Reduction of Concrete Deterioration by Ettringite Using Crystal Growth Inhibition Techniques

Final Report
May 2001

Iowa DOT TR-431

Submitted to the Highway Division
of the Iowa Department of Transportation
and
The Iowa Highway Research Board

Robert D. Cody, Anita M. Cody,
Paul G. Spry, and Hyomin Lee
Department of Geological and Atmospheric Sciences
Iowa State University
Ames, IA 50011

TABLE OF CONTENTS

ABSTRACT vii

PROBLEM STATEMENT 1
RESEARCH OBJECTIVES 2

PART I.
EFFECT OF CRYSTALLIZATION INHIBITORS ON ETTRINGITE GROWTH IN CONCRETE

INTRODUCTION 3
CRYSTALLIZATION INHIBITION 4
EXPERIMENTAL MATERIALS AND METHODS 6
- Selection of Crystallization Inhibitors 6
- Concrete Sample Preparation 9
- Experimental Methods 9
- First Series of Experiments 9
- Second Series of Experiments 13
- Analytical Methods and Instrumentation 14

RESULTS AND DISCUSSION 15
- First Series of Experiments – Crystallization Inhibitor Effects on Ettringite 15
  - *Sodium Sulfate Experiments* 15
  - *Sulfate + Crystallization Inhibitor Experiments* 16
  - *Experimentally-Induced Concrete Expansion by Sulfate Ions* 16
  - *Effects of Crystallization Inhibitors on Expansion* 20
  - *Effects of Crystallization Inhibitors on Ettringite Nucleation and Growth* 25
- Second Series of Experiments – Concentration Effects of Crystallization Inhibitors 37
  - *Introduction* 37
  - *Visually-Evident Concrete Deterioration* 42
  - *Microanalysis Results* 44

PART II.
ETTRINGITE SOLUTION GROWTH EXPERIMENTS

INTRODUCTION 46
DETERMINATION OF CRYSTAL GROWTH METHOD 46
1. Method of Strubble and Brown (1984). 47
2. Method of Mylius (1933) described in Taylor (1990) 47
3. Method developed for this study 48

EXPERIMENTS 48
RESULTS 56
Dequest 2010 (ethanol diphosphonate) 56
Dequest 2060 (5-phosphonic acid) 56
Good-rite K752 (polyacrylic acid) 58
Wayhib S (3-phosphate ester) 58
CONCLUSIONS 58
EFFECT OF ENVIRONMENTAL FACTORS ON ETTRINGITE FORMATION 59
EXPERIMENTAL PROCEDURES 60
RESULTS AND DISCUSSION 61
Ionic Species 61
Carboxylic Acids and Borates 63
Amino Acids and NH Compounds 64
Enzymes 65
Sugars and Sugar-Based Chemicals 65
Phosphates and Nucleotides 67
Stains, Lignins, and Surfactants 68
Overview of Experimental Results 69

PART III.
SUMMARY, CONCLUSIONS, AND RECOMMENDATIONS

SUMMARY FOR PART I. THE EFFECTS OF CRYSTALLIZATION INHIBITORS ON ETTRINGITE GROWTH IN CONCRETE 71
Ettringite Roles in Premature Concrete Deterioration 71
Experiment-Based Conclusions on Ettringite-Induced Deterioration 71
Significance of Crystallization Inhibitor Experiments 73
SUMMARY FOR PART II. SOLUTION GROWTH EXPERIMENTS 74
RECOMMENDATIONS 75
ACKNOWLEDGMENTS 76
REFERENCES 76

TABLES

Table 1. Organic crystallization inhibitors used in study 8
Table 2. Samples and procedures, first series of experiments 10,11
Table 3. Samples and procedures, second series of experiments (effects of concentration) 12

Table 4. Visually-detectable effects on concrete blocks after 40 cycles with different concentrations of Dequest 2060 38
Table 5. Effect of commercial inhibitors on ettringite solution growth 57

FIGURES

Fig. 1. Chemical structures of organic crystallization inhibitors used in study 7
Fig. 2. Expansion of concrete by sodium sulfate treatment. 17
Fig. 3. Expansion of newly-made concrete by Na_2SO_4 and Na_2SO_4 + 0.01 % crystallization inhibitors. 21
Fig. 4. Expansion of durable concrete by Na_2SO_4 and Na_2SO_4 + 0.01 % crystallization inhibitors. 22
Fig. 5 Expansion of non-durable concrete by Na_2SO_4 and Na_2SO_4 + 0.01 % crystallization inhibitors. 23
Fig. 6. Triangular diagram and atomic ratio plot for ettringite in void-fillings of untreated concretes. 26
Fig. 7. Ettringite formed by continuous immersion in 0.75M sodium sulfate. 27
Fig. 8. Triangular diagram and atomic ratio plot for void-fill substances, Na_2SO_4. 28
Fig. 9. Triangular diagram and atomic ratio plot for void-fill substances, Na_2SO_4 + 0.01% Dequest 2010. 30
Fig. 10. Triangular diagram and atomic ratio plot for void-fill substances, Na_2SO_4 + 0.01% Dequest 2060. 31
Fig. 11. Triangular diagram and atomic ratio plot for void-fill substances, Na_2SO_4 + 0.01% Good-rite K752. 32
Fig. 12. Triangular diagram and atomic ratio plot for void-fill substances, Na_2SO_4 + 0.01% Wayhib S. 33
Fig. 13. SEM/EDAX images of void-fill substances, 0.0001% Dequest 2060 39
Fig. 14. SEM/EDAX images of void-fill substances, 0.001% Dequest 2060 40
Fig. 15. SEM/EDAX images of void-fill substances, 0.01% Dequest 2060 41
Fig. 16. Triangular diagram of Ca, Al, S for void-fills produced by second series of experiments at different concentrations of Dequest 2060. 43
Fig. 17. Apparatus used for ettringite growth from solution. 50
Fig. 18. Changes in optical transmittance over time in solutions in which 0, 10, 50, 75, 250, 500, and 1,000 µl of Dequest 2010 were added. 52

Fig. 19. Changes in optical transmittance over time in solutions in which 0, 10, 50, 75, 250, 500, and 1,000 µl of Dequest 2060 were added. 53
Fig. 20. Changes in optical transmittance over time in solutions in which 0, 10, 50, 75, 250, 500, and 1,000 µl of Good-rite K752 were added. 54
Fig. 21. Changes in optical transmittance over time in solutions in which 0, 10, 50, 75, 250, 500, and 1,000 µl of Wayhib S were added. 55
Fig. 22. 62
A. Six-sided needle-like morphology of ettringite grown in solution without additives.
B. Short 'pointed' ettringite crystals formed with arabinic acid (exp. 81).
C. Elongate, thin ettringite crystals grown with Alizarin Red S (exp. 153) exhibit growth defects on their long faces.
Fig.23. Ettringite Structure (Appendix B) 95

APPENDICES

Appendix A. EXPANSION MEASUREMENT DATA 83
Appendix B. ETTRINGITE CRYSTAL STRUCTURE 91
Appendix C. SUMMARY OF CRYSTALLIZATION EXPERIMENTAL RESULTS 95

ABSTRACT

For the Final Report TR-431
Reduction of Concrete Deterioration by Ettringite
Using Crystal Growth Inhibition Techniques
by
Robert D. Cody, Anita M. Cody, Paul G. Spry, and Hyomin Lee

Many researchers have concluded that secondary or delayed ettringite is responsible for serious premature deterioration of concrete highways. In some poorly performing Iowa concretes, ettringite is the most common secondary mineral but its role in premature deterioration is uncertain since some researchers still maintain that secondary ettringite does not itself cause deterioration. The current research project was designed to determine experimentally if it is possible to reduce secondary ettringite formation in concrete by treating the concrete with commercial crystallization inhibitor chemicals. The hypothesis is such that if the amount of ettringite is reduced, there will also be a concomitant reduction of concrete expansion and cracking. If both ettringite formation and concrete deterioration are simultaneously reduced, then the case for ettringite induced expansion/cracking is strengthened.

Our experiments used four commercial inhibitors – two phosphonates, a polyacrylic acid, and a phosphate ester. Concrete blocks were subjected to continuous immersion, wet/dry and freeze/thaw cycling in sodium sulfate solutions and in sulfate solutions containing an inhibitor. The two phosphonate inhibitors, Dequest 2060 and Dequest 2010, manufactured by Monsanto Co. were effective in reducing ettringite nucleation and growth in the concrete. Two other inhibitors, Good-rite K752 and Wayhib S were somewhat effective, but less so than the two phosphonates. Rapid experiments with solution growth inhibition of ettringite without the presence of concrete phases were used to explore the mechanisms of inhibition of this mineral.

Reduction of new ettringite formation in concrete blocks also reduced expansion and cracking of the blocks. This relationship clearly links concrete expansion with this mineral – a conclusion that some research workers have disputed despite theoretical arguments for such a relationship and despite the numerous observations of ettringite mineralization in prematurely deteriorated concrete highways. Secondary ettringite nucleation and growth must cause concrete expansion because the only known effect of the inhibitor chemicals is to reduce crystal nucleation and growth, and the inhibitors cannot in any other way be responsible for the reduction in expansion. The mechanism of operation of the inhibitors on ettringite reduction is not entirely clear but our solution growth experiments show that they prevent crystallization of a soluble ettringite precursor gel.

The present study shows that ettringite growth alone is not responsible for expansion cracking because our experiments showed that most expansion occurs under wet/dry cycling, less under freeze/thaw cycling, and least under continuous soaking conditions. It was concluded from the different amounts of damage that water absorption by newly-formed, minute ettringite crystals is responsible for part of the observed expansion under wet/dry conditions, and that reduction of freeze resistance by ettringite filling of air-entrainment voids is also important in freeze/thaw environments.

On the basis of these experiments, we conclude that the reduction of ettringite formation and expansion cracking in highway concretes is chemically feasible in laboratory experiments. The chemicals used in the project are relatively inexpensive and are of low toxicity. We strongly recommend additional research to determine whether treatment of highways with a commercial phosphonate inhibitor will reduce secondary ettringite formation and premature deterioration under field conditions.

PROBLEM STATEMENT

Cody et al., (HR-384, 1997) cocluded that ettringite was responsible for major concrete deterioration in Iowa highways although the precise mechanism of deterioration remained uncertain. In many Iowa highway concretes that exhibit premature concrete deterioration, ettringite, $Ca_6Al_2(SO_4)_3(OH)_{12}\cdot 26H_2O$, $3CaO\cdot Al_2O_3\cdot 3CaSO_4\cdot 32H_2O$, or $C_6A\overline{S}_3H_{32}$, completely fills smaller voids and lines the walls of large voids. Microscopic ettringite is also disseminated through the paste of many samples. Severe cracking of cement paste is spatially associated with ettringite and many research workers conclude that this association is evidence that ettringite contributed to the cracking. There is disagreement, however, about whether ettringite creates expansion pressures and actively promotes cracking, or whether it is passive and forms in cracked concrete because of easy access of sulfate-bearing solutions. It should also be noted that the decomposition of pyrite in dolomite coarse aggregate enhances ettringite formation (Cody et al. 1997). Pyrite, FeS_2, decomposes in concrete to produce sulfate ions, SO_4^{2-},which react with concrete components to produce ettringite. Many pyritic dolomites contain large amounts of available soluble sulfate as observed by Dubberke (pers. comm. 1996) who found magnesium sulfate efflorescence on the surfaces of these rocks. Ettringite growth in highway concrete can also be caused by deicer applications that may be contaminated with up to 4 wt. % soluble sulfate in the form of gypsum or magnesium sulfate.

Is it possible to chemically reduce new secondary ettringite growth in highway concrete and thereby reduce premature deterioration? The reduction of ettringite growth in concrete might be accomplished by treating highways with inexpensive commercial crystallization

inhibitors but much research on ettringite growth reduction is needed before such highway treatments are attempted.

RESEARCH OBJECTIVES

The major object of the present research is to determine whether concrete treatment with crystallization inhibitor chemicals under closely-controlled experimental conditions will reduce or eliminate ettringite growth. A co-objective is to determine if cracking and other types of expansion-related deterioration are simultaneously reduced with the reduction of ettringite formation. If ettringite formation and expansion cracking are reduced, then ettringite growth must be the cause of the deterioration. Linking the two will show that at least some types of premature cracking of concrete can be minimized by crystallization inhibitor treatment.

To achieve these objectives, two types of experiments were conducted. The results are presented in two parts. The first part were experiments in which concrete samples were immersed in solutions containing $NaSO_4$ and selected inhibitors. These experiments were designed to explore the potential reduction of ettringite growth by crystallization inhibitors and the relationship between ettringite growth and cracking caused by the expansion of concrete.

The second set of experiments involved the solution growth of ettringite in the absence of concrete. These experiments provided a more rapid evaluation of crystallization inhibitor effectiveness than was possible in the first type of experiments and were designed to explore the reactions leading to crystallization inhibition of this mineral. In this part of the project, we also investigated various factors governing inhibitor effectiveness.

PART I

THE EFFECT OF CRYSTALLIZATION INHIBITORS ON ETTRINGITE GROWTH IN CONCRETE

INTRODUCTION

Considerable progress has been made in reducing premature failure of Iowa highway concrete but occasionally failures still occur. Most of the early highway concrete failures in Iowa are construction related, but a few failures are due to chemical processes in the concrete. For the latter type of failure there is often abundant secondary mineral formation in the concretes. As shown in previous DOT research projects (Cody et al. 1994, 1997), a variety of secondary minerals form in highway concrete by internally-induced reactions and perhaps by deicer applications. The major secondary minerals that form are calcite ($CaCO_3$), brucite ($Mg(OH)_2$), and ettringite ($Ca_6Al_2(SO_4)_3(OH)_{12}\cdot 26H_2O$). We found in our previous research that ettringite was the most deleterious mineral that grew in non-durable highway concrete under highway use conditions, and that it was most common in concretes made with dolomite coarse aggregate containing oxidized pyrite inclusions (Cody et al. 1994, 1997). Our previous experiments documented that abundant secondary ettringite was formed in pre-existing highway concrete by sodium sulfate treatment. Extensive concrete expansion cracking accompanied experimental ettringite growth, and as such, we concluded that cracking was caused by ettringite formation.

CRYSTALLIZATION INHIBITION

Crystallization inhibitors are used widely to prevent or minimize unwanted crystallization in industrial processes, as in commercial boilers and water treatment plants. The basic concepts of crystallization inhibition were originally developed in the 1950's (Buckley 1951). Numerous experimental studies have subsequently led to the understanding of the mechanisms involved in the crystallization inhibition processes (Smith 1967; Smith and Alexander 1970; Tuan-Sarif 1983, Black et al. 1991; Davey et al. 1991). The two major effects of inhibitors are the prevention or reduction of undesired precipitation and modification of precipitate morphologies. Many studies have concluded that inhibitors prevent crystallization from solutions chiefly by preventing the growth of "pre-critical nuclei" – that is, crystal nuclei that are too small to be stable in solution. Growth of pre-critical nuclei is prevented so that the unstable crystallites never attain a stable (critical) size, and rapidly dissolve. The result is that macroscopic crystals never develop and precipitation is prevented. A large degree of supersaturation is required for precipitation in the presence of small concentrations of effective inhibitors. Almost all commercial inhibitors are organic chemicals, chiefly polycarboxylates and phosphonates, and most are effective in inhibiting the precipitation of a wide variety of slightly soluble minerals such as calcite, gypsum, and barite (Cody 1991). It has also been proposed that small amounts of certain naturally occurring organic substances act as crystallization inhibitors in modifying precipitation processes in natural sedimentary environments (Cody 1991).

No research has been published on inhibiting secondary mineral precipitation in concrete with a goal of preventing highway deterioration, but some research has been performed on the effects of these chemicals in retarding concrete setting. Organic compounds, such as sugars, hydroxylated carboxylic acids, lignosulfonates, and polyacrylic acids are added to cement in

order to retard the setting process (Young, 1972; Collepardi et al. 1984; Jolicoeur and Simard, 1998). Researchers have generally concluded that mechanisms of cement retardation are due to: (1) adsorption of organic compounds on the surface of cement compounds; (2) complexation between organic compounds with Ca and Si of paste components; (3) precipitation of insoluble hydrates by control of solubility; and (4) crystal nucleation inhibition. However, the precise mechanism for retardation appears to be unresolved because of the complex physicochemical mechanisms involved in cement hydration (Taylor, 1990; Jolicoeur and Simard, 1998).

Very recently, Coveney and coworkers conducted experiments on the effectiveness of phosphonate-based organic inhibitors in the cement retardation process (Coveney and Humhries, 1996; Coveney et al., 1998). They found that some phosphonates are effective in inhibiting the growth of ettringite and that the effectiveness of phosphonates is largely controlled by their molecular structure. Binding of phosphonate radicals to cation sites of ettringite slows the growth rates of the crystals. The most effective phosphonate molecules are those with interatomic distances between phosphonate radicals that are identical to distances between adjacent sulfate ions of ettringite {0001} surfaces. With suitable fit, the inhibitors are adsorbed onto ettringite precritical nuclei which effectively prevent the nucleation and growth processes that transform ettringite gel into its crystalline form. Retardation of ettringite growth delays the concrete setting process. According to the chemical clock model suggested by Billingham and Coveney (1993), hydration of cement is the rate-determining step. The setting process commences when impermeable ettringite gel transforms into permeable mass of needle-like crystalline ettringite. This transformation results in the renewed hydration of the aluminate and silicate phases so that setting begins. The fact that polyphosphonates inhibit ettringite growth in lab experiments suggests that crystallization inhibitors may be effective in reducing

secondary ettringite growth in highway concrete and may possibly reduce highway deterioration.

EXPERIMENTAL MATERIALS AND METHODS

Selection of Crystallization Inhibitors

According to Cody (1991), there are three major chemical groups of commercial organic inhibitors: (1) organic phosphate esters, (2) phosphonates, and (3) polyelectrolytes. The effectiveness of crystallization inhibition is related to the functional groups present on the organic molecules and the interatomic distances between those functional groups. Those molecules which are negatively charged by deprotonation under alkaline condition are the most effective inhibitors (Cody 1991). Additional factors considered important in effectiveness of crystallization inhibitors are pH of solution, inhibitor concentration, and solution concentration (Tuan-Sarif 1983; Cody 1991). The most effective pH ranges vary slightly for different inhibitors, but all commercial inhibitors are effective at moderate to high pH, and thus should be effective in the concrete environment. Effectiveness of inhibitors increase with concentration and the degree of inhibition for a specific concentration of inhibitor depends on the degree of supersaturation of the potential precipitate.

Four different crystallization inhibitors were used in our experiments; two phosphonates, a phosphate ester, and a polyelectrolyte (polyacrylic acid). A brief description of these inhibitors and their general structures are shown in Figure 1 and Table 1.

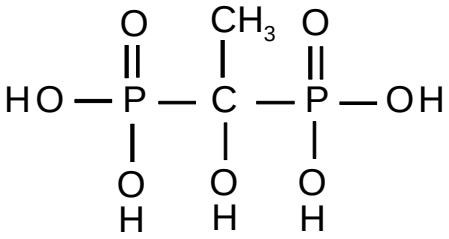

Dequest 2010
1-Hydroxyethylidene 1,
1-Diphosphonic Acid
after Monsanto Tech Bull. No. IC/SCS-314

A.

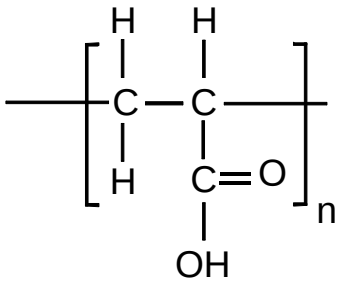

Good-Rite K752
Polyacrylate
after BF Goodrich Tech. Bull. No. GC-62

C.

Phosphonates

Non-Phosphonates

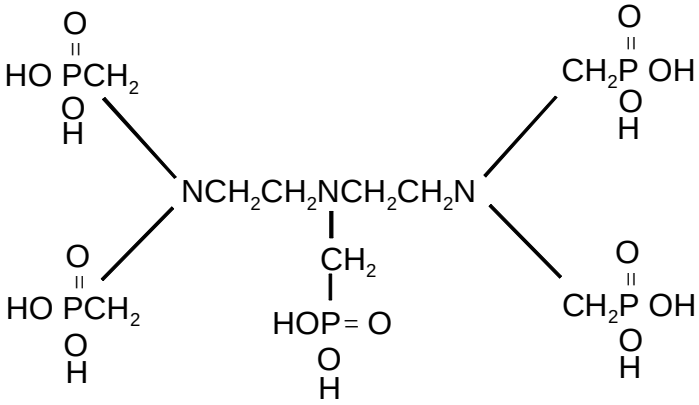

Dequest 2060
Diethylenetriaminopenta
(methylenephosphonic acid)
after Monsanto Tech. Bull. No. IC/SCS-322

B.

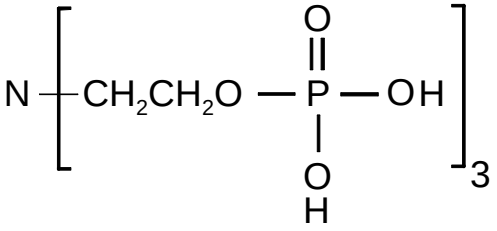

Wayhib S
Phosphate Ester
Nitrilo Tri(ethyl acid Phosphate)
after Phillip A Hunt product
safety data sheet

D.

Fig. 1. Chemical structures of organic crystallization inhibitors used in study.

Table 1. Organic crystallization inhibitors used in study

Trade Names	Chemical groups	Molecular wt.	Natural pH	Manufacturer
Dequest 2010	Phosphonate	206	< 2 (1% solution at 25 ^{o}C)	Monsanto Co.
Dequest 2060	Phosphonate	573	< 2 (1% solution at 25 ^{o}C)	Monsanto Co.
Good-rite K-752	Polyelectrolyte	2100	2.6 (2.2-3)	BF Goodrich, Inc.
Wayhib S	Phosphate Ester	389	4.6 (5 % solution at 25 ^{o}C)	Phillip A. Hunt Co.

Concrete Sample Preparation

Experiments used concrete from existing Iowa highway cores collected by IDOT personnel (Cody et al., 1997), and a newly-made and cured type I concrete. One durable (Sundheim Quarry dolomite aggregate, US 20) and one non-durable (Nelson Quarry dolomite aggregate, US 63) highway concrete were selected (in this study, durable is defined as concrete with a service life > 30 years and non-durable as one with a service life < 16 years). A list of samples and the experimental parameters used in our experiments are presented in Tables 2 and 3. Newly made concrete was mixed with the following specifications; Type I portland cement, limestone coarse aggregate, sand fine aggregate, w/c ratio of 0.6, air content of 6 %, and cured for 10 days in a moisture room. The newly-made concrete was added to experiments for comparative purposes and to eliminate the possible effects of secondary minerals such as ettringite that might have developed in older concrete during highway use. Small 3 cm x 1.5 cm x 1.5 cm blocks used in the experiments were cut from selected highway core samples and newly-made concrete.

Experimental Methods

All experiments were conducted according to the experimental methods described in previous DOT research (Cody et al., 1997). Two series of experiments with concrete blocks were performed in the present study.

First series of experiments

For most experiments, an inhibitor concentration of 0.01% in 0.75M Na_2SO_4 was used. To compare the effectiveness of concentration, inhibitor concentrations of 0.01 and 0.001% were

Table. 2. Samples and procedures, first series of experiments

Type of Experiment	Type of Concretes		Type of Crystallization inhibitors	W/D**	F/T**	Continuous**
Na_2SO_4	Highway concrete	Durable*	-	1	1	1
		Non-durable*	-	1	1	1
	Newly-made		-	2	2	2
Na_2SO_4 + 0.01% inhibitor	Highway concrete	Durable	Dequest 2010	1	1	-
			Dequest 2060	1	1	-
			Good-rite K-752	1	1	-
			Wayhib S	1	1	-
		Non-durable	Dequest 2010	1	1	-
			Dequest 2060	1	1	-
			Good-rite K-752	1	1	-
			Wayhib S	1	1	-
	Newly-made concrete		Dequest 2010	1	1	-
			Dequest 2060	1	1	-
			Good-rite K-752	1	1	-
			Wayhib S	1	1	-
Na_2SO_4 + 0.1% inhibitor	Highway concrete	Durable	Dequest 2010	-	-	1
			Dequest 2060	-	-	1
			Good-rite K-752	-	-	1
			Wayhib S	-	-	1
		Non-durable	Dequest 2010	-	-	1
			Dequest 2060	-	-	1
			Good-rite K-752	-	-	1
			Wayhib S	-	-	1
	Newly-made concrete		Dequest 2010	-	-	1
			Dequest 2060	-	-	1
			Good-rite K-752	-	-	1
			Wayhib S	-	-	1

Numbers indicate the number of samples.

*Durable is concrete from US 20, Dubuque Co., with Davenport type 1 cement and coarse aggregate from the Sundheim Quarry in the Hopkinton Formation. Non-durable concrete is that taken from US 63, Howard Co., with Dewey type I (= Davenport type I) cement and coarse aggregate from the Nelson Quarry in the Cedar Valley Formation. The chemical composition of these concretes is not available.

**W/D = wet/dry cycling. F/T = freeze/thaw cycling. Continuous = continuous immersion in solutions.

Table. 2 (continued). Samples and procedures, first series of experiments

Type of Experiment	Type of Concretes		Type of Crystallization inhibitors	W/D	F/T	Continuous
Na_2SO_4 + 0.001% inhibitor	Highway concrete	Durable	Wayhib S	-	-	1
			Dequest 2010	-	-	1
			Dequest 2060	-	-	1
			Good-rite K-752	-	-	1
		Non-durable	Wayhib S	-	-	1
			Dequest 2010	-	-	1
			Dequest 2060	-	-	1
			Good-rite K-752	-	-	1
	Newly-made concrete		Dequest 2010	-	-	1
			Dequest 2060	-	-	1
			Good-rite K-752	-	-	1
			Wayhib S	-	-	1
H_2O (Controls)	Highway concrete	Durable	N/A	1	1	1
		Non-durable	N/A	1	1	1
	Newly-made concrete		N/A	2	2	2
H_2O with 0.01 % inhibitors (Controls)	Newly-made concrete		Dequest 2010	2	2	2
			Dequest 2060	2	2	2
			Good-rite K-752	2	2	2
			Wayhib S	2	2	2

Numbers indicate the number of samples.

Table 3. Samples and procedures, second series of experiments (effects of concentration)

Type of Experiment (wet/dry cycling)	Inhibitor concentration (Dequest 2060)	# of Blocks	Cycles
Na_2SO_4	N/A	4	W/D
Without change solution during experiment	5.0 %	2	W/D
	1.0 %	2	W/D
	0.1 %	2	W/D
	0.01 %	2	W/D
	0.001 %	2	W/D
	0.0005 %	2	W/D
	0.0001 %	2	W/D
With change solution after 5 cycles	5.0 %	2	W/D
	1.0 %	2	W/D
	0.1 %	2	W/D
	0.01 %	2	W/D
	0.001 %	2	W/D
	0.0005 %	2	W/D
	0.0001 %	2	W/D
Total		28	

used in selected experiments (Table 2). Because the inhibitors usually are in the acid form, the initial solution pH was adjusted with NaOH to a pH of 10 to prevent deterioration of concrete by adverse pH conditions. Four blocks of concrete were immersed in 100 ml of solutions, sealed in polymethylpentene containers, and stored at 58°C in a constant temperature chamber. Experimental procedures for wet/dry and freeze/thaw cycling were described in previous IDOT research (Cody et al. 1997). Experiments that contained inhibitor concentrations of 0.1% and 0.001% inhibitor were only subjected to continuous immersion conditions whereas wet/dry and freeze/thaw cycling was performed only with 0.01% solutions. Fewer experiments were performed under continuous immersion because this condition was found in previous experiments to be least damaging to concrete, and continuous immersion in a sulfate-bearing solution is unlikely to occur under highway conditions. Experiments with the addition of 0.01% inhibitor in distilled water (without Na_2SO_4) were performed to observe any adverse effects of the inhibitor itself. Identical experiments without inhibitor were also conducted for comparison to those with crystallization inhibitors. Additional inhibitors were added to the solutions after 6 cycles of wet/dry and freeze/thaw in order to offset potential time-dependent decomposition of the organic substances at the elevated experimental temperatures. One cycle consisted of 132 hr. of immersion at 58°C, removal of the sample from solution, and either air-drying or freezing at –3°C. At the beginning of the next cycle the sample was returned to the solution and again stored in the oven.

Second series of experiments

After it was found that crystallization inhibitors actually decreased ettringite formation in the concrete samples of the first series of experiments, a second set of experiment was conducted

to test the effects of different concentrations of a representative inhibitor (Dequest 2060). Concrete blocks (1.5 x 1.5x 1.5 cm) made from cores of highway US 20 that contain Sundheim Quarry coarse aggregate were used. Experiments were conducted with 0.75M sodium sulfate solution with inhibitor concentrations of 5, 1, 0.1, 0.01, 0.001, 0.0005, and 0.0001 %. Solution pH was adjusted to pH = 10 (Table 3). Only wet/dry experiments were performed because these conditions were found to be most damaging to concretes in the first series of experiments. Somewhat different procedures were used in these experiments compared to those of the first series. In order to prevent possible kinetics effects of different diffusion rates of sulfate and inhibitor molecules into the immersed concrete sample, the concrete blocks were immersed in a solution containing the proper concentration of inhibitor but no sulfate for 2 weeks before the experiments were started. Also, rather than adding extra inhibitor to the initial solution after 6 cycles as implemented in the first series of experiments, two different procedures were followed. In one group of experiments, a specific concentration of inhibitor and 0.75 M sulfate solution were added at the beginning of the experiment and the blocks were wet/dry cycled to the end of the experiments. In the second group, the starting solution was poured off after the 6^{th} cycle and fresh solution of the same inhibitor and sulfate concentration was added in order to offset possible inhibitor decomposition and resultant decrease in effectiveness. Solutions changes were implemented after each successive 6^{th} cycles until the end of the experiments.

Analytical Methods and Instrumentation

All experiments were continued until visual signs of deterioration were detected in samples treated without inhibitors, at which time all experiments performed with a specific type of concrete under the same conditions (continuous soak, wet/dry, or freeze/thaw cycling) were

terminated. The length change of each block was carefully measured using calipers (0.01 mm scale) to detect expansion presumably due to formation of secondary minerals. All Na_2SO_4 treated blocks without inhibitors and selected blocks with 0.01 % inhibitor treatment were thin-sectioned and examined with polarizing and scanning electron microscopes. Sample selections for detailed petrographic/SEM study were based on obtaining a representative of each inhibitor effect, covering different experimental conditions, and showing comparatively serious deterioration (Table 2 and 3). Using a low-vacuum scanning electron microscope (SEM), back-scattered images were obtained and energy dispersive analytical X-ray (EDAX) area mapping was performed for Si, Al, K, Na, O, Ca, Mg, S, Cl, P, and Fe. Detailed semi-quantitative microanalyses were carried out by EDAX point analysis in order to identify the composition of void filling materials. An accelerating voltage of 20 KV was generally used for EDAX point analyses with the SEM.

RESULTS AND DISCUSSION

First Series of Experiments – Crystallization Inhibitor Effects on Ettringite

Sodium Sulfate Experiments

Sodium sulfate treatments without the addition of crystallization inhibitors had the same effects as described in the IDOT HR-384 Final Report (Cody et al., 1997). The treated concrete samples developed large randomly-oriented cracks in the paste and softening of the outer paste surface. The physical appearance and the in-void occurrence of ettringite were identical to that found in untreated concrete after prolonged highway use. The newly-made concrete deteriorated faster than the older highway concrete samples. New concrete showed visually-detectable deterioration after 18 cycles of wet/dry conditions (125 days). All other experiments were run for 24 cycles (168 days). Under wet/dry cycling, durable concrete (Sundheim Quarry dolomite

aggregate, US 20) that may initially have contained a minor amount of ettringite exhibited deterioration similar to that of the new concrete. Non-durable concrete that initially contained abundant ettringite showed relatively less experimentally-induced deterioration than the other concretes after 24 cycles in wet/dry experiments. Samples subjected to freeze/thaw and especially to continuous immersion conditions showed less deterioration after the same number of cycles than those subjected to wet/dry cycling.

Sulfate + Crystallization Inhibitor Experiments

Cracking was nearly eliminated with the addition of the crystallization inhibitors in the sulfate solutions. Wet/dry and freeze/thaw cycling with 0.01% inhibitor chemicals produced only minor cracking in a few durable concrete blocks under wet/dry conditions. All blocks developed similar surface softening as those in experiments without inhibitor chemicals. Continuous immersion experiments were performed with 0.1% and 0.001% inhibitor solutions and resulted in no visually detectable deterioration except for surface softening. Continuous immersion in sulfate-free distilled water and in sulfate-free distilled water with inhibitors produced no visible effects on any concrete samples.

Experimentally-Induced Concrete Expansion by Sulfate Ions

An important aspect of sulfate attack on concrete is expansion that leads to cracking, strength loss, and disintegration (Neville 1969; Mehta, 1983; Lawrence 1990; Schneider and Piasta 1991; Al-Amoudi et al. 1992; Tumidjski and Turc 1995). Sodium sulfate treatment in the absence of inhibitor molecules produced measurable expansion under continuous immersion, wet/dry and freeze/thaw cycling (Fig. 2, and Appendix A). The amount of expansion was

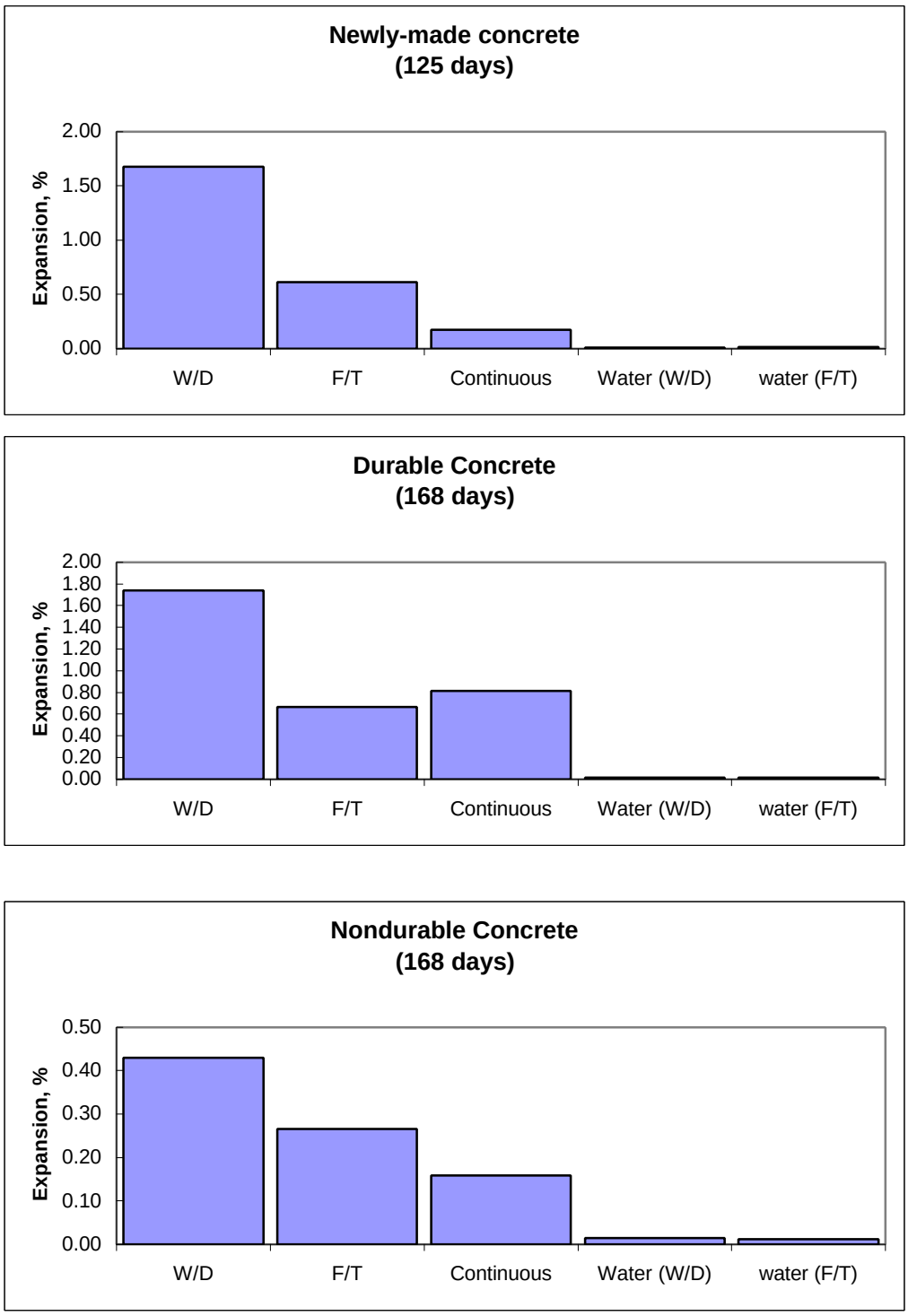

Fig. 2. Expansion of concrete by sodium sulfate treatment. Freeze/thaw (F/T), wet/dry (W/D) and continuous immersion experiments. The largest expansion results from wet/dry experiments regardless of concrete type. Note, however, that much less expansion occurred for non-durable concrete in all sulfate solution experiments.

closely related to the physical conditions during experiments. Greatest expansion developed in concretes subjected to wet/dry cycles. This observation coincides with those of Fu and Beaudoin (1997) who found that accelerated expansion resulted from an increased number of wet/dry cycles. Freeze/thaw conditions produced less expansion, and continuous soaking resulted in the least expansion except, surprisingly, for the durable concrete sample. These results document that different environmental conditions are important factors in deterioration by sulfate attack. Assuming that ettringite growth is the fundamental cause of expansion, there are two principal expansion mechanisms that should be considered. Expansion and cracking may develop because of crystal growth pressures exerted by ettringite or it may occur as a result of swelling of ettringite by water adsorption (Appendix B). In addition, another cause of damage may be present in freeze/thaw conditions – ettringite growth typically fills air-entrainment voids, which are important to freeze resistance, so that loss of voids indirectly affects expansion produced by pore water freezing (Diamond 1996; Wolters 1996).

In the following discussion, it is assumed that ettringite was fundamentally responsible for expansion, either by exerting growth pressures, by swelling during water absorption, and/or by reducing freeze resistance. The justification of this assumption will be discussed later. Continuous immersion produced the least measured expansion because crystal growth of newly-formed ettringite is the only available expansion mechanism since water absorption pressures are unlikely and freeze damage is impossible. Preliminary experiments suggested that crystal growth pressures caused some expansion. However, it was subsequently found that expansion by this mechanism was relatively unimportant because expansion was minimal when samples were subjected to continuous immersion. Upon further consideration, we now believe that wet/dry cycling increases nucleation of ettringite crystals and creates many submicroscopic

crystals because drying creates increasingly concentrated solutions that are saturated or supersaturated in ettringite. Typically, highly-concentrated solutions precipitate numerous, tiny crystals (Klein and Hurlburt 1986). Soaking in sulfate solutions during the wetting part of the cycle causes additional growth of the submicroscopic crystals, and the next drying episode creates many new submicroscopic crystals, which will subsequently grow coarser during the next sulfate solution soaking. Hence, wet/drying cycles produce more ettringite than continuous immersion in a constant concentration sulfate solution.

Because of the larger surface area of fine crystals, submicroscopic ettringite crystals will adsorb more water and swelling will be greater than with coarser crystals. Wet/drying cycles consequently produce more water absorption pressures than continuous immersion, so that greater expansion from wet/dry cycling probably results from pressures exerted by more numerous ettringite crystals and by greater water absorption. Concrete expanded more under freeze/thaw than under continuous immersion, and less under wet/dry cycling. The inferences are that ettringite in larger interstitial pores and air-entrainment voids caused loss of void effectiveness and facilitated expansion produced by freezing of water in addition to expansion caused by ettringite crystal growth.

Newly-made concrete exhibited almost equivalent expansion as durable concrete samples, but over a shorter time span (Fig 2). According to Siedel et al. (1993) and Tumidajski and Turc (1995), accelerated sulfate-induced expansion occurs in mortar of high w/c ratio. They concluded that the sulfate penetration front migrates quickly with an increase in w/c ratio because higher ratios produce a more porous/permeable concrete. Since newly-made concrete was mixed with higher w/c ratio (0.6) than older highway concrete (about 0.43), its accelerated expansion may be due to this reason.

Non-durable concrete that contained large amounts of ettringite before the start of experiments showed the least expansion. The small expansion may result from three possible causes: (1) the existing non-durable highway concrete already had undergone expansion by ettringite during road use conditions, and thus late expansion may be reduced, (2) only relatively small amounts of C_3A necessary for ettringite formation may be available in these older concrete to produce more new ettringite, because C_3A had already been consumed by ettringite under highway conditions, and (3) reduced porosity and permeability resulting from secondary mineral growth during highway road use reduced permeability and the rate of advance of the sulfate ions into the concrete.

Effects of Crystallization Inhibitors on Expansion

Crystallization inhibitors reduced expansion under all environmental conditions and in all types of concrete used in the experiments (Figs. 3-5). The fact that none of the inhibitors completely prevented expansion suggests that none of crystallization inhibitors were completely effective in preventing the formation of ettringite. SEM/EDAX mapping confirms that ettringite void-fill growth was reduced but not completely prevented. Some of the expansion, however, may also result from a form of ettringite that is completely unaffected by crystallization inhibitors. Ettringite produced by sulfate attack on concrete typically exists in two forms: relatively large crystals and nodules that fill voids and which form by direct precipitation from pore solutions, and much smaller ettringite masses that form by replacement of C_3A. Replacement-reaction ettringite may be unaffected by crystallization inhibitors that are effective in preventing ettringite nucleation from solutions. There is some external evidence that replacement reactions are not affected by crystallization inhibitors. Experiments by Cody

Newly-made concrete
(after 125 days)

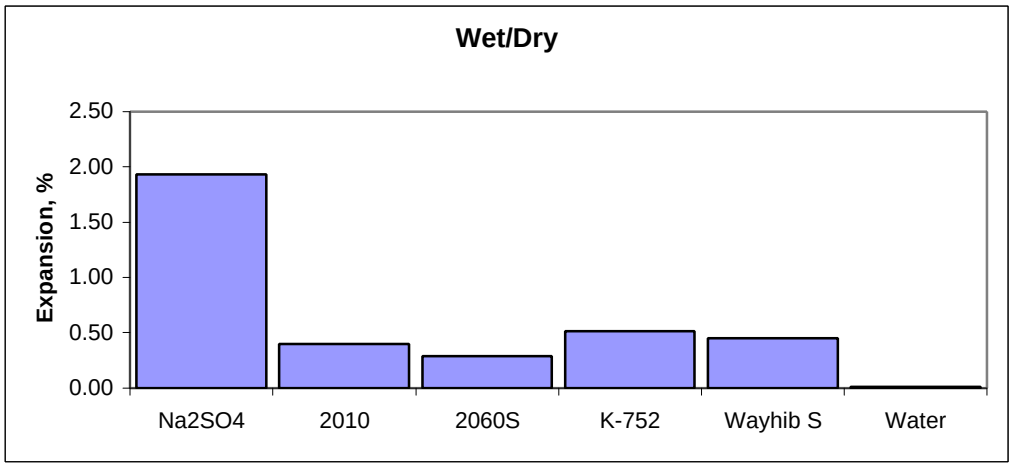

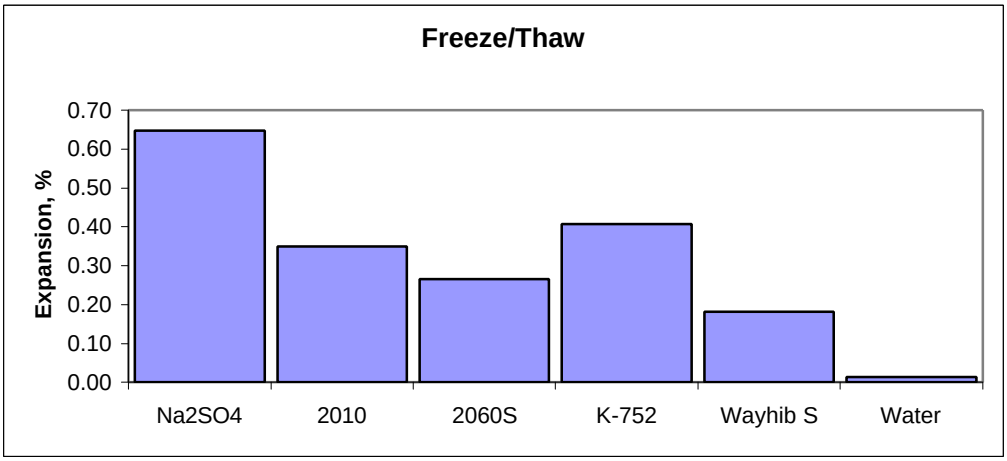

Fig. 3. Expansion of newly-made concrete by Na_2SO_4 and Na_2SO_4 + 0.01 % crystallization inhibitors. Na_2SO_4 treatment without inhibitors, Dequest 2010 phosphonate inhibitor, Dequest 2060 phosphonate inhibitor, Good-rite K-752 polyacrylate inhibitor, Wayhib S phosphate ester inhibitor, and distilled water. Note the different vertical scales in the two diagrams, and that the greatest reduction in expansion occurred in wet/dry experiments. Dequest 2060 was the most effective inhibitor for newly-made concrete.

Durable Concrete
(after 168 days)

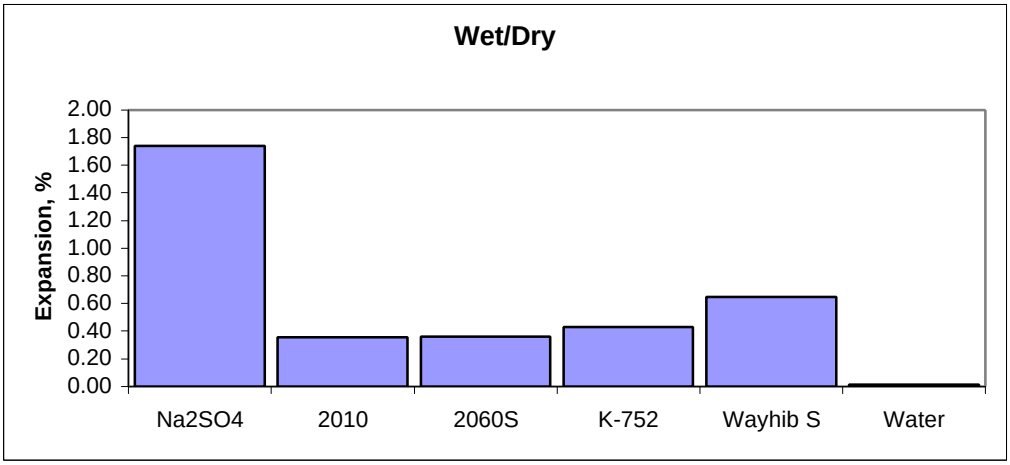

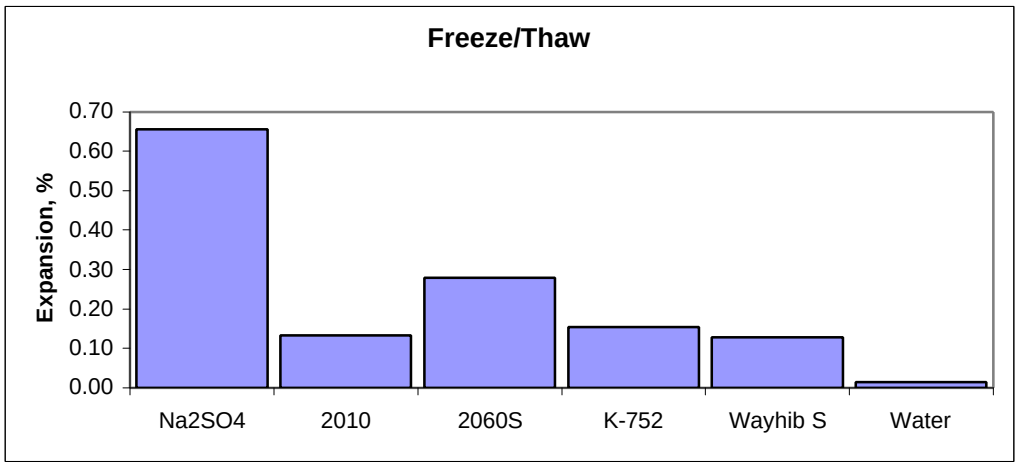

Fig. 4. Expansion of durable concrete by Na_2SO_4 and Na_2SO_4 + 0.01 % crystallization inhibitors. Na_2SO_4 treatment without inhibitors, Dequest 2010 phosphonate inhibitor, Dequest 2060 phosphonate inhibitor, Good-rite K-752 polyacrylate inhibitor, Wayhib S phosphate ester inhibitor, and distilled water. Note the different vertical scales in the two diagrams, and that the greatest reduction occurred in wet/dry experiments. The two phosphonate inhibitors were the most effective in wet/dry experiments, whereas Wayhib S and Dequest 2010 were best in freeze/thaw experiments.

Non-Durable Concrete
(after 168 days)

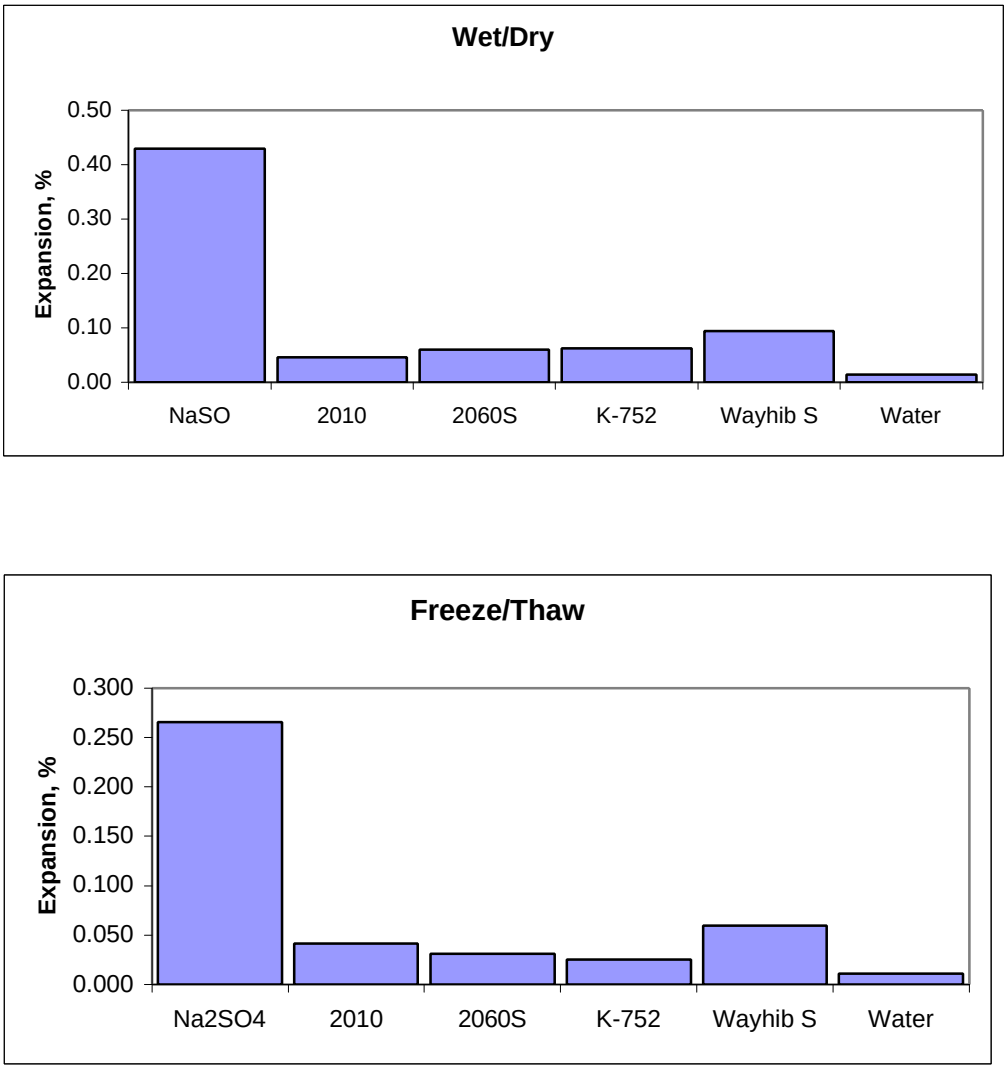

Fig. 5. Expansion of non-durable concrete by Na_2SO_4 and Na_2SO_4 + 0.01 % crystallization inhibitors. Na_2SO_4 treatment without inhibitors, Dequest 2010 phosphonate inhibitor, Dequest 2060 phosphonate inhibitor, Good-rite K-752 polyacrylate inhibitor, Wayhib S phosphate ester inhibitor, and distilled water. Note the different vertical scales in the two diagrams. Dequest 2010 was the most effective inhibitor in wet/dry experiments whereas Good-rite K-752 was most effective in freeze/thaw experiments.

(unpublished) show that crystallization inhibitors did not affect the conversion of gypsum to anhydrite in elevated temperature solutions even though the specific inhibitors very effectively prevented gypsum nucleation and favored anhydrite precipitation for identical experimental conditions.

Lack of complete prevention of void-fill ettringite may be a result of poor interatomic fit of inhibitor molecules on ettringite surfaces. According to Coveney and Humphries (1996) and Coveney et al. (1998), the effectiveness of inhibitors is related to the binding of inhibitor molecules to the growth surface of crystal. The best inhibitors will have similar interatomic distances between phosphonate groups of the inhibitor and sulfate groups on ettringite surfaces. With a suitable fit, an inhibitor might completely prevent the nucleation and growth of precipitated ettringite. Synthesis of better inhibitors to closely approximate the interatomic distances between sulfate ions exposed on ettringite surfaces might be possible, but the cost of synthesizing ettringite-specific inhibitors may be cost-prohibitive for highway applications.

Reduction of expansion by inhibitors was greatest under wet/dry, less in freeze/thaw, and least in continuous immersion conditions (Figs. 3-5). Based on the assumption that the same inhibitor is equally efficient in reducing and/or preventing ettringite crystallization under different environmental conditions, the greater reduction in expansion under wet/dry conditions supports a conclusion that swelling of ettringite by water adsorption probably is a factor in expansion. Only with wet/dry cycling should water absorption swelling be significant. The production of numerous small ettringite crystals, which should produce the greatest water absorption pressures, is favored by drying episodes as discussed previously. Furthermore, the greater reduction of expansion by inhibitors occurred in non-durable concrete compared to the other concretes. This suggests that crystallization inhibitors are more effective in preventing

further growth of pre-existing ettringite (more abundant in non-durable concretes before the experiments) than in preventing nucleation and growth of new experimentally-produced ettringite. The effectiveness of each inhibitor varied with the concretes used and experimental conditions. The phosphate ester Wayhib S was less effective than the other inhibitors in reducing expansion.

Under the conditions of the first series of experiments, increasing an inhibitor concentration from 0.001% to 0.1% in continuous immersion resulted in very little additional reduction in expansion. It should be pointed out again, that additional inhibitor was added to the initial solutions during the course of the experiment in order to compensate for possible decomposition at the elevated temperatures used. Because there was no estimate of the amount of decomposition, inhibitor additions may have increased the total effective concentrations of inhibitor in the experiments, and thereby obscured the effect of initial concentrations. The second series of experiments was designed to address this issue and is discussed in a later section.

Effects of Crystallization Inhibitors on Ettringite Nucleation and Growth

In a previous IDOT study (Cody et al., 1997), Na_2SO_4 treatment was shown to produce abundant ettringite which formed in open spaces such as microscopic interstitial pores, air voids, and the boundaries between aggregate and cement paste in non-durable concretes that had only small amounts of ettringite before sulfate treatment.

In the current study, continuous immersion in 0.75M $NaSO_4$ also produced abundant ettringite with identical features to those previously documented (Figs. 6 and 7) and essentially identical features to those formed under highway use conditions (Fig. 8). The addition of

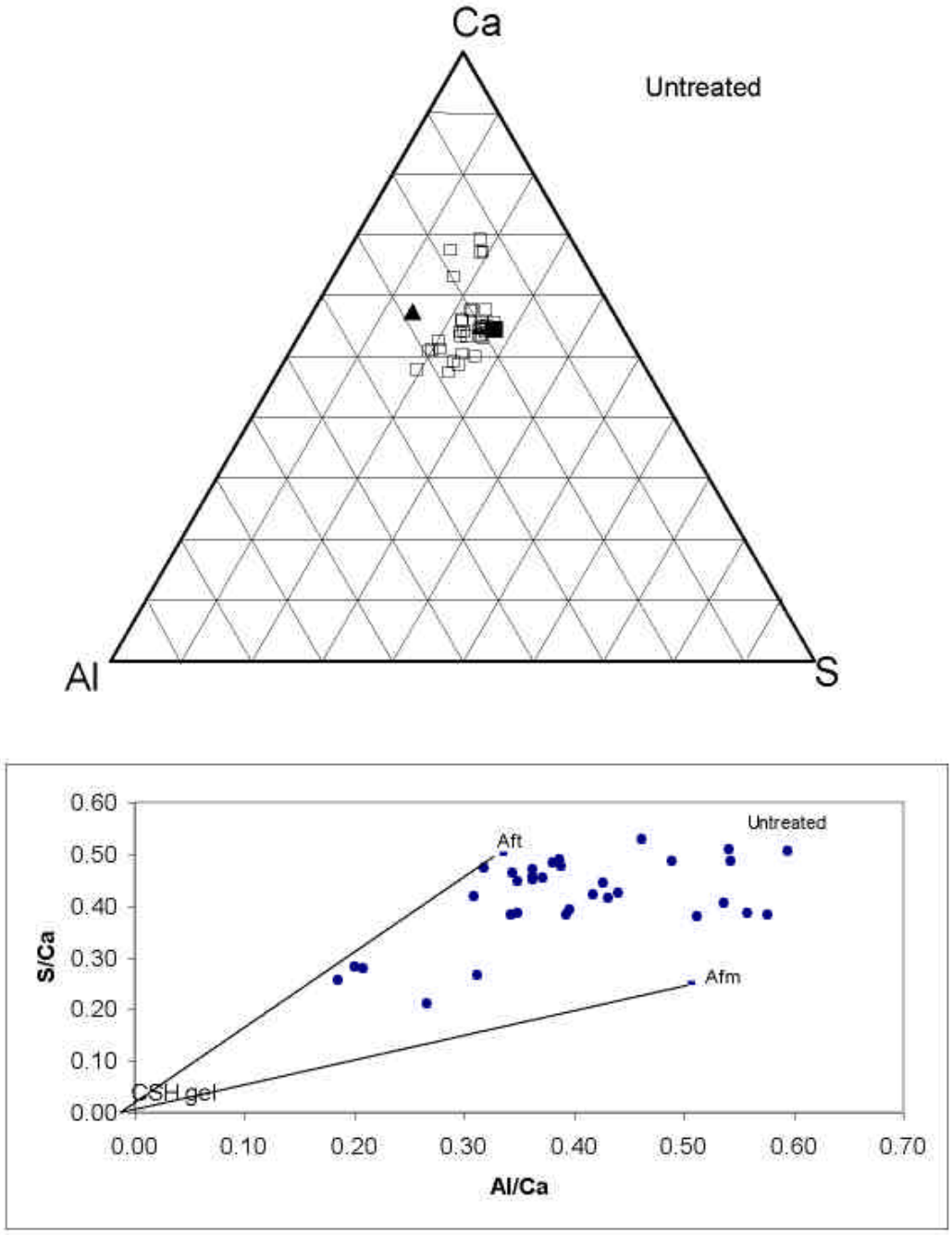

Fig. 6. Triangular diagram and atomic ratio plot of ettringite in void-fillings of untreated concretes (semiquantitative analyses). Ettringite was produced during highway road use, and not by sodium sulfate solutions. In the triangular diagram, the solid square = ettringite and the solid triangle = monosulfate composition. In the atomic ratio plot, AFt = pure ettringite, and AFm = pure monosulfate; CSH = calcium silicate hydrate.

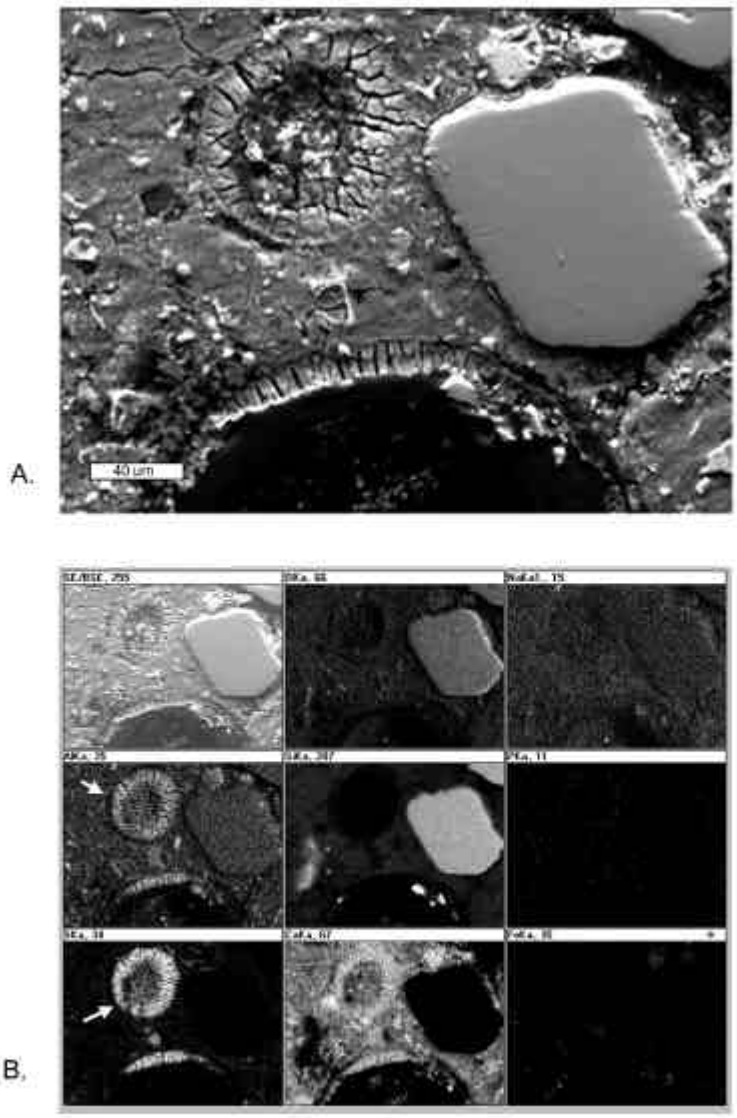

Fig 7. Ettringite formed by continuous immersion in 0.75 M sodium sulfate. A. SEM image, B. EDAX element map. Note the two arrows in the map. The upper arrow points to Al present in an ettringite void fill, and the low arrow points to sulfur in the same void filling. The occurrence of these two elements together with Ca in the bottom middle map indicates the presence of ettringite or substances of close chemical composition.

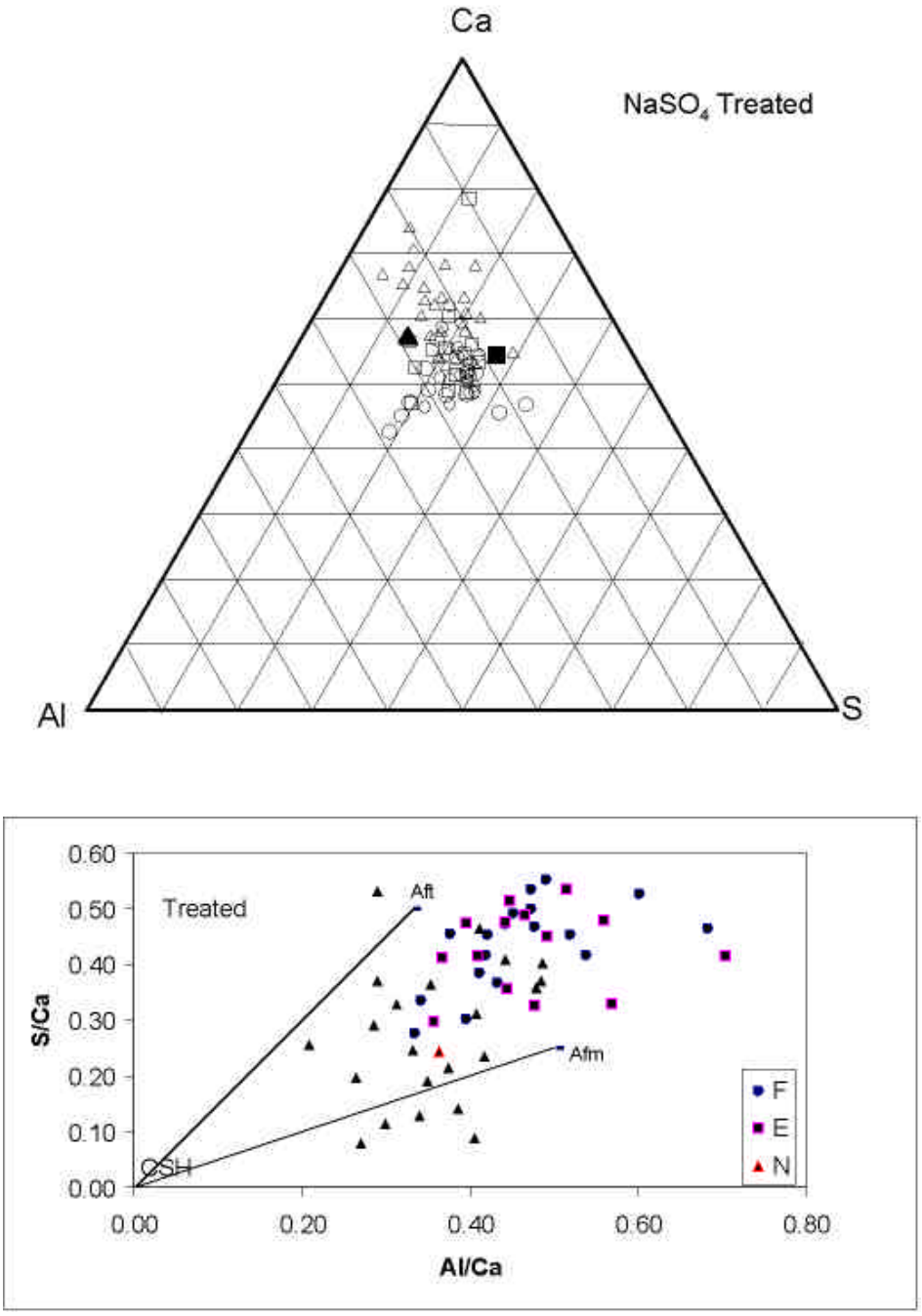

Fig. 8. Triangular diagram and atomic ratio plot of void-fill substances, Na_2SO_4 treated (semiquantitative analyses). In the triangular diagram, the solid square = ettringite and the solid triangle = monosulfate composition. In the atomic ratio plot, AFt = pure ettringite, and AFm = pure monosulfate; CSH = calcium silicate hydrate. Note that the majority of analyses plot between lines connecting AFt and AFm, thus suggesting that the substances are chiefly a mix of the two minerals.

crystallization inhibitors to the sulfate solutions produced a striking change in secondary mineralization. Many voids were filled with newly-formed substances that morphologically resembled ettringite, but showed optically amorphous characteristics different from the optical features of crystalline ettringite. Detailed observations of SEM and analysis by EDAX showed that the chemical composition and morphology of void-filling materials were highly variable and different from the ideal composition of ettringite. Each crystallization inhibitor produced substances with variable chemical and physical characteristics. Detailed microanalyses were carried out by EDAX point analysis in order to determine the approximate composition of filling materials in voids.

Ternary diagrams showing the atomic ratios of Ca, Al, and S combined with atomic ratio plots of Al/Ca and S/Ca proved to be valuable in investigating the character of new precipitates (Gollope and Taylor 1992; Scrivener and Taylor 1993; Thaulow et al. 1996). Microanalyses of void-filling materials together with that of stoichiometric ettringite and monosulfate are presented in ternary diagrams. The atomic ratio plots of Al/Ca against S/Ca are also shown (Figs. 9-12). In the atomic ratio plots, lines are marked between CSH-gel phase and pure ettringite (AFt) or pure monosulfate (AFm) because ettringite and monosulfate are intimately intermixed with CSH (calcium silicate hydrate) gel in cement paste.

Figure 6 shows analyses of void-filling substances in untreated non-durable Iowa highway concretes. The majority of ternary diagram analyses showed compositions close to ettringite, although some show enrichment in Al or Ca and depletion in S, and some indicate enrichment in Si (2-5%) compared to pure ettringite. Deviation from the pure stoichiometric composition of ettringite may be partly due to substitution of SiO_4^{4-} for SO_4^{2-} in the ettringite lattice (Thaulow et al. 1996). The atomic ratio plots of Al/Ca against S/Ca show that most

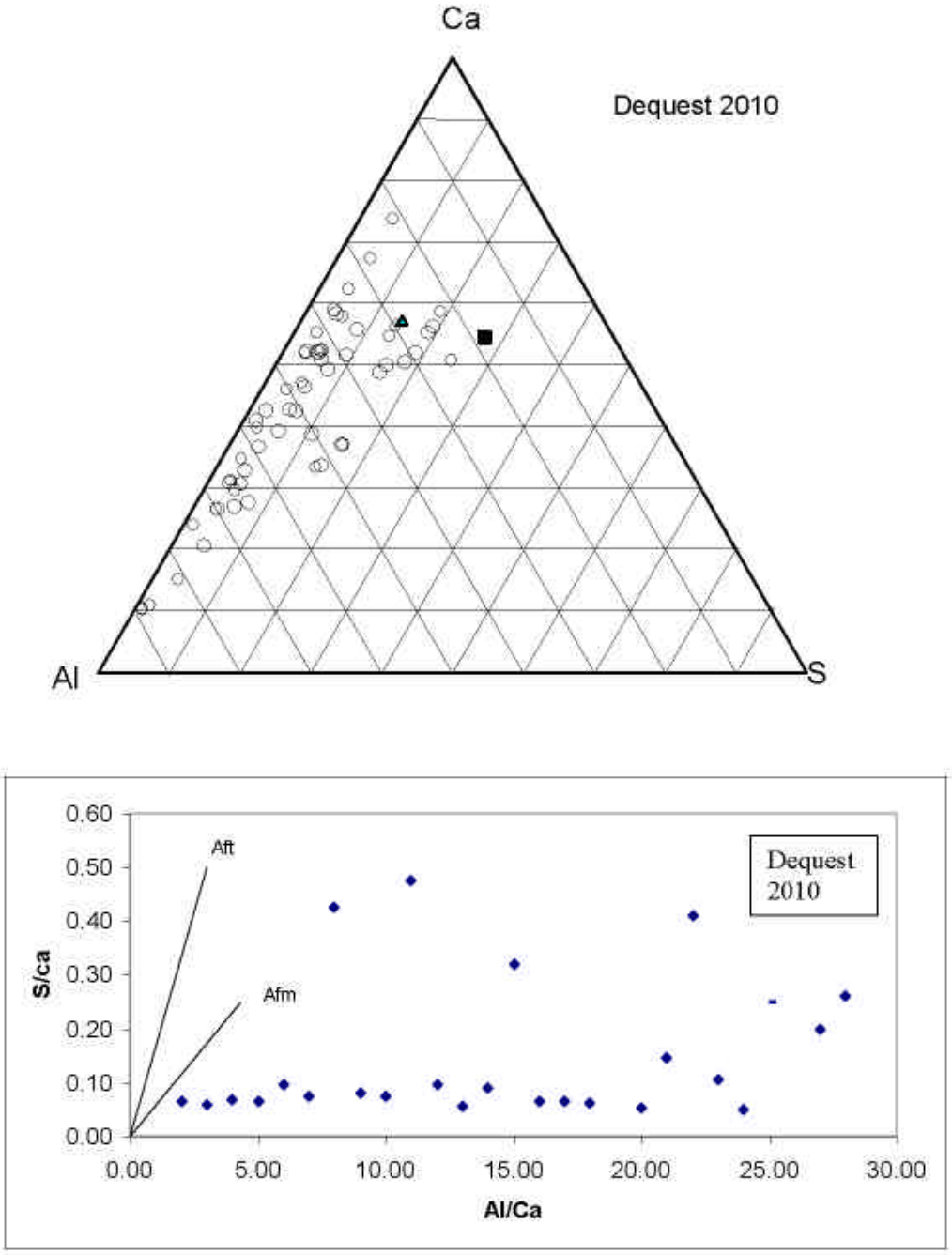

Fig. 9. Triangular diagram and atomic ratio plot of void-fillings substances, Na_2SO_4 + 0.01% Dequest 2010 (semiquantitative analyses). In the triangular diagram, the solid square = ettringite and the solid triangular = monosulfate composition. In the atomic ratio plot, AFt = pure ettringite, and AFm = pure monosulfate; CSH is calcium silicate hydrate. Note that the analyses do not plot between the AFt and AFm lines but rather indicate a very low sulfur-bearing material that cannot be either ettringite or monosulfate or a mixture of the two.

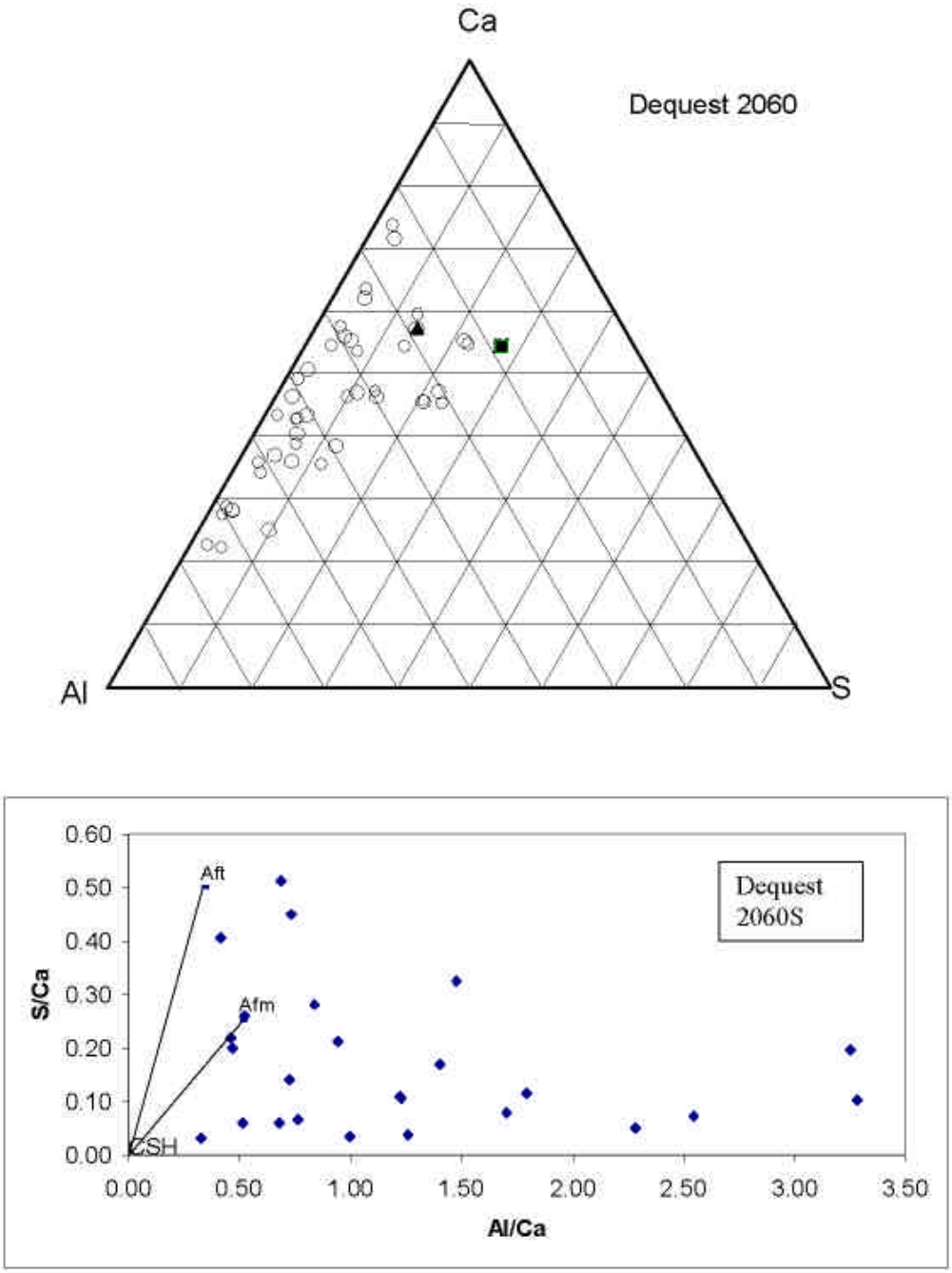

Fig. 10. Triangular diagram and atomic ratio plot of void-fill substances, Na_2SO_4 + 0.01% Dequest 2060 (semiquantitative analyses). In the triangular diagram, the solid square = ettringite and the solid triangle = monosulfate composition. In the atomic ratio plot, AFt = pure ettringite, and AFm = pure monosulfate; CSH is calcium silicate hydrate. Note that most of the analyses do not plot between the AFt and AFm lines but rather indicate a low sulfur-bearing material that cannot be either ettringite or monosulfate or a mixture of the two.

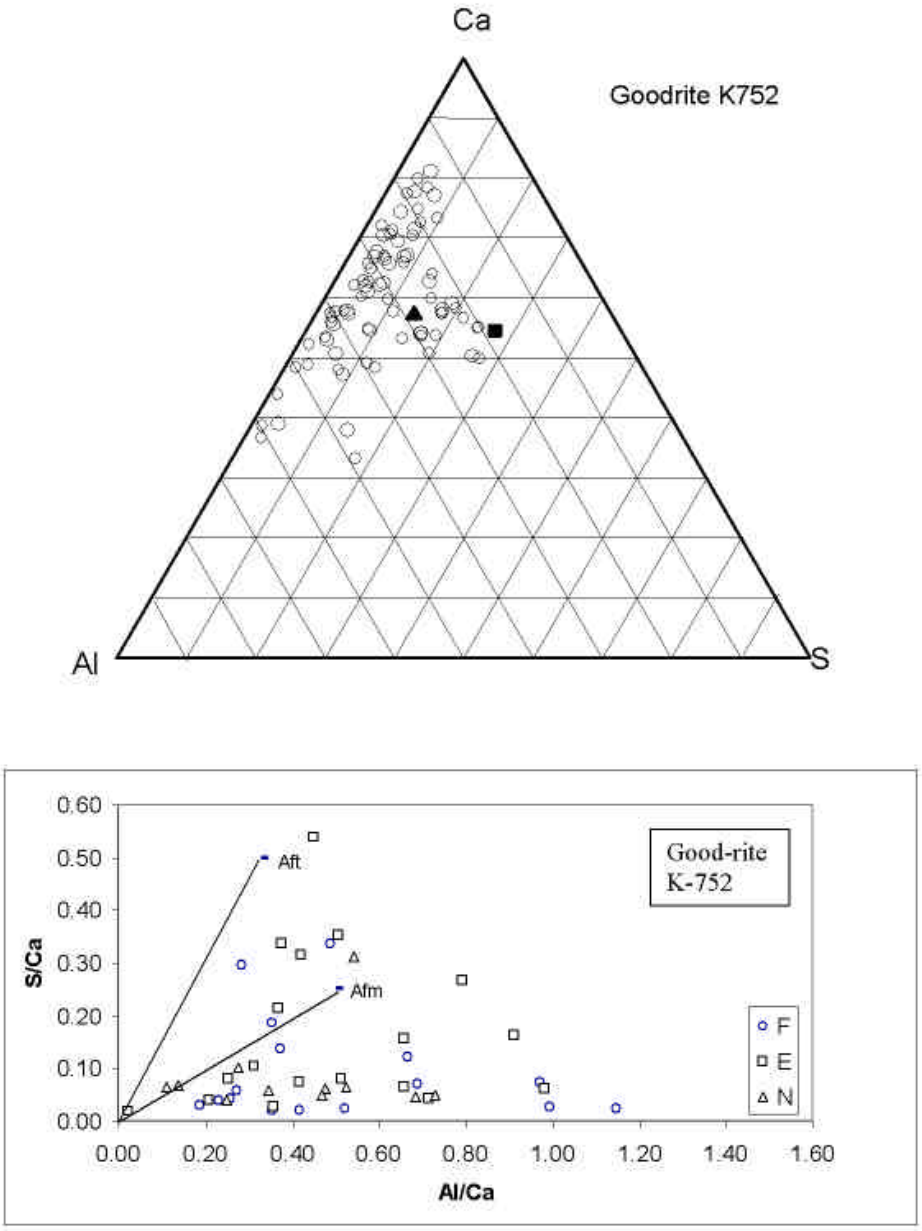

Fig. 11. Triangular diagram and atomic ratio plot of void-fill substances, Na_2SO_4 + 0.01% Good-rite K-752 (semiquantitative analyses). In the triangular diagram, the solid square is ettringite and the solid triangle represents monosulfate compositions. In the atomic ratio plot, AFt is pure ettringite, and AFm is pure monosulfate. CSH is calcium silicate hydrate. Note that most of the analyses do not plot between the AFt and AFm lines but rather indicate a very low sulfur-bearing material that cannot be either ettringite or monosulfate or a mixture of the two.

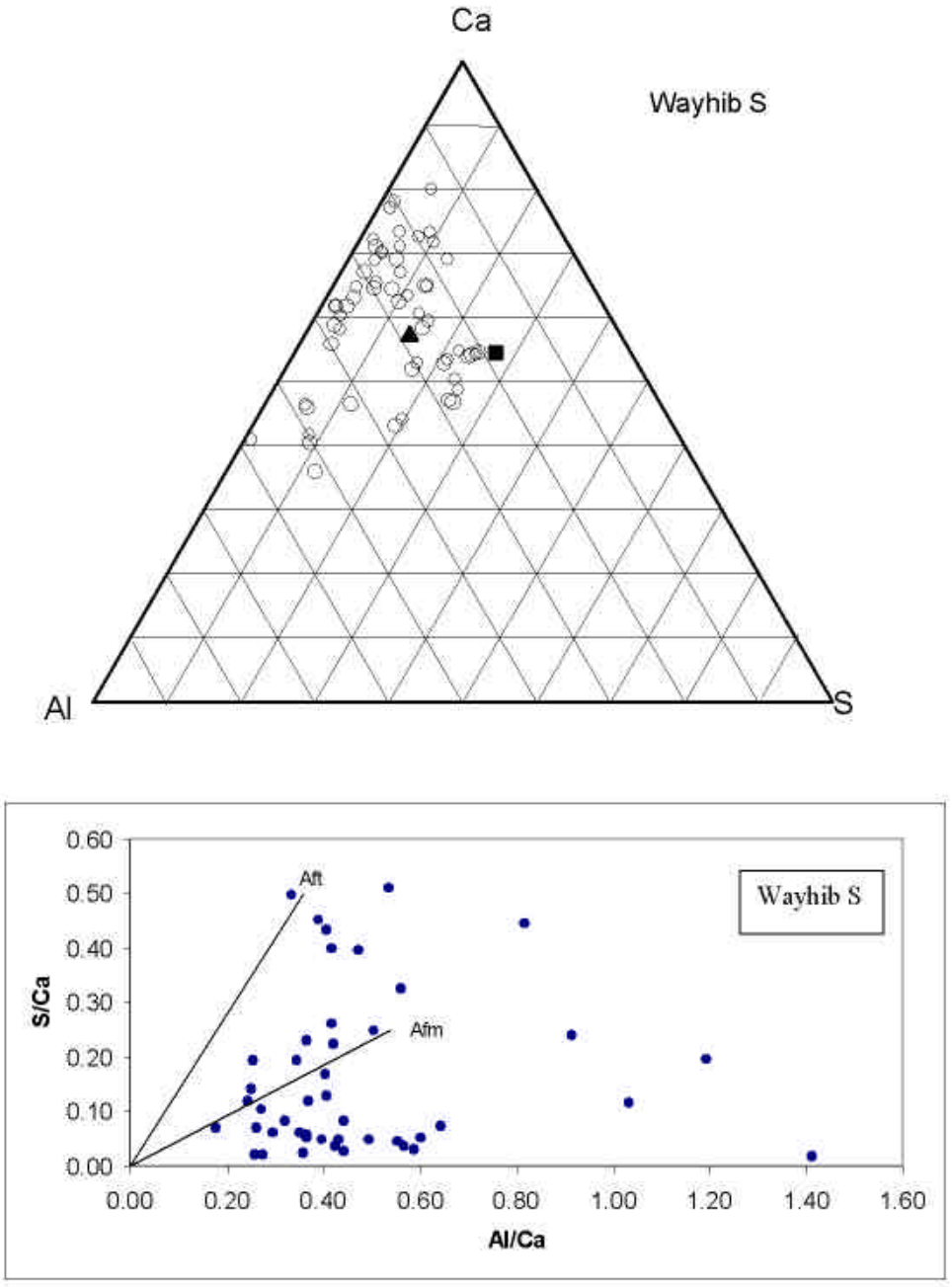

Fig. 12. Triangular diagram and atomic ratio plot of secondary mineralization in void-fillings. Na_2SO_4 + 0.01% Wayhib S (semiquantitative analyses). In the triangular diagram, the solid square is ettringite and the solid triangle represent monosulfate compositions. In the atomic ratio plot, AFt is pure ettringite, and AFm is pure monosulfate. CSH is calcium silicate hydrate. Note that most of the analyses do not plot between the AFt and AFm lines but rather indicate a very low sulfur-bearing material that cannot be either ettringite or monosulfate.

compositions are close to that of ettringite. A few results that plotted at high Ca/low S in the ternary diagram appear to be intermixed with CSH. It should be pointed out, however, that a large deviation in Al and Ca could be partly caused by analytical constraints. EDAX microanalysis is a semi-quantitative method, and errors may result from differences in calibration of standards, thickness and geometry of the measurement samples, acquisition time, and acceleration voltage. The precision of repeated measurements is very high but the accuracy is moderately low (personal communication with Straszheim, 1999).

SEM/EDAX views of typical void-fillings produced by sodium sulfate treatment without added inhibitor are shown in Figure 7, and analyses of void-fillings are shown in Figure 8. Older concrete samples chiefly contain phases that are close to the ettringite (AFt) composition, and a few that are close to the monosulfate (AFm) composition. Newly-made concretes show wider variation in composition than the old concrete. Part of the variation in composition may result from early termination of the experiments, which occurred after 18 cycles when cracking and paste softening became evident. Upon sulfate attack, unstable monosulfate is the first reaction product and later it transforms to the stable ettringite in the presence of sufficient sulfate (Cohen 1983a; Diamond 1996). The most likely explanation for the wide variation in phase compositions in newly made concrete is that there was not enough time for complete transformation to ettringite. Upon sulfate attack, abundant Al and Ca are produced by the decomposition of C_4AH_x and C-S-H phases. Unstable monosulfate forms as a result of the decomposition, then later transforms to ettringite by further replacement (topochemical) reactions with sulfate solutions. Insufficient reaction time allows the coexistence of a variety of early-forming, metastable phases with high Al and Ca, in addition to monosulfate and some ettringite.

Some of the variation in sulfoaluminate phases may also result from progressive changes in the chemical compositions of reacting solutions migrating through the concrete. These changes may affect monosulfate and ettringite stability relationships. When pore solutions are highly Al-rich, the monosulfate is stable and ettringite is unstable, but when the pore solutions are highly SO_4^{2-}-rich, ettringite is stable and monosulfate is unstable (Day 1992). Progressive and also local variations in pore solution compositions during the course of experiments might result in different minerals or different ratios of minerals.

The most extreme changes in mineral formation occurred in the presence of the two phosphonate inhibitors. In all three types of concretes (newly-made, older durable, and older non-durable types), void-filling materials produced by the phosphonate inhibitor Dequest 2010 consist of Al and Ca, and contain no or very low sulfur content. The ternary diagram and atomic ratio plots (Figs. 9, 10) confirm that only minor amounts of monosulfate and ettringite formed. Void-filling materials produced by the phosphonate inhibitor Dequest 2060 have a morphology and composition (Fig. 10) similar to that of materials formed in the presence of Dequest 2010. However, Dequest 2060 seems to favor minerals that are slightly enriched in sulfur content (although results of Part II experiments show that it is generally a more effective inhibitor for ettringite under solution growth conditions than Dequest 2010). Both inhibitors are effective in the inhibiting growth of sulfoaluminate phases. In the absence of inhibitor ions, when sulfate solutions progress into the concrete, the sulfate ions attack paste components to produce Ca- and Al-rich pore solutions that would normally react with sulfate ions to precipitate monosulfate and ettringite. Phosphonate ions apparently prevent precipitation of sulfate-rich materials and allow the precipitation Al- and Ca-rich gel phases (as discussed in Part II of this report) of variable

composition that would normally not be preserved in the presence of sulfate. Later, these gel phases crystallize into low sulfur void-filling material of variable composition.

The void-filling materials produced by addition of the polyacrylate inhibitor (Good-rite K752) also show well-developed chemical compositions and composition zoning in voids. A mixture of abundant monosulfate (AFm), small amounts of ettringite (AFt), and a highly Al-rich phase occur at the edge of voids. A high Ca- and low Al-phase without detectable sulfur is present in the center of the voids. The ternary diagram and atomic ratio plot confirm the presence of a minor amount of AFm and AFt (Fig. 11).

The morphology and occurrence of void-filling material produced by the addition of the phosphate ester (Wayhib S) inhibitor are similar to those produced by polyacrylate. Accicular ettringite crystals are clearly visible in SEM views. Analytical data show that larger amounts of ettringite formed in the presence of Wayhib S than in experiments with other inhibitors and the high Al-phase is relatively minor in abundance (Fig. 12). Expansion data, however, are equivocal. Wayhib S reduced expansion more than the phosphonates for newly made (Fig. 3) and durable concrete (Fig. 4) but less for nondurable concrete (Fig. 5) in freeze/thaw experiments. For wet/dry experiments, however, Wayhib S was less effective in reducing expansion for all concretes than the two phosphonates (Figs. 3-5). The different relative effectiveness of freeze/thaw and wet/dry experiments suggests that Wayhib S may be less effective than the phosphonates for reducing excessive ettringite precipitates that normally should form during drying cycles, as discussed earlier, or that Wayhib S, modifies ice crystallization in a way to reduce freeze expansion.

Compositional zoning in void-fillings were observed in all of the inhibitor-mediated samples, but were less evident with the two phosphonates, and somewhat less evident with the

polyacrylate Good-rite K752 than with the phosphate ester Wahib S. Zonation probably results from kinetic effects during experiments. The earliest mineralization occurs on the outside edges of voids, near to the paste, and the minerals in the center of voids were the last to form. Inhibitor molecules are large polymers and probably migrate into concrete slower than small SO_4^{2-} ions. Early in an experiment, there will be no or little inhibitor molecules at sites of mineral nucleation and growth, so ettringite and/or monosulfate will precipitate. Later in experiments, the inhibitor molecules will have diffused to sites of potential ettringite nucleation and will prevent or reduce additional AFt/AFm precipitation, thus causing the observed pattern of greater AFt/AFm on the outer rim of voids compared to the void centers.

Second Series of Experiments – Concentration Effects of Crystallization Inhibitors

Introduction

In the second set of experiments, the effect of inhibitor concentrations on crystallization effectiveness were evaluated using Dequest 2060, and wet/dry cycling. Seven different concentrations were tested: 5%, 1%, 0.1%, 0.01%, 0.001%, 0.0005% and 0.0001%. Control experiments with sodium sulfate and no inhibitor were also included. Although in the first series of experiments, Dequest 2010 was a slightly more effective crystallization inhibitor than 2060, Dequest 2060 was chosen because Coveney et al. (1998) concluded that longer chain phosphonates such as Dequest 2060 should be more effective than shorter chain chemicals such as Dequest 2010, and because Dequest 2060 is generally considered a superior inhibitor by its manufacturer (Monsanto representative, pers. comm. 1998). The solution growth experiments (Part II) also suggest that Dequest 2060 was more effective than Dequest 2010 in preventing ettringite formation in the absence of concrete material. Duplicate experiments were performed;

Table 4. Visually-detectable effects on concrete blocks after 40 wet/dry cycles with different concentrations of Dequest 2060

Type of Experiment	Dequest 2060 Concentration	Cracks	Surface Roughness	Other Characteristic Features
Na_2SO_4	N/A	++	+	Slightly darker color
Without change solution during experiment	5 %	no	++	Brown color
	1 %	no	+	Yellowish brown color
	0.1 %	no	+	Slightly darker color
	0.01 %	no	+	Slightly darker color
	0.001 %	no	+	Slightly darker color
	0.0005 %	no	+	Slightly darker color
	0.0001 %	+	+	Slightly darker color
With change solution after 5 cycles	5 %	no	++	Brown color
	1 %	no	+	Pale brown color
	0.1 %	no	+	Slightly darker color
	0.01 %	no	+	Slightly darker color
	0.001 %	no	+	Slightly darker color
	0.0005 %	no	+	Slightly darker color
	0.0001 %	+	+	Slightly darker color

+ = some effect. ++ = much effect.

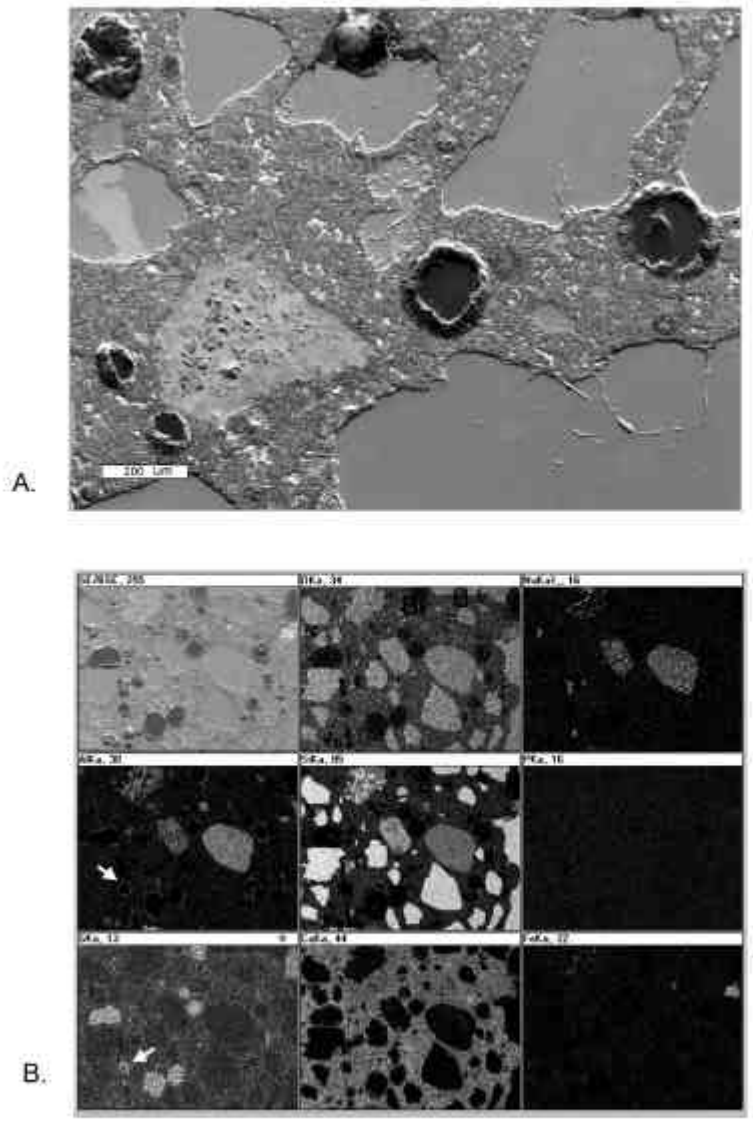

Fig. 13. SEM/EDAX images of void-fill substances, Na_2SO_4 + 0.0001% Dequest 2060. A. SEM image. B. EDAX element map. Note in B. that abundant Al and S (shown by arrows) occur in the void-filling material.

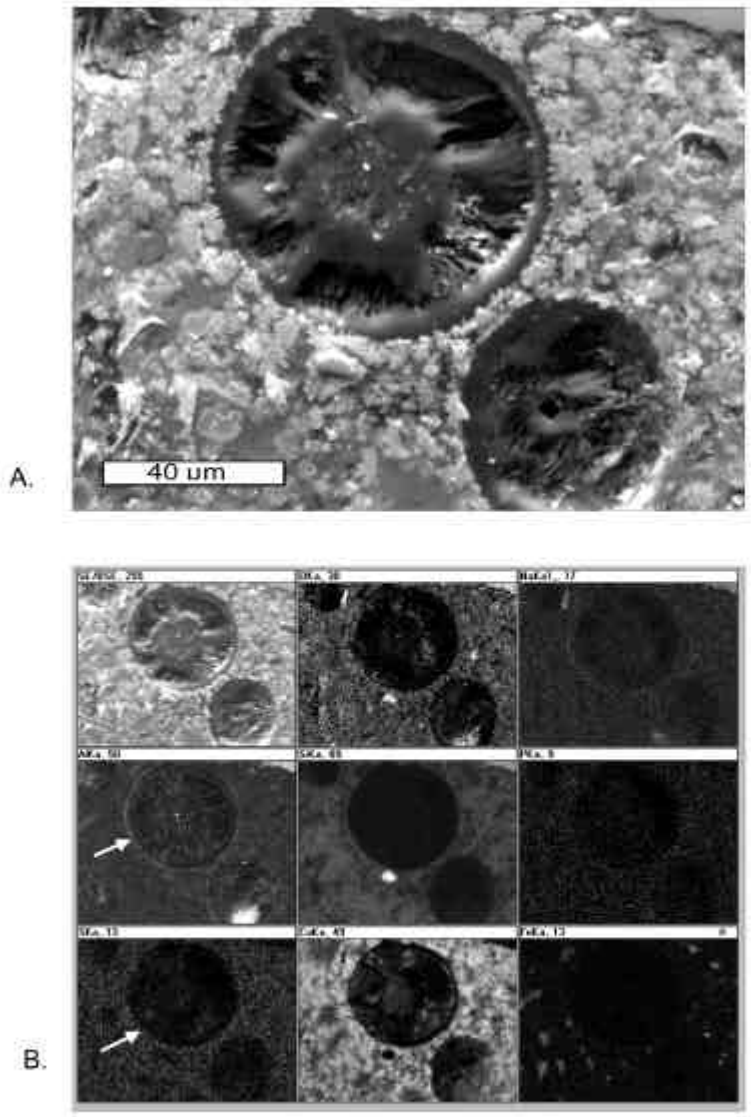

Fig. 14. SEM/EDAX images of void-fill substances, Na_2SO_4 + 0.001% Dequest 2060. A. SEM image. B. EDAX element map. Note in B. that Al and S (shown by arrows) occur only in very small amounts in the void-filling material.

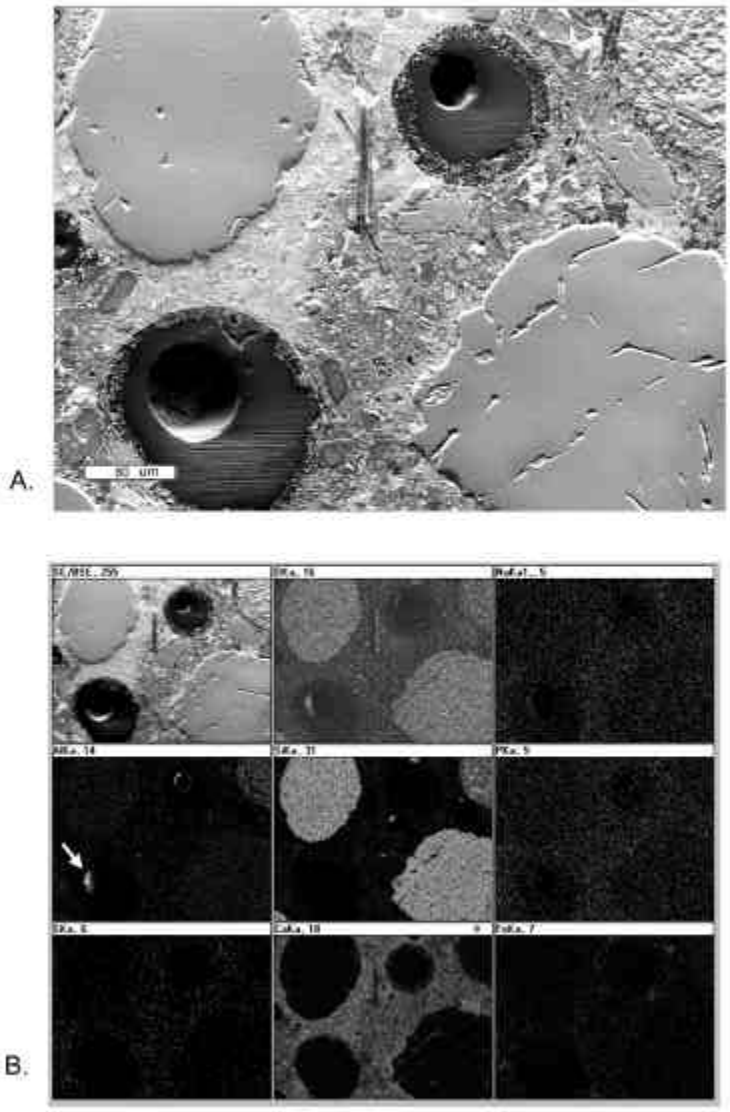

Fig. 15. SEM/EDAX images of void-fill substances, Na_2SO_4 + 0.01% Dequest 2060. A. SEM image. B. EDAX element map. Note in B. that abundant Al occurs in very small amounts (shown by arrow) and S is not detectable in void-filling material.

one set was terminated after 23 cycles for petrographic microscope study, and the other set was concluded after 36 cycles.

Visually-Evident Concrete Deterioration

Typical deterioration features of the concentration experiments are listed in Table 4. With sodium sulfate and no crystallization inhibitor, deterioration, which is characterized by abundant expansion cracking, was identical to deterioration in concrete samples of series I experiments. With Na_2SO_4 + inhibitors, cracking only occurred in samples subjected to sulfate attack with the lowest concentration of 0.0001 % crystallization inhibitor. No visually-detectable cracks were observed in any of the other samples. Thus, inhibitor concentrations <0.0001% probably will not significantly inhibit ettringite nucleation and growth in concrete. Samples treated with 5% crystallization inhibitor developed marked surface roughening and edge crumbling, thus showing that too much inhibitor may be deleterious to concrete. These effects can result from complexing of concrete Ca with inhibitor molecules and resultant dissolution of the concrete.

In series II experiments, two methods for evaluating inhibitor effectiveness and decomposition rate were used. With the first method, a specific concentration of Dequest 2060 was added to the sulfate solution at the beginning of an experiment and the concrete was continuously cycled without changing the solution. With the second method, the original solution was decanted after 6 cycles and replaced with fresh solution at the same sulfate and inhibitor concentration. If Dequest 2060 significantly decomposed over the duration of experiments, then the second method should result in less cracking of the concrete blocks than occurred in experiments in which same solution was used for the entire time interval. No

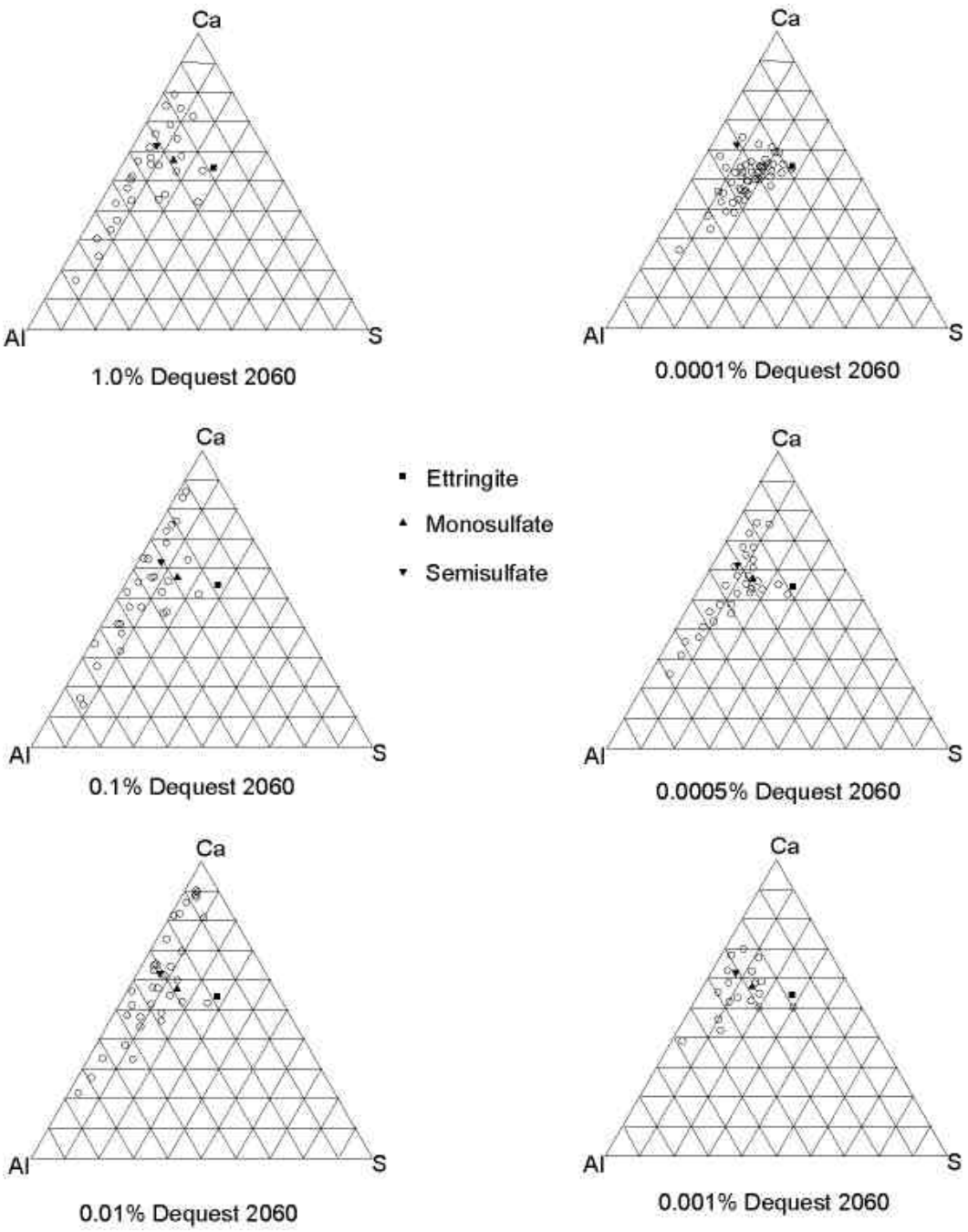

Fig. 16. Triangular diagram in terms of Ca, Al, and S for void-fills produced by series II experiments, at different concentrations of Dequest 2060. This series of diagrams shows the effects of concentration on void-fill compositions. See Fig. 8 for comparison to void-fill compositions produced by $NaSO_4$ treatment. Note that the amount of S is reduced in all experiments, except at the lowest concentration of 0.0001%.

distinguishable differences in the visually-detectable deterioration were found in comparing the two methods, except that slightly darker color changes developed on concrete blocks using the second method (fresh inhibitor solution changes). Apparently Dequest 2060 is resistant to decomposition for considerable amounts of time, even at the relatively high temperatures of 58^{o}C that were used for all experiments.

Microanalysis Results

With sodium sulfate treatment and no inhibitor, abundant void-filling material formed in the cement paste. Data in Figure 16 cluster near AFt/AFm compositions showing that the materials are chiefly sulfoaluminate phases with variable amounts of Ca and Al. With increasing concentration of inhibitor, there is a progressive change in the character of new mineral matter. Even at 0.0001% inhibitor, void-filling materials exhibit a marked difference compared to that produced in the absence of inhibitor (Fig. 8) in that the void-fill at 0.0001% compositions are less clustered near the AFm/AFt locations. EDAX element maps of filling material produced with 0.0001% Dequest 2060, however, show abundant S, Al, and Ca (Fig. 13). With 0.0005% inhibitor concentration, small amounts of sulfoaluminate phase that probably can transform into ettringite are present, but the discrepancy in compositions between these phases and normal ettringite is more marked than with 0.0001% inhibitor. At = 0.01%, the differences between ideal ettringite and the void-filling material are more discernible (Fig. 20). SEM/EDAX plots show that the void-filling material is very low in sulfur (Figs. 13-15). Inhibitor concentrations of 0.001% and 0.01% still allow the formation of significant amounts of void-filling material but most of the void-filling materials are Ca- and Al-rich materials and that only very small amounts of monosulfate and ettringite are present. In concrete samples treated with inhibitor

concentrations of 0.1% and 1.0 %, the quantity of new void-filling materials was greatly reduced. Surprisingly, experiments with 5.0% inhibitor concentration, the highest concentration used, produced more void-filling materials than 0.1% and 1% concentrations. Analyses show that the filling materials produced with 5% Dequest 2060 are enriched in Si but have composition ranges of Ca, Al, and S that are similar to those produced at lower inhibitor concentrations.

PART II

ETTRINGITE SOLUTION GROWTH EXPERIMENTS

INTRODUCTION

The results of Part I documented that the presence of crystallization inhibitors during sulfate attack reduced both new ettringite formation and concrete expansion/cracking. However, those experiments are unable to give any information on the mechanisms by which the inhibitors reduce ettringite formation. Therefore, solution growth experiments were conducted: (1) to assess the relative ettringite-inhibiting ability of four selected scale-inhibitors; (2) to determine the quantity of each inhibitor necessary to inhibit ettringite formation; (3) to study the mechanisms by which the inhibitors were operating; and (4) to determine the duration of inhibitor effectiveness.

Additional experiments were performed to determine the roles of reactant concentration, pH, and environmental chemical additives. Nearly 350 chemical additives of varied molecular and ionic composition, many of which occur in the concrete environment, were tested to determine their effects on ettringite nucleation and morphology. Factors governing the formation of calcium aluminate gel phases, AFm (alumino ferrite monosulfate) and AFt (alumino ferrite trisubstituted = ettringite) phases were also investigated.

DETERMINATION OF CRYSTAL GROWTH METHOD

Most past studies of ettringite formation (Mehta 1973, Odler and Abdul Maula 1984, Baussant et al. 1989) involve the reaction of solid components such as C_3A or $C_4A_3\overline{S}$, $C\overline{S}$, and CH with water in a changing mixture containing many phases. In order to isolate and study only

those reactions pertaining to the nucleation and growth of ettringite, it was decided to grow the crystals from liquid solutions. Several previously-used methods were tested.

1. Method of Strubble and Brown (1984)

A. $Al_2(SO_4)_3$ solution: 340.8 g. $(Al_2SO_4)_3 \cdot 18H_2O$/L

B. $Ca(OH)_2$ solution: dissolve 340.8 g. CaO in 890 ml 10% sucrose solution. 10% sucrose solution: 100 g. sucrose/L.

Add 10 ml solution A to 225 ml solution B and stir for two hours.

Result: the concentration of reactants was too high. The time for the onset of crystallization was too short for changes in nucleation rates to be studied. The resulting crystals were too small to see without high magnification SEM. Over time, the solution developed a brown color and fluoresced green in short wavelength UV, indicating sugar polymerization that could possibly interfere with experiments.

2. Method of Mylius (1933) described in Taylor (1990)

A. Calcium hydroxide solution: 1.2 g CaO/1.2L (1g/L)

B. Gypsum (saturated) solution: Stir excess $CaSO_4 \cdot 2H_2O$ in 1 L distilled water, 12 hours; filter.

C. $Al_2(SO_4)_3 \cdot 18H_2O$ solution: 2.317 g/L.

Combine [72ml A + 31.8 ml B] and add 46.2 ml C.

Result: the induction time (time between addition of C and the first appearance of crystals) was ≈ 45 sec – long enough for induction studies. This method was not reliable in producing ettringite. Calcium aluminate monosulfate

(AFm/monosulfate) sometimes formed. SEM magnification of 2,000x was needed to see the crystals.

3. Method developed for this study

A. Calcium hydroxide solution (saturated ≈ 1.85 g/L): Add excess CaO, stir 2 hr. and filter.

B. $Al_2(SO_4)_3 \cdot 18H_2O$ solution: 2.317 g/L

Combine 75 ml A +75 ml B.

Results: Quantities are not stochiometric but induction time is good (≈ 1 min.) and the method is reliable in producing ettringite crystals that are visible with a light microscope (45x – 320x). The entire reaction occurred in 15 minutes, so carbonation effects are of minimal importance.

EXPERIMENTS

All solutions were made with double-distilled, deionized water, and filtered with Whatman #42 paper to remove all crystalline material. Calcium hydroxide solution was stored in a thick polyproplyene container with a bottom tap. Air that entered the container was bubbled through a carbon dioxide lock containing limewater [$Ca(OH_2)$] to remove CO_2.

Ten percent stock solutions of the four liquid inhibitors tested were made by weighing the quantity of inhibitor before dilution. For example, for Dequest 2060 (SG=1.40), a 10% solution contained 1.4g/100mL or 140,000 ppm. One ml of 10% stock solution A contains 0.140g Dequest 2060. The specific gravities of the other inhibitors tested are Good-rite K527 (1.2), Dequest 2010 (1.45), and Wahib S (1.5). Highly acidic solutions were diluted half-way, adjusted to pH = 8 with 20 ml NaOH, and then diluted to volume.

Experiments were conducted in transparent hard plastic containers of square cross-section with inner diameters 5.3 cm x 5.3 cm x 12 cm height (Fig. 17, apparatus). The containers were cleaned with 28% HCl and rinsed with distilled water after each use.

Solution in the reaction cell was stirred with a Teflon-covered magnetic stir bar. To lessen reflection effects, the cell face was angled toward a beam of light from a fiber optic lamp source. Light passing through the container entered a Beckman photocell and its intensity changes during the duration of the experiment were monitored by passing the photocell output to a high-gain amplifier and then to an analog/digital converter board housed in a Dell P180 microcomputer. Resultant data were imported into Microsoft Excel and graphed.

The onset of crystal formation was marked by a drop in intensity (transmittance) of the beam of light passing through the plastic cell because the newly-formed crystals blocked some of the light beam. A rough estimate of the rate at which new crystals formed could be ascertained by the rate and amount of transmittance drop over a set period of time.

According to crystallization theory, when crystallization first begins, a small number of atoms come together to form 'precritical nuclei' that are in equilibrium with the surrounding solution. The pre-critical nuclei have an equal chance of dissolving back into solution, or of growing to crystal size. When a crystallization inhibitor is added to the solution, it tips the balance toward dissolution and a longer time is required for a crystal to form. The induction time is said to increase. This increase is measured by a delay in initial transmittance drop.

A good crystallization inhibitor is one that will prevent crystallization for the longest time when present in the smallest quantity. Although many commercial inhibitors are used to inhibit

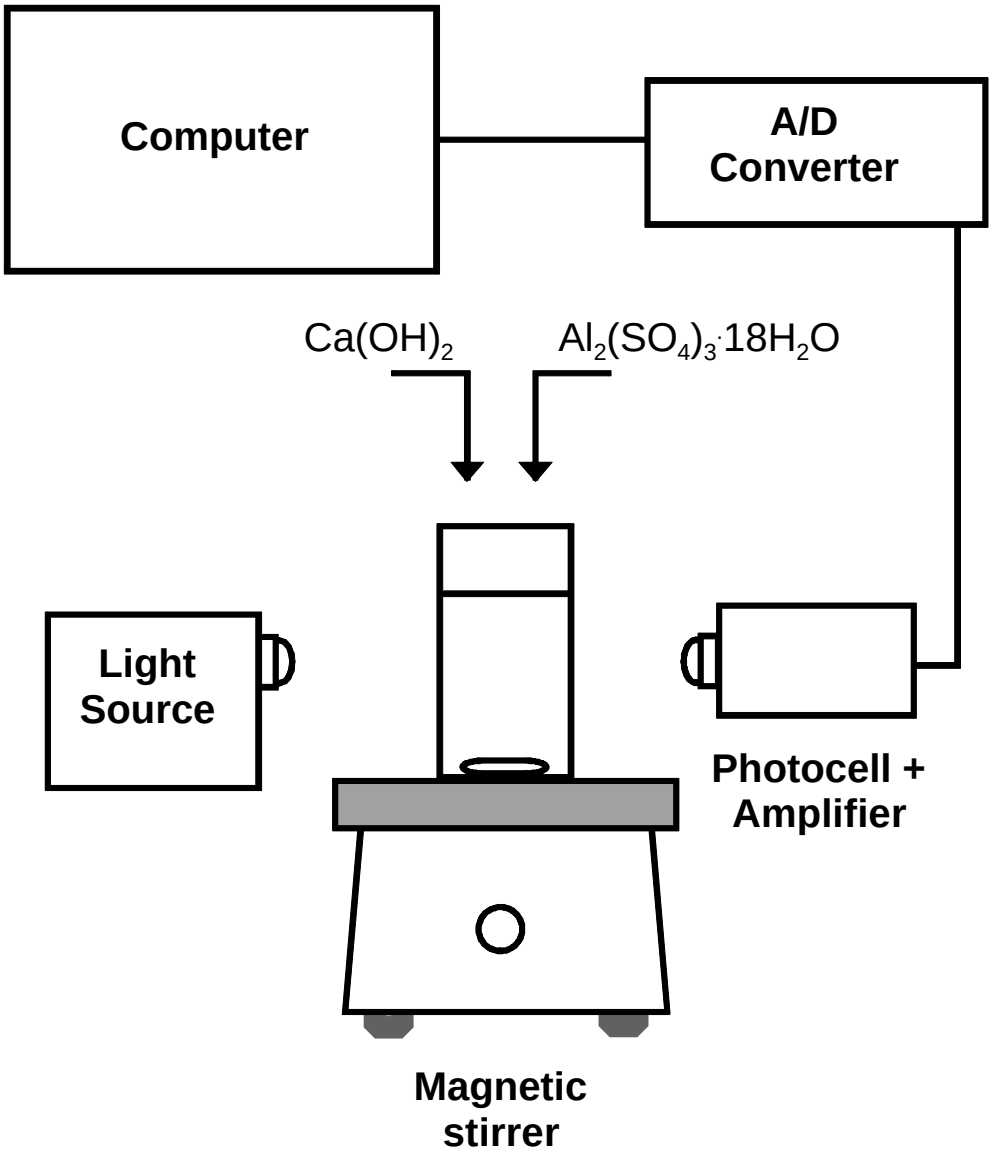

Fig. 17. Apparatus used for ettringite growth from solution.

a number of minerals, the best inhibitor of each individual mineral must be experimentally-determined. It was not our purpose to find the very best possible inhibitor (Coveney et al. 1998) but to find the best inexpensive commercially available inhibitor.

Figs. 18 - 21 show the optical transmittance change over time (in minutes) produced by varying concentrations of the four inhibitors tested. The results of only one of several replicate experiments are shown. It can be seen that the inhibitors not only change the times of the initial drop in transmittance (induction time = i), but they also change the crystallization rate (x) at which crystals form and grow (the slope at which the curves approach their equilibrium lowest horizontal portion). Minor cyclic fluctions on the curves are attributed to solution perturbations from the magnetic stir bar.

At the end of each test, solution pH was measured to ascertain that it was within the pH range 11.0 ± 0.1; well within the pH stability range of 10.5 – 13.0 of ettringite (Damidot and Glasser 1973). The solution was filtered immediately and the precipitate was characterized by X-ray diffraction analysis with CuK_{α} radiation at 35 KV and 20 mA. Patterns were collected between 5.0^{o} and 50.0^{o} 2θ using an angle step of 0.05" and a dwell time of 0.5 sec. Crystals were not crushed before X-ray to avoid carbonation and loss of water from highly-hydrated phases. The crystals were also examined with a petrographic microscope and their morphology or outward appearance [needles: length, solitary/radiating, pointed/not; plates: size, single/clustered, 3/6 sides], and the relative amount of each phase was noted. The optic

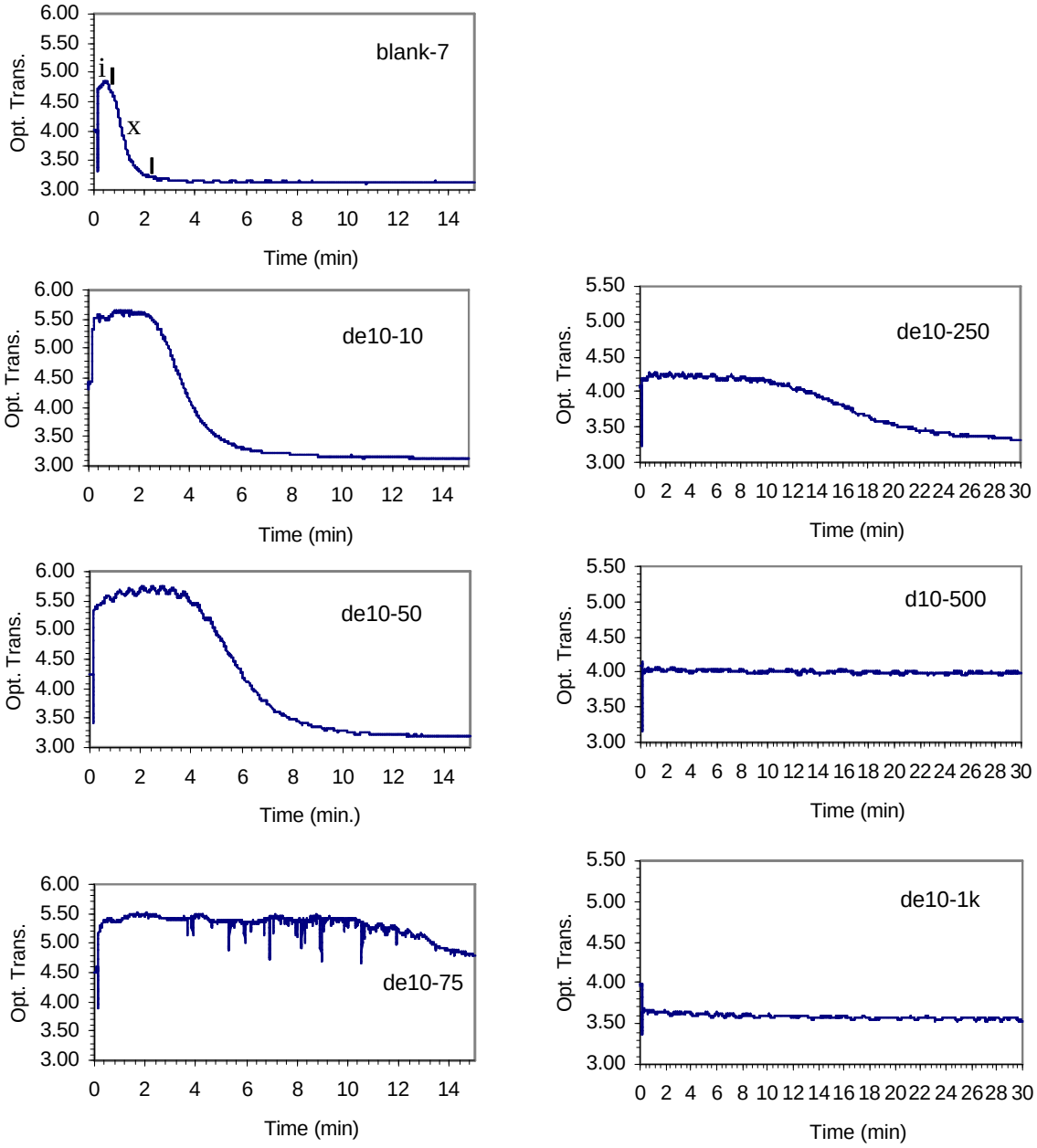

Fig. 18. Changes in optical transmittance over time in solutions in which 0, 10, 50, 75, 250, 500, and 1,000 µl of Dequest 2010 were added. i = induction time, x = crystallization time. Increasing concentration of the inhibitor increased the time before crystal formed (the induction time, i shown in the uppermost diagram of 'blank 7'). Note that inhibitor concentrations of 500 µl and 1000 µl completely prevent crystallization – an amorphous colloidal gel formed and was stable for about one month, after which the gel converted to crystalline ettringite.

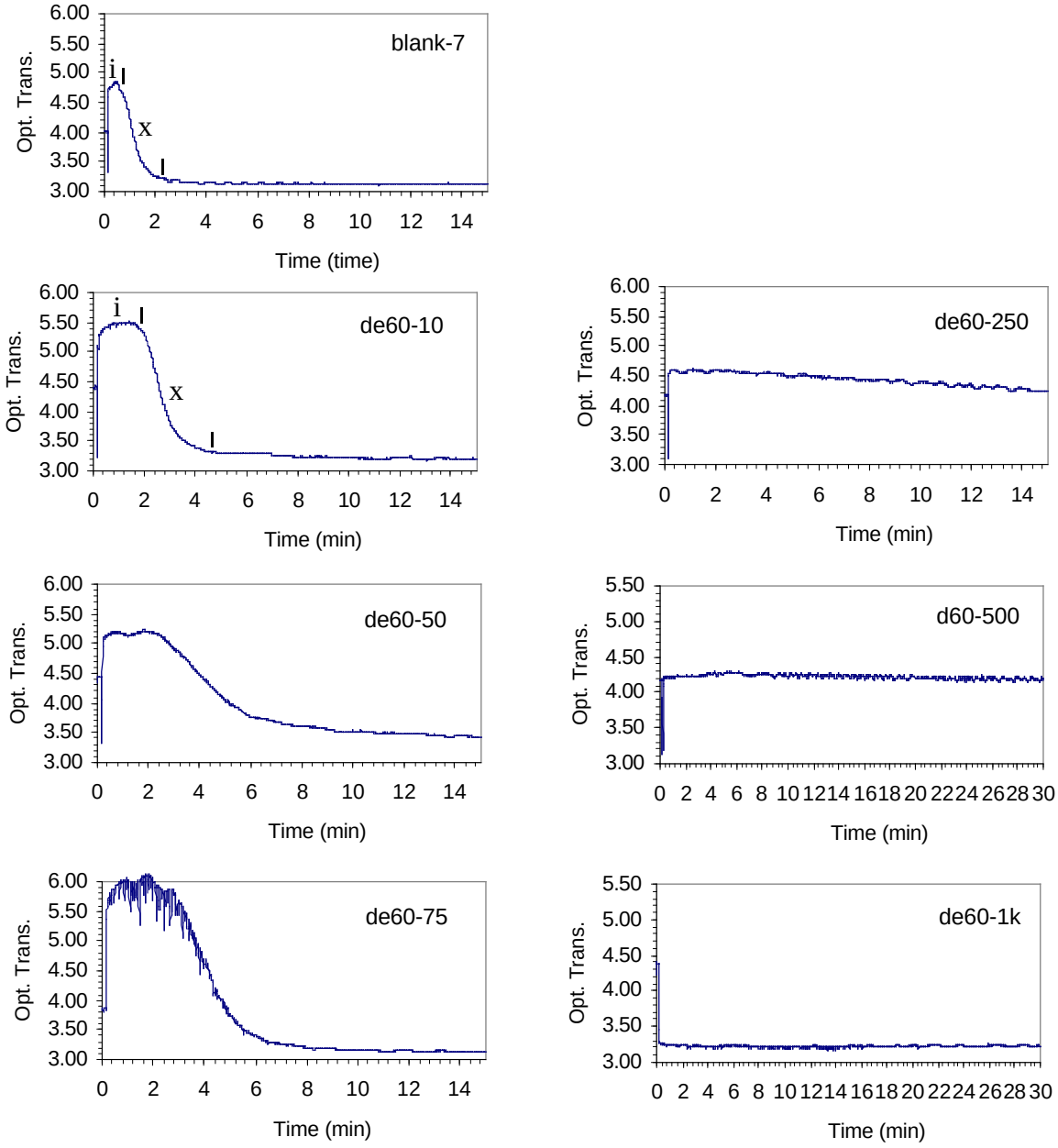

Fig. 19. Changes in optical transmittance over time in solutions in which 0, 10, 50, 75, 250, 500, and 1,000 µl of Dequest 2060 were added. i = induction time, x = crystallization time.

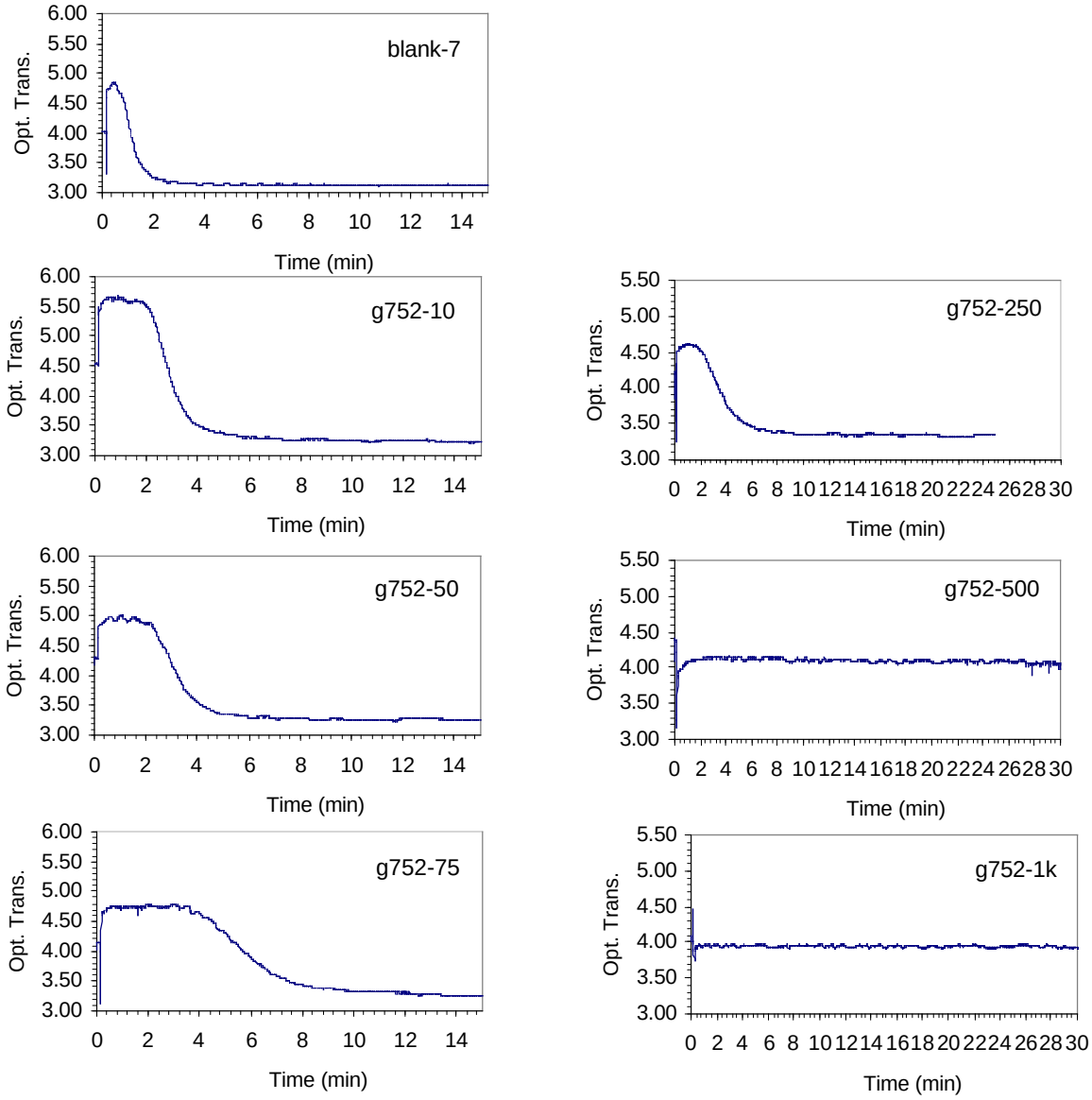

Fig. 20. Changes in optical transmittance over time in solutions in which 0, 10, 50, 75, 250, 500, and 1,000 µl of Good-rite K752 were added.

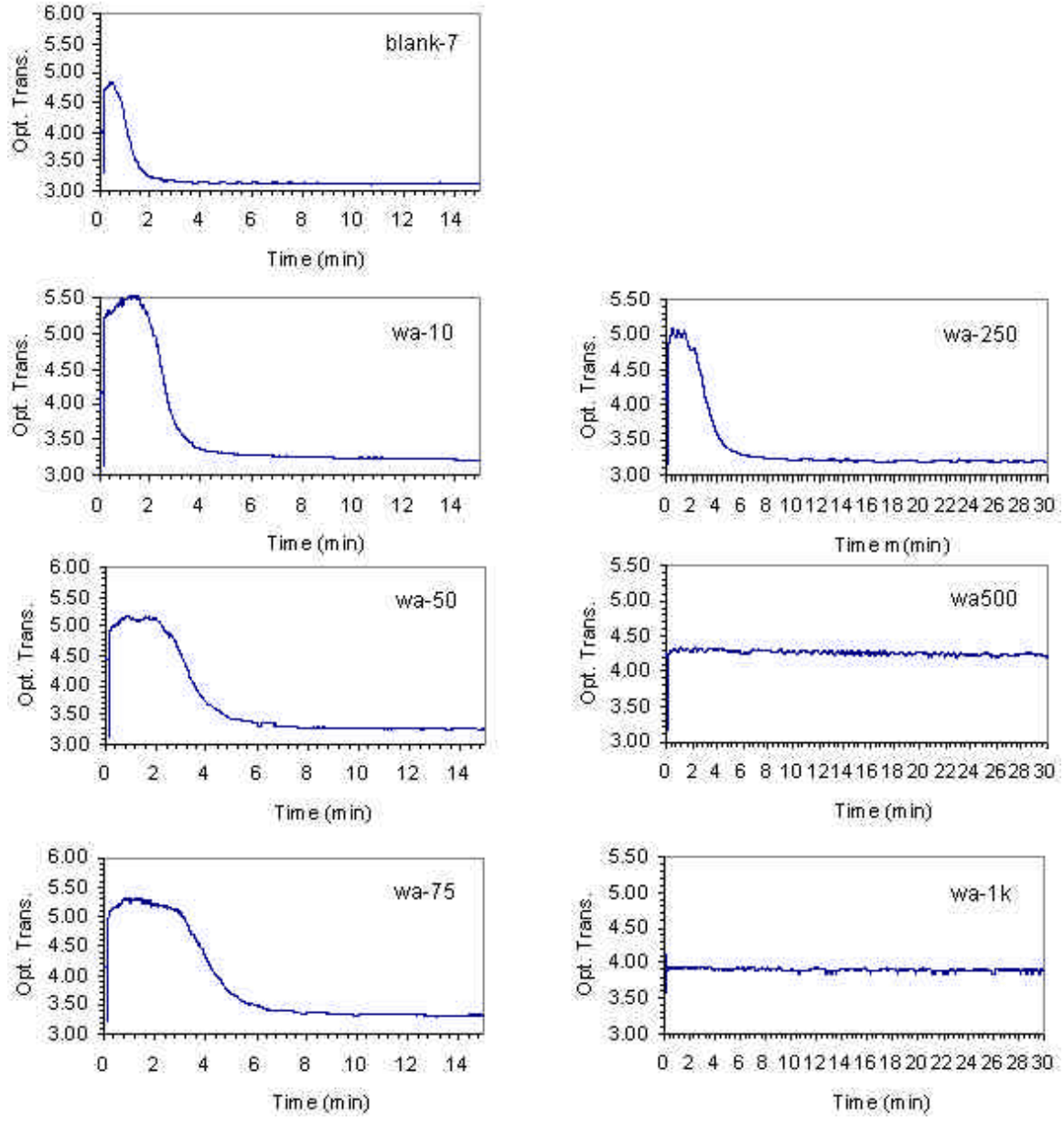

Fig. 21. Changes in optical transmittance over time in solutions in which 0, 10, 50, 75, 250, 500, and 1,000 µl of Wayhib S were added.

orientation and sign of needle-like crystals were determined. Crystals with unusual morphology were tested with 10% HCl to determine if they were calcium carbonate which was seen to form short 6-sided optically negative prisms that resemble short ettringite crystals. Low vacuum SEM and energy dispersive X-ray analysis (EDAX) were used when necessary to distinguish the identity of forms in multi-phase precipitates.

RESULTS

Results of the above tests are shown in Table 5.

Dequest 2010 (ethanol diphosphonate)

Ettringite was formed at all concentrations tested, so this chemical was not considered to be a good inhibitor of ettringite. Induction time (I) increased with concentrations of added Dequest 2010, indicating nucleation inhibition. Crystallization time also increased, and crystal size decreased with increasing inhibitor concentration, indicating that once crystals did form, their growth was somewhat inhibited. A gel was produced at concentrations of 500 µl and 1000 µl but the gels converted to ettringite within one month indicating poor inhibitor durability.

Dequest 2060 (5-phosphonic acid)

Induction time remained constant as inhibitor concentration increased but when crystals finally did nucleate, the thermodynamically more stable ettringite, was partly inhibited at 9.33 ppm (10 µl inhibitor) and the less stable AFm phase (monosulfate) formed also. The quantity of both phases was seen to decrease with increasing inhibitor concentration. At, and above a concentration of 233 ppm (250 µl inhibitor), a gel phase formed and no crystals were seen in samples kept for over one year, indicating very good inhibitor durability.

Table 5. Effect of commercial inhibitors on ettringite solution growth

µL	Dequest 2010 Diphosphonic Acid			Dequest 2060 5-Phosphonic Acid			Good-rite K752 Polyacrylic Acid			Wayhib S Phosphate Ester		
10	E 9.67 ppm	L.Amt. S.Sz.	I=2.2 X=4.8	E+M 9.33 ppm	L.Amt. L.Sz.	I=2 X=3	E 8 ppm	L.Amt. L.Sz.	I=3 X=3	E 15 ppm	L.Amt. L.Sz.	I=2 X=2.5
50	E 48.39 ppm	S.Amt S. Sz.	I=3 X=7	E+M 46.65 ppm	M.Amt. L.Sz.	I=2 X=6	M + E 40 ppm	L.Amt. L.Sz.	I=3 X=3	M 75 ppm	L.Amt. L.Sz.	I=2 X=4
75	E 72.53 ppm	S.Amt. V.S.Sz.	I=10 X=?	E+M 69.98 ppm	S.Amt. L.Sz.	I=2 X=6	E + M 60 ppm	S.Amt. L.Sz.	I=4 X=6	S 112.5 ppm	M.Amt. L. Sz.	I=2 X=6
250	E 242 ppm	S.Amt. V.S.Sz.	I=10 X=20	Gel +S/M (Tr) +E (Tr) 233 ppm	L.Sz. S.Sz.	I=2.5 X=?	S+M 200 ppm	V.S.Amt. S.Sz. (Spheres)	I=1.5 X=8.5	S + Gel 375 ppm	M.Amt. L.Sz.	I=1.5 X=6.5
500	M(Tr) +E(Tr) ? +Gel? E 483.5 ppm	Sm.Sz. V.L.Sz. L.Amt.	I=? X >1 mo.	Gel 466 ppm		I >1 yr.	Gel 400 ppm		I > 1 yr.	S + Gel 700 ppm	S.Amt. S.Sz. Poor XRD peaks.	I=?.
1000	E ? +Gel? E 966 ppm	 V.L.Sz.	I=? X >1 mo	Gel 932 ppm		I >1yr	Gel 800 ppm		I >1yr.	? Gel? E 1500 ppm	No XRD peaks	I=? X=15 days

E = ettringite $3CaO{\cdot}Al_2O_3{\cdot}3CaSO_4{\cdot}32H_2O$ M = monosulfate $3CaO{\cdot}Al_2O_3{\cdot}CaSO_4{\cdot}12H_2O$ L. = Large Amt. = Amount ?

S = semisulfate $3CaO{\cdot}Al_2O_3{\cdot}1/2CaSO_4{\cdot}1/2Ca(OH)_2{\cdot}12H_2O$ M. = Medium Sz. = Size ? = Converts to..

I = Induction Time (min.) X = Crystallization Time (min.) S. = Small V. = Very Tr. = Trace.

Good-rite K752 (polyacrylic acid)

Similar to the behavior of Dequest 2060, the induction time for crystal nucleation remained nearly constant with increasing Good-rite 752 concentration, but when crystals finally did nucleate, there was a change in the phases that formed. Ettringite nucleation was progressively inhibited and monosulfate nucleation was favored. At high concentrations (200 ppm or 250 µl), monosulfate nucleation was also inhibited and calcium aluminate semisulfate nucleation was favored. The size of crystals and the quantity of all crystals decreased with inhibitor increase. All phases were inhibited at and above a concentration of 400 ppm (500 µl) where a gel formed and persisted for over one year.

Wayhib S (3-phosphate ester)

Wayhib S inhibited nucleation of ettringite and monosulfate at a concentration lower than all other inhibitors. The crystal size of those hydrates was large indicating that once they did nucleate, their growth was not inhibited. At 113 ppm (75µl) Wayhib S, unstable calcium aluminate semisulfate was the only phase to nucleate; all others were inhibited. With increasing concentration, the size and quantity of semisulfate crystals decreased and the X-ray pattern of the crystals was degraded. Only gel was formed in experiments where 1,500 ppm (1,000µl) Wayhib S was tested. A few crystals formed 3 days later and more formed over 15 days. The crystals had the morphology of ettringite needles but their X-ray pattern was totally degraded and indicated a very disordered lattice structure.

CONCLUSIONS

In solution experiments, the 5-phosphonic acid Dequest 2060 was found to be the best inhibitor of ettringite formation. It was effective at a concentration of 0.02%, in agreement with

results obtained with concrete block experiments. Its inhibiting capacity was also found to be long-lived, lasting more than one year at room temperature, and over 1 ½ years at 58°C.

The advantage of the crystal growth method devised for this study was seen in several experiments in which more than one phase was formed. The major (signature) X-ray peaks used to identify ettringite and monosulfate are centered respectively at 9.72 Å and 8.90 Å or at angles of 9.15° 2θ and 9.85° 2θ. The actual peak separation is approximately 4 mm on X-ray charts. Because the peaks are broad, when both phases are present, the two peaks coalesce to form one and it is difficult to determine what is present, and the relative amount of each phase. Because the crystals were visible with light microscopy, the six-sided needle morphology of ettringite could be distinguished easily from the hexagonal plate morphology of the monosulfate phase (Lerch et al. 1928). Calcium aluminate semisulfate is formed by substitution of hydroxide for half the sulfate ions in the AFm monosulfate lattice (Pollmann 1987) making the two phases visually indistinguishable but easily-separable by X-ray diffraction.

EFFECT OF ENVIRONMENTAL FACTORS ON ETTRINGITE FORMATION

Of more academic interest was a general understanding of the effects of chemical environment on ettringite growth. Road deicers, fly ash, lignosulfonate and hydroxycarboxylic acid water reducers, plasticizers, superplasticizers, air entrainment chemicals, environmental contaminants, and numerous other chemicals are present in highway concrete. It is important to know the effects of these chemicals on the formation and stability of ettringite, specifically. Over 300 chemical additives were tested to determine their effects on the nucleation and growth of ettringite, or more correctly the AFt (alumino ferrite trisubstituted) phase. The structure of

pure ettringite is explained in Appendix C. The effects of different additives on ettringite are, however, not straightforward because considerable substitution in the basic formula $[Ca_3Al(OH)_6]_2?24H_2O?SO_4?2H_2O$ can occur. Calcium can be replaced by Pb and Sr (Taylor 1973); Al by Cr, Si, Ti, Co, Mn, Fe, Ga, and Ge (Taylor 1973, Struble and Brown 1984) and sulfate may be partly or completely replaced by CO_3^{-2}, CrO_4^{-2}, IO_3^{-}, and BO_3^{2-} (Taylor 1973, Struble and Brown 1984, Ogawa and Roy 1982). The effects that these replacements have on the morphology and the stability of the AFt phase is not yet clear.

EXPERIMENTAL PROCEDURES

The same solutions described in part B of this section were used. In most cases 25 ml of $Al_2(SO_4)_3$ solution were placed in a hard plastic container with an additive and swirled to dissolve the additive. Then, 20 ml of saturated $Ca(OH)_2$ solution were added, the container was capped, and the contents swirled. In some cases where a precipitate could form in the $Al_2(SO_4)_3$ solution, the additive was mixed with the $Ca(OH)_2$ solution and the sulfate solution was then added.

Ettringite is generally stable in the pH range 10.5 to 13.0 (Damidot and Glasser 1973). For additives that produced a pH below 10.5, pH was adjusted with 5M NaOH. The containers were left for 24 hours, then the contents of containers with visible precipitate were filtered through Whatman #40 filter paper, rinsed with a small quantity of distilled water, and the crystals were examined with a petrographic microscope. Crystal morphology (size and shape) was noted and the relative quantity of air-dried crystals recorded (large, L, medium, M, small, S, trace, Tr). The results of the experiments are shown in Appendix C.

RESULTS AND DISCUSSION

Ionic Species

Different cations and anions were examined because many ions might be expected in concrete. Silica and magnesium are always present. Lithium salts, hydroxides of Ca and K, and sulfates are added as accelerators of concrete setting time. Magnesium chloride and barium nitrate are also used to control set. Sodium chloride and nitrate, potassium chloride and sulfate, as well as barium chloride, are used to retard concrete setting time (Hewlett 1998). Sodium nitrate is also added for its water reducing effect.

Ettringite crystals grown in solutions without additives are long, medium wide, 6-sided in cross section (Fig 22A), have flat terminations, and appear in large quantities (L). Single valent ions, such as Li and K, have little effect on ettringite formation. NH_4, Ba, Co, Cr, Mn, Pb, ZrO, and Ni cause long very thin crystals to form (Appendix C). Although some of these ions are capable of substituting in the ettringite structure, their influence is believed to be mostly a surface effect. That this is the situation will become clearer after the effects of other additives on ettringite growth are examined.

Chen and Mehta (1982) conducted zeta potential measurements of the surface charge on ettringite crystals and found it be negative (-11.6 mV) at pH 7, and even more negative (-13.4 mV) at pH 10.4 in 10^{-3}M $Ca(OH)_2$, This was thought to be due to adsorbed layers of water and/or hydroxide ions on the long crystal surfaces. It would not be unreasonable to imagine highly charged positive ions being attracted to the long crystal surfaces where they would shield the faces from further growth layers. Growth on the ends of the needle-like crystals would result

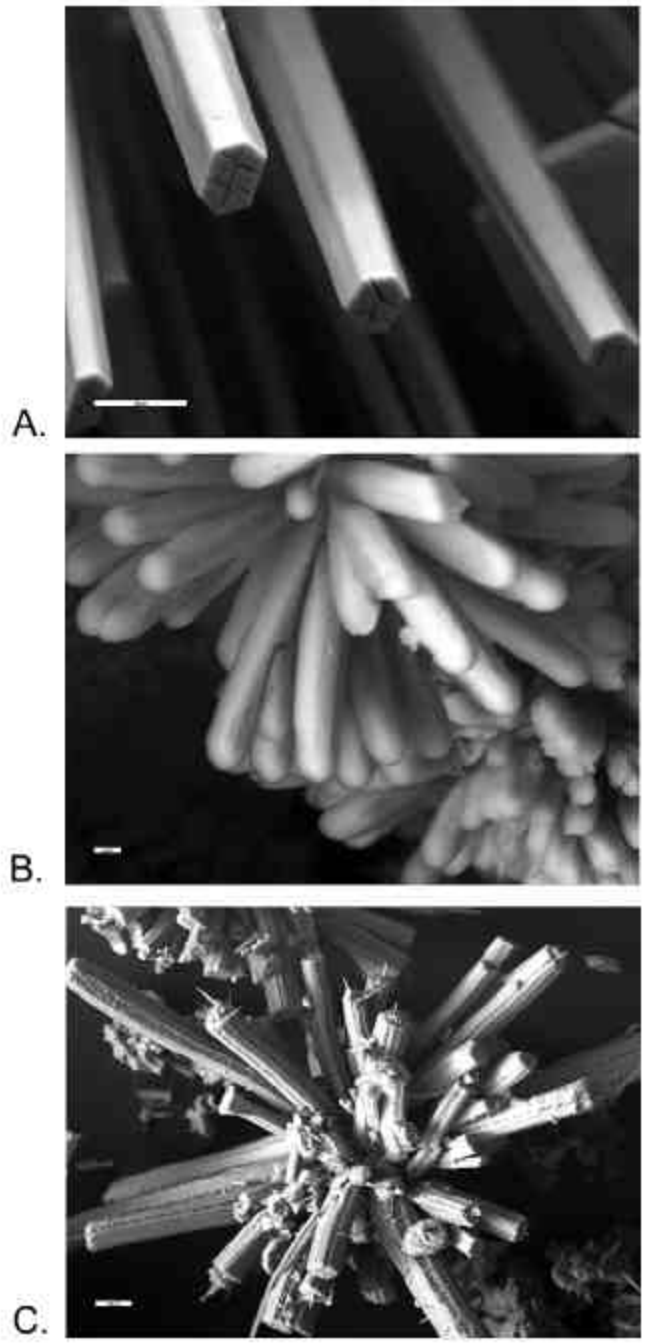

Fig. 22.

A. Six-sided needle-like morphology of ettringite grown in solution without additives. Bar is 20 µm.

B. Short 'pointed' ettringite crystals formed with arabinic acid (exp. 81). Bar is 2 µm.

C. Elongate, thin ettringite crystals grown with Alizarin Red S (exp. 153) exhibit growth defects on their long faces/edges. Bar is 20 µm.

in the very elongate thin morphology that was observed. Magnesium ions are closest in size to Ca ions and would more easily substitute for them. Crystals grown with Mg chloride were short (0.03 mm long).

Crystals formed in several experiments are described as pointed. Crystals with pointed or rounded terminations (Fig 22B) are formed by the chlorides of ions capable of substitution in the crystal structure, by the chloride ion itself, and by certain carboxylic acids.

Carboxylic Acids and Borates

This group of chemicals was tested because they were found to be very effective in altering the growth of many calcium minerals including gypsum (Cody and Cody 1991) and the calcium oxalates (Cody and Cody 1994). Carboxylic acids were found to bind to crystal surface calcium ions and to prevent further growth on those surfaces. Molecules with carboxylate spacing equal to the calcium spacing of the mineral were the most effective in preventing this growth. Citrate and tartrate ions are also powerful chelators of solution Ca^{2+} and Al^{3+} and would be expected to influence the nucleation and growth of calcium phases. Borax and tartaric acid and its salts are used as Type B (ASTM C494) set retarders, and the hydroxylated carboxylic acids, discussed here in the sugar section, are used as Type A water reducers (ASTM C494) (Kosmatka and Panarese 1988). Citric, tartaric, glycolic, salicylic, heptonic, and malic acids have all been used as water-reducing plasticizers (Taylor 1990).

Most carboxylic acids had no effect on the morphology of ettringite crystals because the calcium ions of the crystals are buried in a sheath of negatively-charged hydroxyl molecules and water molecules. The negatively charged carboxylate groups appeared to be repelled by the negatively charged crystals. Citrate and tartrate molecules, as expected, affected the nucleation of ettringite. Fewer crystals were formed and the crystals were short because the nutrients for

their growth were chelated. It was also possible that molecules chelated to calcium ions, which become part of the crystals, blocked rapid growth on the terminal faces. A small quantity of the AFm phase was formed when small quantities of isocitric acid was used.

A concentration of 0.22 ppt mucic/galactaric acid produced pointed ettringite crystals. At a concentration of 0.66 ppt mucic acid, a long-lasting gel was formed, indicating this to be a powerful inhibitor of ettringite.

Boric acid and its sodium salt inhibited the nucleation of ettringite, allowing the metastable AFm phase to form in its place. This was important because borate ions are believed to partially substitute for sulfate ions in the lattice of ettringite to form the mineral sturmanite. If metastable primary AFm is formed in concretes in which borax is used as a set retarder, there is the possibility that it could easily convert over time to deleterious secondary ettringite. It would be of interest to know if the reported cases of concretes with primary monosulfate (or monosulfate that supposedly converted from ettringite) were concretes that were made with borax or lignosulfonate inhibitors to be discussed later. A concentration of < 44 ppm borax was capable of inhibiting ettringite and producing only the AFm phase.

Amino Acids and NH Compounds

Amino acids and NH compounds were tested because they form positively-charged NH_2^+ and NH_3^+ groups on relatively large organic molecules. These positively-charged groups may adsorb onto crystal faces and allow the large molecules to shield and prevent growth of those faces. Nearly all of the compounds tested produced long thin ettringite crystals because they were attracted to the negatively-charged elongate faces.

Enzymes

Enzymes are formed in concrete in small quantities produced mainly via microbiological processes. The effect of these very large molecules on the formation of ettringite in concrete has probably not been tested previously.

Many enzymes produced very thin needles, as might be expected because they were composed of amino acids, which produced very thin needles of ettringite. Maltase, enterokinase, lipase, and protease were unusual in producing large quantities of spheres composed of relatively short ettringite needles. These chemicals were interpreted to be nucleation enhancers. When a large quantity of crystals nucleates, each individual crystal will have less nutrient to grow to large size. Mehta (1976) observed that ettringite forms slender needles and spherulites in solution growth and in high water/cement experiments, and that short prisms formed in low w/c experiments where the supersaturation is much higher and rapid nucleation of a greater number of crystals is expected. Each crystal in the latter environment will have less nutrient to grow and will be short.

Sugars and Sugar-Based Chemicals

Sugars have been studied extensively because of their effects in retarding setting time especially in hot weather and in deep geothermally-heated oil wells. Taylor (1990) suggested that "sugars are capable of attacking concrete by complexing with calcium with consequential dissolution of CH and hydrated silicate and aluminate phases". Thomas and Birchall (1983) described three categories of retarding sugars: (1) trihalose and a methyl glucosides which are ineffective; (2) glucose, maltose, lactose, and cellobiose, which are good retarders, and (3) sucrose and raffinose, which are outstanding retarders. Thomas and birchall (1983) believe that

sugars shield the surfaces of CH and thereby delay its dissolution and the rate of the setting reactions.

Sugars are capable of complexing calcium and possibly aluminum because they contain numerous hydroxyl groups that deprotonate to form multi-dentate negatively-charged molecules that can tightly bind solution ions. Ettringite formation is additionally prevented because the deprotonated hydrogen ions can lower solution pH below the pH stability range of ettringite. For this reason, control of solution pH was especially important in studying this group of additives.

The six-carbon (hexose) sugars that Thomas and Birchall (1983) found to be effective in retarding total concrete set had little effect on ettringite growth. Five-carbon (pentose) sugars such as arabinose, ribose, and xylose were, however, found to be very effective in inhibiting both nucleation and growth of ettringite. In experiments, only a small quantity of crystals was formed and the crystals were short thick hexagonal prisms rather than needles. Shortening of the prisms was found to correspond with the amount of pentose sugar added. Other chemicals that contained pentose sugar moities (groups) were also effective in inhibiting crystal length. They included arabinic acid, galacturonic acid, adenosine, and cytidine. Sorbitol, a six-carbon, six-hydroxyl aliphatic sugar alcohol is used as a plasticizer because of its resistance to alkali attack. It was highly effective in inhibiting ettringite nucleation and linear growth.

Coveney et al. (1998) proposed a model in which phosphonate compounds could inhibit the growth of ettringite by fitting into the lattice sites normally occupied by sulfate. They designed and synthesized a ring-shaped (“crown”) triphosphonate molecule with the proper spacing of functional phosphonate groups to fit into the sulfate positions of the lattice on the terminal {0001} faces of the crystals. The ring shape of the crown triphosphonate molecule is analogous to the ring of pentose sugars with hydroxyl functional groups replacing phosphonate

groups. In the lattice structure of ettringite (Appendix B), there are three hydroxyl groups positioned between each calcium and aluminum ion. We first considered the possibility that sugar hydroxyl groups might fit into the lattice like the phosphonate groups proposed by Coveney et al. We later discarded the idea because the spacing of the three hydroxyl groups in the effective pentose inhibitors ribose, arabinose, and xylose was different in each case. Also, if the hydroxyl groups of the sugar molecules were incorporated into the ettringite lattice, the remainder of the molecule would have to be overgrown by the crystal and would result in lattice and structural disruptions that would be visible. Because the crystals were perfectly clear and showed no surface or optical disruption, it was concluded that the molecules functioned by chelating calcium and possibly aluminum ions that were incorporated into the crystals. Their shielding effect and their detachment slowed the rate at which the crystals could grow to elongation. This conclusion is supported by the fact that sorbitol, tartaric and citric acids and their salts, all linear molecules that are know calcium chelators, were found in this study to inhibit ettringite nucleation and linear growth. This raises the possibility that Covey et al.'s expensive, tailor-made ettringite inhibitor might only be a better calcium chelator.

Phosphates and Nucleotides

Certain phosphates have been added to concrete to reduce steel reinforcement corrosion by chloride ions. Many of those tested here formed gels showing that they were powerful AFt and AFm inhibitors. When potassium phosphate monobasic was added to Al_2SO_4 and $Ca(OH)_2$ in separate containers, a gel was formed in the hydroxide container indicating that a hydroxy, rather than an aluminate gel, was involved. Further detailed study of phosphates and nucleotides is warranted.

Stains, Lignins, and Surfactants

Salts of lignosulfonates, alkylbenzene sulfonates, sulfonated hydrocarbons, and synthetic detergents are added to concrete as air-entraining admixtures and to improve workability (ASTM C260). Most of the biological stains tested in this study were sulfonated hydrocarbons of varied molecular weight and structure. Several also contained benzene rings. Stains containing between 0 and 4 sulfonic acid groups were tested. Nearly all of the stains produced a large quantity of long thin needles indicating that they did not inhibit nucleation and that they were adsorbed along the long axis of the crystals. It was difficult to understand why molecules with negatively-charged carboxyl groups had no effect on the growth of negatively-charged ettringite crystals, whereas molecules with negatively-charged sulfonic acid groups did. It is hypothesized that a sulfonic acid group may be incorporated into the crystal as a substitute for sulfate. The remainder of the molecule would then shield the sides of the crystal from rapid growth until the molecule is overgrown. Linear surface and growth defects would be expected if this occurred. Crystals grown with Alizarin Red S (Fig. 22C) exhibit these defects on the edges between their long faces. Carboxylic acid groups are probably incapable of substituting for any of the lattice components in ettringite, and so they have no effect on growth.

Commercial lignosulfonate chemicals had more powerful effects on ettringite than the biological stains. Polyfon O with one sulfonic acid group, inhibited ettringite, and the metastable AFm phase formed instead. Again, as with borax, later decomposition of the metastable phase could possibly contribute to the formation of secondary ettringite. Reax 6BW, a lignocarboxylate with 1.5 sulfonic acid groups produced very long (>0.3 mm) ettringite needles and behaved as a nucleation inhibitor, as did the lignosulfonate Reax 100.

The most amazing results were found when a very small quantity of the surfactant sodium lauryl sulfate (a sulfate ester) was tested. A large 3 cm block of dense latex-appearing 'clot' formed in the solution and could be removed in one piece. It was found to consist of long, extremely fine fiber-like crystals that could bend without breaking. When the mass dried, it shrank to the size of a standard (L) large quantity precipitate, thus showing that much of the large initial volume was due to water adsorption. The fact that great water adsorption and expansion was seen with fiber-like crystals having large surface areas associated with the elongate crystal faces indicates that these faces play a major role in the expansion of ettringite during water adsorption. It is not just small crystal size that causes large water-induced expansion (Mehta 1973), but rather it is the large surface area of the elongate water-adsorbing crystal faces that adsorb large volumes of water. This observation may find application in the commercial use of ettringite to produce fire-resistant wallboard.

Overview of Experimental Results

As tabulated in Appendix C, the additives tested could be divided into groups that produce several different types of effects: (1) those that have no effect, and produce elongate, six-sided, medium thick ettringite crystals with flat {0001} terminating faces. The crystals were either single or in spheres composed of radiating elongate crystals (Fig. 22A); (2) additives that modify ettringite crystal morphology; (3) those that selectively inhibit ettringite and allow the precipitation of other crystal phases such as the monosulfate or semisulfate rather than ettringite; and (4) additives that inhibit precipitation of all crystalline phases and cause the formation of a gel/colloid phase.

The modification of ettringite morphology (Type 2 effects), were of different varieties and resulted because of growth reduction on specific crystal faces. This reduction occurred

because the additives were selectively adsorbed onto those faces, and the additive blocked or slowed the growth on the adsorbing faces. Typical morpological changes were: (a) reduction in growth of terminating {0001} faces (the small six-sided end faces perpendicular to the axis of crystal elongation), thus producing short, stubby crystals; and (b) reduction in growth of elongate prism faces (those faces parallel to the axis of crystal elongation, the ***c*** axis) thus producing very thin, elongate crystals. In some cases, strongly-grooved elongate faces occurred probably because of adsorption along the edges separating the elongate faces (Fig. 22C). Other less pronounced habit modifications occurred, such as the production of pyramidal (pointed or rounded) terminating surfaces instead of the normal flat faces perpendicular to the axis of elongation (Fig. 22 B).

Generally with habit-modifying additives, higher concentrations often lead to either selective or general inhibition of crystal precipitation so that phases other than ettringite precipitate or a gel/colloid phase results.

PART III

SUMMARY AND RECOMMENDATIONS

SUMMARY FOR PART I. THE EFFECTS OF CRYSTALLIZATION INHIBITORS ON ETTRINGITE GROWTH IN CONCRETE

Ettringite Roles in Premature Concrete Deterioration

Previous research on the role that secondary ettringite plays in premature deterioration of highway concrete has led to two opposing viewpoints: (1) the formation of secondary ettringite causes expansion and eventually leads to concrete damage even though the mechanism that produces deterioration remains unclear (Cohen 1983b), and (2) the formation of secondary ettringite accompanies cracking but is not the cause of the cracking (Mather 1984).

Experiment-Based Conclusions on Ettringite Induced Deterioration

The results obtained in this research project have considerable implications about the role of ettringite in premature concrete deterioration. Concrete expansion and cracking were caused by sulfate attack and ettringite was the predominant new mineral formed during the experiments. Degree of expansion depended on the concrete type and the experimental conditions during experiments. Severity of deterioration varied and was found to decrease in the series wet/dry cycles, freeze/thaw cycles, and continuous immersion conditions. The presence of crystallization inhibitor chemicals simultaneously reduced new ettringite formation and the amount of expansion cracking.

Continuous immersion of concrete blocks in sodium sulfate solutions caused ettringite-induced expansion that was almost certainly due to crystal growth pressures. Greater expansion

occurred during the wet/dry experiments than during continuous immersion, which supports the concept that ettringite swelling pressures caused by water adsorption is partly responsible for expansion. Expansion was particularly evident under wet/dry conditions because drying allowed the rapid precipitation of tiny crystals in agreement with the conclusions of Klien and Hurlbut (1986). These crystals have high surface areas that readily adsorb large volumes of water. We conclude that expansion during wet/dry conditions is due to the simultaneous action of both crystal growth and water adsorption pressures. The greater abundance of small crystals produced by drying intervals also probably creates greater crystal growth pressures as these small crystals grow during wetting intervals.

Measured expansion of concrete was greater during freeze/thaw cycling than during continuous immersion and was less than expansion produced by wet/dry conditions. These observations suggest that ettringite void-filling also produces some expansion under freeze/thaw conditions. Expansion during freeze/thaw experiments probably is due to both crystal growth pressures and to pore clogging during freezing.

Concrete type was important to expansion caused by ettringite during sulfate attacks. The new concrete with high water/cement (w/c) ratio exhibited large expansion within relatively shorter times than old low w/c concrete. The higher porosity and permeability of higher w/c concrete allowed rapid ingress of sulfate solution into concrete. Non-durable concrete, that contained large amounts of ettringite before the experiments, exhibited the least amount of expansion. Previous growth of the ettringite depleted C_3A in the concrete and left insufficient C_3A for new ettringite formation. During our experiments, sulfate ions caused the precipitation of gypsum rather than ettringite. Other minerals, such as brucite and calcite, produced during highway use probably also reduced concrete permeability in the non-durable concrete samples

and reduced the rate of sulfate ingress into concrete and thereby reduced the amount of ettringite formed during experiments.

Significance of Crystallization Inhibitor Experiments

All crystallization inhibitors reduced concrete expansion during sulfate attack, although none were totally effective. They significantly reduced expansion under all experimental conditions. Because the inhibitors can only alter nucleation and growth of new ettringite, these results provide powerful evidence that the formation of secondary ettringite is a direct cause of expansion and cracking.

Petrographic microscope and SEM observations of sulfate + inhibitor treated concrete samples showed that many voids were filled with newly-formed materials. Detailed EDAX point analysis revealed that the chemical composition and morphology of filling materials were not ettringite. These analyses also showed that the filling materials produced by each crystallization inhibitors had different chemical and physical characteristics. Phosphonate inhibitors were generally more effective than polyacrylic acid and the phosphate ester in preventing the nucleation and crystal growth of both monosulfate and ettringite. Void-filling materials formed by sodium sulfate solutions with phosphonate inhibitors are Al- and Ca-rich phases with very low sulfur content, and contain only a few sub-microscopic sulfoaluminate masses. The phosphate ester was not as effective in inhibiting sulfoaluminate formation, and void-filling materials consisted of crystalline ettringite, monosulfate, and a low S, high Al - Ca phase. The increased volume of sulfoaluminate phases resulted in slightly higher expansion when compared to that from phosphonate inhibitors.

Experiments that tested effectiveness of different phosphonate concentrations (5%, 1%, 0.1%, 0.01%, 0.001%,0.0005%, and 0.0001%) indicated that an inhibitor concentration in the range between 0.1% and 0.001% is probably the most cost effective in preventing ettringite growth.

SUMMARY FOR PART II. SOLUTION GROWTH EXPERIMENTS

A new method of crystal growth was devised to reliably produce ettringite crystals that could be seen with a light microscope (45x – 320x). Solution growth experiments were then conducted to determine the relative ability of four commercial scale inhibitors to prevent ettringite nucleation and growth. The phosphonic acid, Dequest 2060 (Monsanto, Inc.), was found to be the most effective inhibitor at = 0.02% concentration, comparable to the effective concentration determined in concrete block experiments. It retained its effectiveness for over one year, both at room temperature and at 58^{o}C.

Nearly 300 chemicals, many of which are present in the concrete environment, were also tested to determine their effects on ettringite growth and morphology. Most carboxylic acids had no effect on ettringite formation except for the known calcium chelators (and water-reducing plasticizers) citrate and tartrate, which prevented nucleation and growth. Hydroxylated carboxylic acids such as mucic/galactaric and its further-hydroxylated form, the plasticizer sorbitol, were very effective in inhibiting ettringite nucleation and growth. A smaller quantity of short, stubby ettringite crystals formed. Pentose sugars also inhibited elongation growth, whereas hexose sugars, which are used as concrete set retarders, had little effect on ettringite nucleation and growth.

Sodium tetraborate (borax), which is used as a type B set retarder, was found to inhibit ettringite nucleation at a concentration < 44 ppm. Borax caused the metastable phase AFm to form instead. Further study is needed to determine if this reaction occurs in concrete, and if later conversion of the metastable AFm phase to ettringite contributes to the formation of secondary ettringite. Some commercial lignosulfonates were found to cause the same effect.

Chemicals with sulfonic acid groups produced very long thin fiber-like ettringite crystals which adsorbed an exceptionally large quantity of water that produced significantly greater volume expansion. Knowledge of the effects of the chemical environment on the AFm and AFt phases is important to producing better, more durable concrete.

RECOMMENDATIONS

Many researchers have concluded that secondary or delayed ettringite is responsible for serious premature deterioration of concrete highways, although the precise expansion mechanism exerted by ettringite is uncertain. Based on the conclusions of previous studies and the results of the present contribution concerning the strong link between ettringite formation and concrete expansion, it is essential to reduce additional damage to existing highways that already have undergone ettringite-induced expansion cracking and to prevent damage to new highways that may in the future experience such cracking. Ideally, new highways may eventually be constructed from materials using techniques that will eliminate such premature deterioration. In the meantime, however, efforts are necessary to discover methods of reducing secondary ettringite formation and resultant damage.

Our results suggest that it is feasible that the application of inexpensive crystallization phosphonate-based inhibitor chemicals will both reduce secondary ettringite formation and

ettringite-induced expansion cracking of concrete highways. Further research involving field testing of phosphonate inhibitors at different concentrations should be undertaken to determine if laboratory results are comparable to those obtained under highway use conditions.

ACKNOWLEDGEMENTS

The project was funded by the Iowa Department of Transportation, Project TR-431. This support is gratefully acknowledged. We particularly want to thank Mark Dunn. Wallace Rippie, and Robert Dawson of the Iowa DOT and Jim Myers and Wendell Dubberke for their advice, suggestions, and support of this project. We thank Max Porter of the ISU Civil and Construction Engineering Department for his advice, and Jerry Amenson and Scott Schlorholtz of the ISU Materials Research Laboratory for their assistance with SEM analyses.

REFERENCES

AL-AMOUDI, O. S. B.; ABDULJAUWAD S. N.; RASHEEDUZZARFAR; AND MASLEHUDDIN, M., 1992, Effect of chloride and sulfate contamination in soils on corrosion of steel and concrete: *Transportation Research Record.* No. 1345, pp. 67-73.

BAUSSANT, J. B.; VERNET, C.; AND DEFOSSE, C. 1989, Growth of ettringite in diffusion controlled conditions influence of additives on the crystal morphology: *Proceeding of the 11th International Conference on Cement Microscopy*, April 1989, New Orleans, pp. 186-197.

BILLINGHAM, J. AND COVENEY, P.V, 1993, Simple chemical clock reactions: Application to cement hydration: *Journal of Chemistry Society Faraday Transactions*, Vol. 89, No. 16, pp. 3021-3028.

BLACK, S. N.; BROMLEY, L. A.; COTTIER, D. C.; DAVEY, R. J.; DOBBS, B.; AND ROUT, J. E., 1991, Interactions at the organic/inorganic interface: Binding motifs for phosphates at the surface of barite crystals: *Journal of Chemistry Society Faraday Transactions*, Vol. 87, No. 20, pp. 3409-3414.

BUCKLEY, H. E., 1951, *Crystal Growth*: New York, John Wiley & Sons, Inc., 571 p.

CHEN, SUH-SHIANG AND MEHTA, P. K., 1982, Zeta potential and surface area measurements on ettringite: *Cement and Concrete Research*, Vol. 12, No. 2, pp. 257-259.

CODY, R. D., 1991, Organo-crystalline interactions in evaporite systems: The effects of crystallization inhibition: *Journal of Sedimentary Petrology*, Vol. 61, No. 5, pp. 704-718.

CODY, A. M. AND CODY, R. D., 1991, Chiral habit modifications of gypsum from epitaxial-like adsorption of stereospecific growth inhibitors: *Journal of Crystal Growth*, Vol. 113, pp. 508-519.

CODY, A. M. AND CODY, R. D., 1994, Calcium oxalate trihydrate phase control by structurally-specific carboxylic acids: *Journal of Crystal Growth*, Vol. 135, pp. 235-245.

CODY, R. D.; SPRY, P. G.; CODY, A. M.; AND GAN, G., 1994, *The role of magnesium in concrete deterioration*: Iowa Department of Transport, Final Report HR-355, 171p.

CODY, R. D.; CODY, A. M.; SPRY, P. G.; AND LEE, H., 1997, *Expansive mineral growth and concrete deterioration*: Iowa Department of Transport, Final Report HR-384, 201p.

COHEN, M. D., 1983a, Modeling of expansive cement: *Cement and Concrete Research*, Vol. 13, No. 4, pp. 519-528.

COHEN, M. D., 1983b, Theories of expansion in sulfoaluminate-type expansive cements: schools of thought: *Cement and Concrete Research*, Vol. 13, pp. 809-818.

COLLEPARDI, M; MONOSI, S.; MORICONI, G; AND PAURI, M, 1984, Influence of gluconate or glucose on the C_3A hydration in the presence of gypsum with without lime: *Cement and Concrete Composites*, Vol. 14, No. 1, pp. 105-112.

COVENEY, P. V.; DAVEY, R. J.; GRIFFIN, J. L. W.; AND WHITING, A., 1998, Molecular design and testing of organophosphonates for inhibition of crystallization of ettringite and cement hydration: *Chemical Communication*, pp.1467-1468.

COVENEY, P. V. AND HUMPHRIES, W., 1996, Molecular modeling of the mechanism of action of phosphonate retarders on hydrating cements, *Journal of Chemistry Society Faraday Transactions*, Vol. 92, No. 5, pp. 831-841.

DAMIDOT, D. AND GLASSER, F. P., 1993, Thermodynamic investigation of the CaO-Al_2O_3-$CaSO_4$-H_2O system at 25^oC and the influence of Na_2O: *Cement and Concrete Research*, Vol. 221-238, No. 1, pp. 221-238.

DAVEY R. J.; BLACK, L. A.; BROMLEY, L.A.; COTTIER, D.; DOBBS, B; AND ROUT, J. E., 1991, Molecular design based on recognition at inorganic surface, *Nature*, Vol. 353, No. 10, pp. 549-550.

DAY, R. L., 1992, The effect of secondary ettringite formation on durability of concrete: A literature analysis: *PCA Research and Development Bulletin* RD108T, pp.1-115.

DIAMOND, S., 1996, Delayed ettringite formation - processes and problems: *Cement and Concrete Composites*, Vol. 18, No. 3, pp. 205-215.

FU, Y. AND BEAUDOIN, J. J., 1997, Expansion of portland cement mortar due to internal sulfate attack: *Cement and Concrete Research*, Vol. 27, No. 9, pp. 1299-1306.

GOLLOPE, R. S. AND TAYLOR, H. F. W., 1996, Microstructural and microanalytical studies of sulfate attack. I. Ordinary portland cement paste: *Cement and Concrete Research*, Vol. 22, No. 6, pp. 1027-1038.

HEWLETT, P. C. (ed.), 1998, *Lea's Chemistry of Cement and Concrete*, 4th ed., New York, John Wiley & Sons, 1053 p.

JOLICOEUR, C. AND SIMARD, M., 1998, Chemical admixture-cement interactions: Phenomenology and physico-chemical concepts: *Cement and Concrete Composites*, Vol. 20, pp. 87-101.

KLEIN C. AND HURLBUT, C. S. JR., 1985, *Manual of Mineralogy*, 20th Ed., New York, John Willy & Sons, Inc, 505p.

KOSMAIKA S. H. AND PANARESE W. C., 1988, *Design and Control of Concrete Mixtures*, Skokie, IL, Portland Cement Association, 205 p.

LAWRENCE, C. D., 1990, Sulfate attack on concrete, *Magazine of Concrete Research*, Vol. 42, No. 153, pp. 249-264.

LERCH, W.; ASHTON, F. W.; AND BOGUE, R. H., 1928, The sulphoaluminates of calcium: *Journal of Research, National Bureau of Standards*, Vol. 2, No. 4, pp. 715-731,

MATHER, B., 1984, A discussion of the paper "Theories of expansion in sulfoaluminate-type expansive cements: schools of thought", by M. D. Cohen: *Cement and Concrete Research*, Vol. 14, No. 4, pp. 603-609.

MEHTA, P. K., 1973, Mechanisms of expansion associated with ettringite formation: *Cement and Concrete Research*, Vol. 3, No. 1, pp. 1-6.

MEHTA, P. K., 1976, Scanning electron micrographic studies of ettringite formation: *Cement and Concrete Research*, Vol. 6, No. 2, pp. 169-182.

MEHTA, P. K., 1983, Mechanism of sulfate attack on Portland cement concrete - another look: *Cement and Concrete Research*, Vol. 13, No. 3, pp. 401-406.

NEVILLE, A. M., 1969, Behavior of concrete in saturated and weak solutions of magnesium sulphate or calcium chloride: *Journal of Materials*, Vol. 4, No. 4, pp.781-816.

ODLER, I. AND ABDUL MAULA, 1984, Possibilities of quantitative determination of the AFt- (ettringite) and AFm – (monosulphate) phases in hydrated cement pastes: *Cement and Concrete Research*, Vol. 14, No. 1, pp. 133-141.

OGAWA, K. AND ROY, D. M.., 1982, $C_4A_3\overline{S}$ hydration, ettringite formation, and its expansion mechanism: effect of CaO, NaOH, and NaCl; conclusions: *Cement and Concrete Research*, Vol. 12, No. 2, pp. 247-255.

POLLMANN, H. 1987, SEM, X-ray, and thermoanalytical studies on hydration products of tricalcium aluminate in the presence of sulfates, carbonate, and hydroxide ions: *Proceedings of the 9th International Conference on Cement Microscopy*, Reno, NV, pp. 426-445.

SCHNEIDER, U. AND PIASTA, W. G., 1991, The behavior of concrete under Na_2SO_4 solution attack and sustained compression or bending: *Magazine of Concrete Research*, Vol. 43, No. 157, pp. 281-289.

SCRIVENER, K. L. AND TAYLOR, H. F. W., 1993, Delayed ettringite formation: a microstructural and microanalytical study: *Advances in Cement Research*, Vol. 5, No. 20, pp. 139-146.

SIEDEL, H; HUMPEL, S; AND HUMPEL, R, 1993, Secondary ettringite formation in heat treated portand cement concrete: Influence of different w/c ratios and heat treatment temperatures: *Cement and Concrete Composites*, Vol. 23, No. 2, pp. 453-461.

SMITH, B. R., 1967, Scale prevention by addition of polyelectrolytes: *Desalination*, Vol. 3, pp. 263-268.

SMITH, R. B. AND ALEXANDER, A. E., 1970, The effect of additives on the process of crystallization: II. Further studies of calcium sulfate, *Journal of Colloid and Interface Science*, Vol. 34, pp. 81-90.

STRUBLE, L. J. AND BROWN, P. W., 1984, *An evaluation of ettringite and related compounds for use in solar energy storage*: National Bureau of Standards, Progress Report, NBSIR 84-2942, 42 p.

TAYLOR, H. F. W., 1973, Crystal structures of some double hydroxide minerals: *Mineralogical Magazine*, Vol. 39, No. 304, pp. 377-389.

TAYLOR, H. F. W., 1990, *Cement Chemistry*: New York, Academic Press Ltd. 475 p.

THAULOW, N.; HJORTH, U.; AND CLARK, B., 1996, Composition of alkali silica gel and ettringite in concrete railroad ties: SEM-EDAX and X-ray diffraction analyses, *Cement and Concrete Research*, Vol. 26, No. 2, pp. 309-318.

THOMAS, N. L. AND BURCHELL J. D. 1983, The retarding action of sugars on cement hydration: *Cement and Concrete Research*, Vol. 13, No. 6, pp. 830.

TUAN-SARIF, T. B. B., 1983, The influence of organic inhibitors on the crystallization of gypsum [Unpublished M.S. thesis]: Iowa State University, 107 p.

TUMIDAJSKI, P. J. AND TURC, I, 1995, A rapid test for sulfate ingress into concrete, *Cement and Concrete Research*, Vol. 25, No. 5, pp. 924-928.

WOLTER, S., 1996, *Ettringite. Cancer of Concrete*: New York, Burgess Publishing Co., 172 p.

YOUNG, J. F. 1972, A review of the mechanisms of set-retardation in portland cement paste containing organic admixtures: *Cement and Concrete Research*, Vol. 2, No. 4, pp. 415-433.

Appendix A

EXPANSION MEASUREMENT DATA

EXPANSION MEASUREMENT DATA

0.75 M Sodium Sulfate Solutions without Crystallization Inhibitors.

Type of concrete	Sample No. .	Physical Condition	Before treatment (Length Avg.)	Stdv	After Treatment (Length Avg.)	Stdv	Expansion, %
Newly-made	N1-S	W/D	35.2355	0.0092	35.9155	0.0064	1.9299
Newly-made	N1-S2	W/D	33.6070	0.0028	34.0840	0.0127	1.4193
Newly-made	N1-S2	F/T	33.8285	0.0120	34.0475	0.0035	0.6474
Newly-made	N2-S2	F/T	35.8155	0.0064	36.0230	0.0382	0.5794
Newly-made	N3-S	Continuous	37.4820	0.0028	37.5475	0.0035	0.1748
Newly-made	N3-S2	Continuous	38.5455	0.0064	38.6100	0.0071	0.1673
Non-durable	E1-S	W/D	36.7820	0.0042	36.9400	0.0071	0.4296
Non-durable	E2-S	F/T	33.3490	0.0042	33.4375	0.0064	0.2654
Non-durable	E3-S	Continuous	35.3470	0.0071	35.4030	0.0085	0.1584
Durable	F1-S	W/D	36.2720	0.0042	36.9025	0.0177	1.7383
Durable	F2-S	F/T	32.9535	0.0106	33.1725	0.0106	0.6646
Durable	F3-S	Continuous	32.8135	0.0064	33.0800	0.0085	0.8122

0.75 M Sodium sulfate Solution with 0.01% Crystallization Inhibitor, Dequest 2010

Newly-made	N1-SD1	W/D	36.8195	0.0064	36.9660	0.0085	0.3979
Newly-made	N2-SD1	F/T	36.6245	0.0021	36.7525	0.0035	0.3495
Non-durable	E1-SD1	W/D	35.8845	0.0078	35.9010	0.0156	0.0460
Non-durable	E2-SD1	F/T	35.8515	0.0035	35.8665	0.0064	0.0418
Durable	F1-SD1	W/D	33.2400	0.0028	33.3585	0.0049	0.3565
Durable	F2-SD1	F/T	33.2440	0.0057	33.2880	0.0085	0.1324

Dequest 2060S

Newly-made	N1-SD2	W/D	36.7225	0.0021	36.8275	0.0106	0.2859
Newly-made	N2-SD2	F/T	36.8575	0.0120	36.9550	0.0071	0.2645
Non-durable	E1-SD2	W/D	35.9275	0.0078	35.9490	0.0078	0.0598
Non-durable	E2-SD2	F/T	37.2845	0.0092	37.2960	0.0071	0.0308
Durable	F1-SD2	W/D	33.4240	0.0113	33.5440	0.0014	0.3590
Durable	F2-SD2	F/T	32.8665	0.0092	32.9580	0.0057	0.2784

Good-Rite K752

Newly-made	N1-SK	W/D	35.3525	0.0106	35.5345	0.0134	0.5148
Newly-made	N2-SK	F/T	35.1725	0.0064	35.3155	0.0064	0.4066
Non-durable	E1-SK	W/D	37.0085	0.0120	37.0315	0.0134	0.0621
Non-durable	E2-SK	F/T	35.9165	0.0049	35.9255	0.0049	0.0251
Durable	F1-SK	W/D	32.7960	0.0057	32.9370	0.0113	0.4299
Durable	F2-SK	F/T	33.4010	0.0014	33.4525	0.0106	0.1542

Wayhib S

Newly-made	N1-SW	W/D	36.3945	0.0078	36.5575	0.0064	0.4479
Newly-made	N2-SW	F/T	33.5100	0.0071	33.5710	0.0156	0.1820
Non-durable	E1-SW	W/D	35.8800	0.0113	35.9135	0.0163	0.0934

Non-durable	E2-SW	F/T	37.0540	0.0071	37.0760	0.0057	0.0594
Durable	F1-SW	W/D	36.3375	0.0106	36.5725	0.0177	0.6467
Durable	F2-SW	F/T	34.7340	0.0099	34.7785	0.0049	0.1281

0.75 M Sulfate with Different Inhibitor Concentrations

Type of concrete	Sample No.	Inhibitor concentration (%)	Before treatment (Length Avg.)	Stdv	After treatment (Length Avg.)	Stdv	Expansion, %
Dequest 2010							.
Newly-made	N5-SD1	0.001	35.6405	0.0035	35.6625	0.0177	0.0617
Newly-made	N4-SD1	0.1	36.1750	0.0071	36.1900	0.0141	0.0415
Durable	F5-SD1	0.001	37.1585	0.0064	37.1800	0.0141	0.0579
Durable	f4-SD1	0.1	35.7235	0.0120	35.7350	0.0099	0.0322
Non-durable	D5-SD1	0.001	37.2885	0.0049	37.3125	0.0106	0.0644
Non-durable	D4-SD1	0.1	37.2465	0.0078	37.2645	0.0064	0.0483
Dequest 2060S							.
Newly-made	N5-SD2	0.001	36.6925	0.0134	36.7235	0.0163	0.0845
Newly-made	N4-SD2	0.1	36.8000	0.0028	36.8150	0.0071	0.0408
Durable	F5-SD2	0.001	35.7140	0.0198	35.7310	0.0269	0.0476
Durable	F4-SD2	0.1	36.5530	0.0127	36.6135	0.0049	0.1655
Non-durable	D5-SD2	0.001	35.8725	0.0035	35.8825	0.0035	0.0279
Non-durable	D4-SD2	0.1	37.1925	0.0035	37.2075	0.0106	0.0403
Good-Rite K572							.
Newly-made	N5-SK	0.001	34.7395	0.0049	34.7675	0.0035	0.0806
Newly-made	N4-SK	0.1	36.4300	0.0071	36.4550	0.0141	0.0686
Durable	F5-SK	0.001	35.8715	0.0021	35.8975	0.0106	0.0725
Durable	F4-SK	0.1	36.8250	0.0071	36.8475	0.0035	0.0611
Non-durable	D5-SK	0.001	37.2890	0.0057	37.3230	0.0071	0.0912
Non-durable	D4-SK	0.1	36.5625	0.0035	36.5750	0.0141	0.0342
Wayhib S							.
Newly-made	N5-SW	0.001	34.5580	0.0099	34.5800	0.0141	0.0637
Newly-made	N4-SW	0.1	34.1200	0.0071	34.1475	0.0035	0.0806
Durable	F5-SW	0.001	34.5175	0.0106	34.5365	0.0007	0.0550
Durable	F4-SW	0.1	35.1300	0.0113	35.2270	0.0170	0.2761
Non-durable	D5-SW	0.001	37.3035	0.0092	37.3365	0.0078	0.0885
Non-durable	D4-SW	0.1	34.2535	0.0021	34.2645	0.0064	0.0321

Distilled Water with 0.01% Inhibitors							.
Newly-made	ND1-1	Dequest 2010	34.5475	0.0064	34.5530	0.0042	0.0159
Newly-made	ND1-2	Dequest 2010	34.9445	0.0092	34.9475	0.0078	0.0086
Newly-made	ND2-1	Dequest 2060S	37.6340	0.0099	37.6380	0.0127	0.0106
Newly-made	ND2-2	Dequest 2060S	35.5245	0.0148	35.5235	0.0078	-0.0028
Newly-made	NK-1	Good-Rite K572	34.9975	0.0177	34.9990	0.0240	0.0043
Newly-made	NK-2	Good-Rite K572	35.8150	0.0099	35.8210	0.0042	0.0168
Newly-made	NW-1	Wayhib S	34.4460	0.0085	34.4530	0.0099	0.0203

Newly-made	NW-2	Wayhib S	34.8915	0.0078	34.8910	0.0099	-0.0014

Distilled Water

Newly-made	N1-W1		35.6190	0.0156	35.6235	0.0078	0.0126
Newly-made	N1-W2		36.8110	0.0060	36.8135	0.0015	0.0068
Newly-made	N2-E1		37.9080	0.0042	37.9125	0.0106	0.0119
Newly-made	N2-E2		34.9445	0.0092	34.9500	0.0170	0.0157
Non-durable	E1-W1		34.7470	0.0099	34.7520	0.0028	0.0144
Non-durable	E1-W2		35.6240	0.0156	35.6235	0.0078	-0.0014
Non-durable	E2-E1		37.8595	0.0035	37.8625	0.0035	0.0079
Non-durable	E2-E2		37.7550	0.0028	37.7600	0.0028	0.0132
Durable	E1-W1		33.4170	0.0156	33.4225	0.0106	0.0165
Durable	E1-W2		34.3465	0.0035	34.3515	0.0106	0.0146
Durable	E1-E1		34.4160	0.0040	34.4210	0.0040	0.0145
Durable	E1-E2		34.8895	0.0106	34.8880	0.0099	-0.0043

0.75 M Ca/Mg Acetate with Different Molar Ratios of Ca/Mg

Sample No.	Ca/Mg ratio	Physical Conditions	Before treatment (Length Avg.)	Stdv	After treatment (Length Avg.)	Stdv	Expansion, %
Newly-made Concrete							.
N1-A1	1:0	W/D	35.9590	0.0010	36.0405	0.0025	0.2266
N2-A1	1:0	F/T	37.0670	0.0040	37.1175	0.0025	0.1362
N1-A2	7:3	W/D	35.8390	0.0030	35.9075	0.0025	0.1911
N2-A2	7:3	F/T	36.0555	0.0045	36.0940	0.0040	0.1068
N1-A3	5:3	W/D	34.1820	0.0030	34.2960	0.0060	0.3335
N2-A3	5:3	F/T	33.8425	0.0025	33.9285	0.0035	0.2541
N1-A4	1:1	W/D	35.7790	0.0010	35.9180	0.0030	0.3885
N2-A4	1:1	W/D	36.7365	0.0035	36.8360	0.0010	0.2708
N1-A5	3:5	F/T	35.6240	0.0040	35.7870	0.0070	0.4576
N2-A5	3:5	W/D	35.2915	0.0055	35.3900	0.0050	0.2791
N1-A6	3:7	F/T	36.6390	0.0030	36.8035	0.0015	0.4490
N2-A6	3:7	W/D	35.5800	0.0020	35.6825	0.0025	0.2881
N1-A7	0:1	F/T	35.1495	0.0035	35.3185	0.0065	0.4808
N2-A7	0:1	W/D	37.6565	0.0015	37.7775	0.0025	0.3213
Durable Concrete							.
F1-A1	1:0	W/D	37.3550	0.0030	37.3940	0.0010	0.1044
F2-A1	1:0	F/T	36.9400	0.0020	36.9750	0.0030	0.0947
F1-A2	7:3	W/D	36.1320	0.0020	36.1705	0.0025	0.1066
F2-A2	7:3	F/T	37.0265	0.0025	37.0515	0.0015	0.0675
F1-A3	5:3	W/D	34.9105	0.0025	34.9550	0.0050	0.1275
F2-A3	5:3	F/T	34.0635	0.0035	34.1060	0.0060	0.1248
F1-A4	1:1	W/D	34.2195	0.0005	34.2750	0.0030	0.1622
F2-A4	1:1	W/D	36.7235	0.0025	36.7720	0.0040	0.1321
F1-A5	3:5	F/T	35.6600	0.0020	35.7165	0.0045	0.1584
F2-A5	3:5	W/D	35.7790	0.0040	35.8275	0.0025	0.1356

F1-A6	3:7	F/T	35.9170	0.0040	35.9815	0.0035	0.1796
F2-A6	3:7	W/D	35.0130	0.0030	35.0550	0.0050	0.1200
F1-A7	0:1	F/T	34.7640	0.0040	34.8230	0.0030	0.1697
F2-A7	0:1	W/D	35.2295	0.0015	35.2750	0.0030	0.1292

Non-durable Concrete							.
E1-A1	1:0	W/D	33.2340	0.0057	33.2750	0.0100	0.1234
E2-A1	1:0	F/T	37.2900	0.0071	37.3300	0.0020	0.1073
E1-A2	7:3	W/D	37.1590	0.0014	37.2110	0.0010	0.1399
E2-A2	7:3	F/T	37.2315	0.0049	37.2825	0.0025	0.1370
E1-A3	5:3	W/D	33.6665	0.0021	33.7090	0.0040	0.1262
E2-A3	5:3	F/T	36.1040	0.0071	36.1470	0.0010	0.1191
E1-A4	1:1	W/D	37.0830	0.0057	37.1370	0.0050	0.1456
E2-A4	1:1	W/D	37.1810	0.0014	37.2315	0.0035	0.1358
E1-A5	3:5	F/T	36.8545	0.0064	36.9025	0.0025	0.1302
E2-A5	3:5	F/T	38.4680	0.0028	38.5230	0.0050	0.1430
E1-A6	3:7	W/D	36.5970	0.0057	36.6755	0.0025	0.2145
E2-A6	3:7	W/D	36.0605	0.0035	36.1360	0.0060	0.2094
E1-A7	0:1	F/T	33.7845	0.0035	33.8525	0.0025	0.2013
E2-A7	0:1	E/T	34.6940	0.0028	34.7445	0.0035	0.1456

0.75 M Calcium Acetate with 0.01% Inhibitors

Sample No.	Inhibitor	Physical Conditions	Before treatment (Length Avg.)	Stdv	After treatment (Length Avg.)	Stdv	Expansion, %
Newly made concrete							.
N1-A1	None	W/D	35.9590	0.0010	36.0405	0.0025	0.2266
N2-A2	None	F/T	37.0670	0.0040	37.1175	0.0025	0.1362
N1-CD1	Dequest 2010	W/D	36.2345	0.0045	36.3075	0.0025	0.2015
N2-CD1	Dequest 2010	F/T	36.7840	0.0010	36.8410	0.0040	0.1550
N1-CD2	Dequest 2060S	W/D	38.4010	0.0040	38.4725	0.0075	0.1862
N2-CD2	Dequest 2060S	F/T	35.7185	0.0035	35.7660	0.0060	0.1330
N1-CK	Good-Rite K752	W/D	35.5415	0.0055	35.5885	0.0065	0.1322
N2-CK	Good-Rite K752	F/T	35.5840	0.0040	35.6295	0.0055	0.1279
N1-CW	Wayhib S	W/D	36.3115	0.0045	36.3780	0.0080	0.1831
N2-CW	Wayhib S	F/T	34.9845	0.0045	35.0310	0.0010	0.1329
Durable concrete							.
F1-A1	None	W/D	37.3550	0.0030	37.3940	0.0010	0.1044
F2-A2	None	F/T	36.9400	0.0020	36.9750	0.0030	0.0947
F1-CD1	Dequest 2010	W/D	32.9350	0.0010	32.9650	0.0050	0.0911
F2-CD1	Dequest 2010	F/T	35.9765	0.0035	36.0010	0.0090	0.0681
F1-CD2	Dequest 2060S	W/D	36.3600	0.0020	36.3850	0.0100	0.0688
F2-CD2	Dequest 2060S	F/T	37.1845	0.0045	37.2150	0.0050	0.0820
F1-CK	Good-Rite K752	W/D	34.4615	0.0005	34.4785	0.0035	0.0493
F2-CK	Good-Rite K752	F/T	34.4335	0.0035	34.4680	0.0020	0.1002
F1-CW	Wayhib S	W/D	34.2420	0.0070	34.2685	0.0025	0.0774
F2-CW	Wayhib S	F/T	34.6545	0.0055	34.6775	0.0035	0.0664
Non-durable Concrete							.

E1-A1	None	W/D	33.2340	0.0040	33.2750	0.0100	0.1234
E2-A2	None	F/T	37.2900	0.0050	37.3300	0.0020	0.1073
E1-CD1	Dequest 2010	W/D	33.7645	0.0045	33.7990	0.0010	0.1022
E2-CD1	Dequest 2010	F/T	37.6040	0.0060	37.6340	0.0240	0.0798
E1-CD2	Dequest 2060S	W/D	35.9420	0.0060	35.9775	0.0025	0.0988
E2-CD2	Dequest 2060S	F/T	38.2380	0.0080	38.2805	0.0015	0.1111
E1-CK	Good-Rite K752	W/D	34.1265	0.0065	34.1740	0.0020	0.1392
E2-CK	Good-Rite K752	F/T	35.1815	0.0035	35.2010	0.0010	0.0554
E1-CW	Wayhib S	W/D	34.1635	0.0055	34.2075	0.0025	0.1288
E2-CW	Wayhib S	F/T	38.0720	0.0030	38.1125	0.0025	0.1064

0.75 M CMA(Ca/Mg = 3/7) with 0.01% Inhibitors

Sample No.	Inhibitor	Physical Conditions	Before treatment (Length Avg.)	Stdv	After treatment (Length Avg.)	Stdv	Expansion, %
Newly made concrete							.
N1-A6	None	W/D	36.6390	0.0030	36.8035	0.0015	0.4490
N2-A6	None	F/T	35.5800	0.0020	35.6825	0.0025	0.2881
N1-CD1	Dequest 2010	W/D	36.0590	0.0040	36.1650	0.0050	0.2940
N2-CD1	Dequest 2010	F/T	37.7830	0.0050	37.8775	0.0025	0.2501
N1-CD2	Dequest 2060S	W/D	36.0425	0.0025	36.1690	0.0010	0.3510
N2-CD2	Dequest 2060S	F/T	37.2305	0.0025	37.3330	0.0040	0.2753
N1-CK	Good-Rite K752	W/D	36.9880	0.0040	37.1320	0.0030	0.3893
N2-CK	Good-Rite K752	F/T	35.8140	0.0070	35.8950	0.0010	0.2262
N1-CW	Wayhib S	W/D	35.9415	0.0035	36.0775	0.0025	0.3784
N2-CW	Wayhib S	F/T	35.5520	0.0040	35.6325	0.0025	0.2264
Durable concrete							.
F1-A6	None	W/D	35.9170	0.0040	35.9815	0.0035	0.1796
F2-A6	None	F/T	35.0130	0.0030	35.0550	0.0050	0.1200
F1-CD1	Dequest 2010	W/D	33.9875	0.0045	34.0415	0.0035	0.1589
F2-CD1	Dequest 2010	F/T	36.1670	0.0020	36.2085	0.0005	0.1147
F1-CD2	Dequest 2060S	W/D	33.6310	0.0040	33.6775	0.0015	0.1383
F2-CD2	Dequest 2060S	F/T	33.5820	0.0200	33.6225	0.0025	0.1206
F1-CK	Good-Rite K752	W/D	31.9990	0.0060	32.0475	0.0125	0.1516
F2-CK	Good-Rite K752	F/T	32.3870	0.0040	32.4190	0.0010	0.0988
F1-CW	Wayhib S	W/D	32.2660	0.0040	32.3275	0.0025	0.1906
F2-CW	Wayhib S	F/T	36.0365	0.0085	36.0775	0.0025	0.1138
Non-durable Concrete							.
E1-A1	None	W/D	36.5970	0.0040	36.6755	0.0025	0.2145
E2-A2	None	F/T	36.0605	0.0025	36.1360	0.0060	0.2094
E1-CD1	Dequest 2010	W/D	35.1420	0.0040	35.1905	0.0155	0.1380
E2-CD1	Dequest 2010	F/T	35.2285	0.0135	35.2940	0.0030	0.1859
E1-CD2	Dequest 2060S	W/D	33.6210	0.0040	33.6775	0.0015	0.1680
E2-CD2	Dequest 2060S	F/T	33.5820	0.0200	33.6225	0.0025	0.1206
E1-CK	Good-Rite K752	W/D	31.9875	0.0055	32.0475	0.0125	0.1876
E2-CK	Good-Rite K752	F/T	32.3700	0.0050	32.4190	0.0010	0.1514
E1-CW	Wayhib S	W/D	34.0910	0.0030	34.1570	0.0050	0.1936
E2-CW	Wayhib S	F/T	37.4295	0.0045	37.4915	0.0065	0.1656

0.75 M Magnesium-Acetate with 0.01% inhibitors

Sample No.	Inhibitor	Physical Conditions	Before treatment (Length Avg.)	Stdv	After treatment (Length Avg.)	Stdv	Expansion, %
Newly made concrete							.
N1-A7	None	W/D	35.1495	0.0035	35.3185	0.0065	0.4808
N2-A7	None	F/T	37.6565	0.0015	37.7775	0.0025	0.3213
N1-MD1	Dequest 2010	W/D	36.3575	0.0025	36.5275	0.0025	0.4676
N2-MD1	Dequest 2010	F/T	34.4410	0.0040	34.5350	0.0050	0.2729
N1-MD2	Dequest 2060S	W/D	35.9345	0.0035	36.0350	0.0050	0.2797
N2-MD2	Dequest 2060S	F/T	35.1095	0.0045	35.1960	0.0010	0.2464
N1-MK	Good-Rite K752	W/D	38.5085	0.0035	38.6590	0.0090	0.3908
N2-MK	Good-Rite K752	F/T	37.4630	0.0020	37.5850	0.0100	0.3257
N1-MW	Wayhib S	W/D	35.5550	0.0050	35.6625	0.0075	0.3023
N2-MW	Wayhib S	F/T	34.6910	0.0210	34.8125	0.0025	0.3502
Durable concrete							.
F1-A7	None	W/D	34.7640	0.0040	34.8230	0.0030	0.1697
F2-A7	None	F/T	35.2295	0.0015	35.2750	0.0030	0.1292
F1-MD1	Dequest 2010	W/D	33.4595	0.0035	33.5205	0.0005	0.1823
F2-MD1	Dequest 2010	F/T	36.1815	0.0035	36.2315	0.0115	0.1382
F1-MD2	Dequest 2060S	W/D	34.0445	0.0035	34.0985	0.0065	0.1586
F2-MD2	Dequest 2060S	F/T	34.0240	0.0030	34.0800	0.0100	0.1646
F1-MK	Good-Rite K752	W/D	33.9945	0.0075	34.0375	0.0025	0.1265
F2-MK	Good-Rite K752	F/T	35.9660	0.0040	36.0025	0.0065	0.1015
F1-MW	Wayhib S	W/D	33.9430	0.0060	33.9755	0.0045	0.0957
F2-MW	Wayhib S	F/T	33.8820	0.0020	33.9375	0.0575	0.1638
Non-durable Concrete							.
E1-A1	None	W/D	33.7845	0.0025	33.8525	0.0025	0.2013
E2-A2	None	F/T	34.6940	0.0020	34.7445	0.0035	0.1456
E1-MD1	Dequest 2010	W/D	32.9700	0.0020	33.0125	0.0005	0.1289
E2-MD1	Dequest 2010	F/T	34.5135	0.0045	34.5715	0.0015	0.1681
E1-MD2	Dequest 2060S	W/D	33.1335	0.0075	33.1890	0.0040	0.1675
E2-MD2	Dequest 2060S	F/T	34.9860	0.0040	35.0415	0.0035	0.1586
E1-MK	Good-Rite K752	W/D	35.2390	0.0010	35.3075	0.0025	0.1944
E2-MK	Good-Rite K752	F/T	33.3185	0.0065	33.3785	0.0035	0.1801
E1-MW	Wayhib S	W/D	33.6880	0.0070	33.7410	0.0010	0.1573
E2-MW	Wayhib S	F/T	35.3500	0.0080	35.3920	0.0080	0.1188

Appendix B

ETTRINGITE CRYSTAL STRUCTURE

ETTRINGITE CRYSTAL STRUCTURE

Ettringite has a composition $\{Ca_6[Al(OH)_6]_2 \cdot 24H_2O\}(SO_4)_3 \cdot 2H_2O$ which is based on columns consisting of $[Ca_3[Al(OH)_6] \cdot 12H_2O]^{3+}$ units. The SO_4^{2-} ions and remaining water molecules are linked between these positively charged columns (Day 1992, Taylor 1990). Its structure consists of columns parallel to the c crystallographic axis, with additional water and sulfate molecules residing in channels parallel to and separating the columns. Ettringite is trigonal with point group 3m and space group P31c and with unit cell dimensions of c = 21.5 A; $a = b$ = 11.23 A. In Fig 23, A. shows the structure of 1/2 the c dimension of a column, and B. shows an a-b view of columns with channels between each column. The unit cell includes portions of four adjacent columns, for a total of one entire column in the cell. Because of orientations of sulfate and water in the channels, the unit cell c dimension is twice that shown in A. and has a complete formula of $\{Ca_{12}[Al(OH)_6]_4 \cdot 48H_2O\}(SO_4)_6 \cdot 4H_2O$.

Clues to the water adsorption swelling of ettringite in concrete are given by the crystal structure, and the morphology of ettringite rims around air entrainment voids. In the absence of a detailed crystallographic analysis of the ettringite in concrete voids, one can speculate that the ettringite rim crystals (Fig 7A) are oriented with their c axes perpendicular to void walls, and the axis of elongation of the crystals is parallel to c (Coveney et al. 1998). Macroscopic crystals are often pseudohexagonal prisms elongate along c and terminated by a pyramid or a pinacoid, or more commonly by both forms. The prominent cracks shown in Fig. 7A are assumed to be oriented parallel to the ettringite c axis and correspond to the orientation of channels parallel to c. Water absorption will increase the a-b spacings and expand the unit cell perpendicular to c. Drying of the crystals with loss of channel water should cause a reduction in the a-b spacings and creates cracks parallel to the c crystal axes.

Coveny et al. (1998) concluded that phosphonates adsorb onto the {0001} crystal faces of ettringite, and that the most effective phosphonate inhibitor molecules will have identical distances between adjacent phosphonate groups as the spacing between sulfate groups exposed on the {0001} faces. Although the inter-phosphonate spacings of the inhibitors used in the present study probably are not ideal, our observations as discussed in Part II provides some doubt that phosphonate inhibitors adsorb strongly on the {0001} faces, reduce growth rates of those faces, and thereby reduce or eliminate precipitation of ettringite from solutions. We observed that none of four inhibitors used in this study markedly decrease elongation, and we conclude that inhibition probably is not because of absorption on faces that terminate the prism.

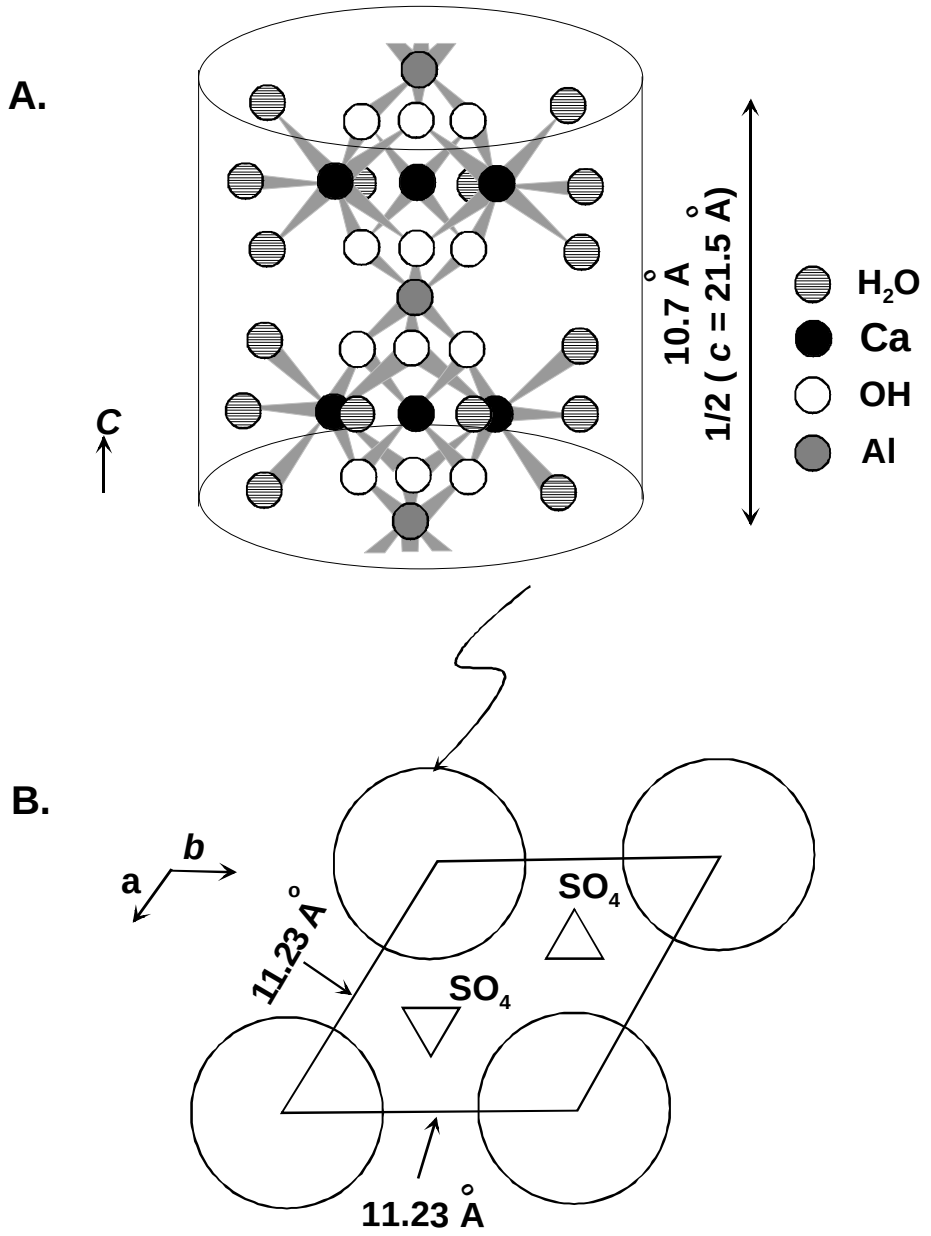

A. Structure of ettringite column, one-half unit cell. Structure is parallel to the **c** crystallographic axis. The *c* spacing is 21.5 Å. Modified from Day 1992.

B. View of a-b plane. The circles represent ettringite columns, and the regions between the columns are channels in which water and sulfate molecules reside. The ***a*** and ***b*** unit cell spacings are 11.23 Å. Modified from Day 1992.

Fig. 23. Ettringite Structure.

Appendix C

SUMMARY OF

CRYSTALLIZATION EXPERIMENTAL RESULTS

SUMMARY OF CRYSTALLIZATION EXPERIMENTAL RESULTS

Abbreviations:
Quantity: L = large; M = medium; S = small; Tr = trace.
Features med. = medium; amt. = amount; dash (-) = composed of ...; dia. = diameter

Ionic Species **A. Chlorides**			
Exp.No.	**Chemical**	**Quant. Precip.**	**Features**
249	NH_4	L	long, thin fiber-like needles
195	Ba	M	spheres - v. long, med. thick needles
159	Co	L	spheres - v. thin needles & a few AFM sphr (plates)
171,253	Cr		clusters of a few long, v. thin needles
198	Cu^{+3}	L	prob. Pointed, spheres - large, with long (0.3mm) needles
162	Li	L	spheres - v. long med. thin needles
17, 163	Mg	ML	small spheres - thin, short (0.03 mm) needles & split calcite
18,19,247	Na	L	Exp. 18 (sm.. amt. NaCl) spheres - small thin needles; Exp. 19 (lrg. amt NaCl) spheres - med. size long (0.25 mm) thin needles.
161	Pb	L	prob. pointed, spheres - very long, very thin needles
256	K	L	med, long thin needles
165	Rb	L	pointed, spheres – needles
217,264	Sn	L	med. long, med thin needles
216, 291	Zn	M	gel & colloidal precipitate
209,267	ZrO	L	v. long (0.2 mm) thin needles, prob. pointed
B. Non-Chlorides			
214	$AgNO_3$	S	pointed, dense spheres – med. long thin needles
197	$CeNHNO_3$	L	small, spheres – tiny, long needles
201	$NiNO_3$	ML	med. long, v. thin needles
191,266	$TiKF_2$	L	med. long, thin needles that hold much surface water
213	Silica gel	M	spheres – med. long, thin needles
192	UAc	L	dense spheres – med. long, thin needles
263	$NaNO_3$	L	med. long thin needles
	NaNitrite	L	long thin needles
Carboxylic Acids/Carboxylates and Borates			
4,177,215	Acetate, Na	M	spheres – long large needles
160	Acetate, Pb	L	very long, very thin needles
192	Acetate, U	L	dense spheres – med. long thin needles; gel
28	EDTA	M	med. long med. thick needles
147	Acetate, Phenyl	M	med. long, thin & med. long thick needles
5	Aconitic	S	large, thick needles
178	Alginic, Na	L	med. long, med. thick needles needles; some large calcite

95, 276	L-ascorbic	M	Ca oxalate dihydrate, short & med. long med. thick crystals
158,250	Boric acid	ML	small (0.63 mm dia.) spheres – AFM plates
2,259,274,275, 276	Borate, Na	L	spheres, AFM & short (0.009 mm) thin needles
141	Cholic	L	pointed, med. long, med thick
7	Citrate, Na	S	small short needles
199	Citrate, Fe^{+3}	L	spheres – long, thin needles, insol (?)
85	Isocitric	M	short needles; some AFM
245	Citrate, NH_4 dibasic	Tr	short needles; calcite spherulites
83	Coumaric	L	clumps – very long thin needles
142	Docosanoic	L	med. long, med. thick needles & small thin needles
167	1,12 Docecane dicarboxylic.	L	spheres – med long, thin needles
108, 279	Galacturonic	S	spheres – short thick prisms
64,261	Glutamic	M	long, broad needles
31,246	Glutamic, Na	M	giant long, broad needles
182,262	Glycolic, Na	M	spheres – short, v. thin needles
112	Thioglycolic, Na	M	0.04 mm needles
211	Maleic anhydride	M	large spheres – med. long med. thick needles
224,254	Malic	L	med long, med thin needles
145	Malonic, Na	M	spheres – long (0.2 mm) med. wide needles
36,212,243,245, 288,289; 292	Mucic/Galactaric	Tr	gel; tr. calcite
125,202	Nicotinic	M	spheres – med. long, med thin needles
203	O-nitrobenzoic	ML	spheres – long, med. long, med thick needles
89	Nucleic	L	large, very long needles
146	Orotic	M	spheres – long, med. thick & thin needles
9	Oxalic, K	M	needles; Ca oxalate dihydr.
175	M-phosphoric	L	spheres - small thin needles
166,218	Salicylic	M	long, broad needles; tr. AFM & calcite
72	Shikimic	M	med. long, wide needles
149	Sorbic	L	med. long, thin needles
150	Suberic	M	med. long, med. thick needles & med. long, thin needles
183	Succinic	L	med. long, med. thick needles
186	Succinate, Na	ML	very long (0.37 mm), med. thick needles
26	Tannic	L	clumps – large needles; tr. gypsum
274	Tartaric, NH_4	S	clusters – short thick crystals
3,281	Tartaric, K	M	clusters – short & med. long thick crystals
184, 286	Tartaric, Na	M	clusters – short & med. long med. thick crystals
34	Uric	M	clusters – med. long, small elongate needles
Amino Acids + NH_2 Compounds			
91,92	D-Alanine	Tr	spheres – long and med. needles
93	L-arginine	ML	long, very thin needles
82,115	L-asparagine	M	clusters – med. long needles w. pointed tips; gel
94,276	L-aspartic acid	L	clusters – med. long med. thick needles
98	L-cystine	M	clusters – short thin needles
103	D-glutamic acid	M	few short, thin needles; large calcite
104,261,280	L-glutamic acid	L	spheres – long ulta-thin needles
31,260	Glutamate, Na	L	spheres – long ultra-thin needles
105,144	Glycine	LM	clusters – med. long thick & thin needles

65	DL-Isoleucene	L	clusters – long broad needles
66	D-Leucine	L	clusters – med. wide needles
67	DL-lysine HCl	L	med. long very thin needles
68	DL-Methionine	ML	med. long thin needles
80	Ornithine HCl	Tr	clusters – small thin pointed needles
69	DL-Phenylalanine	L	med. long (0.12 mm) thin needles
70	Protamine sulfate	L	clumps – long, very thin needles
198,273	L-Pyroglutamic acid	L	long, thin needles
74	D-Threonine	L	large clumps – very thin needles
137,265	Thioproline	L	long med. thick needles (opt +)
87	Tricine	L	spheres – long thick needles
75	DL-Tryptophan	L	spheres – very thin long needles
139,270	Adenosine	L	long thin needles
101	D-Dianisidine	S	clusters – med. long thin needles
151,188	Sulfanilic	M	small thin needles
257	Sulfathiazol	VL	ultra-long very thin needles
187,287	Sulfamic acid	L	long (0.3 mm) thin needles
207	DL-Barbital, Na	L	spheres – long thin needles
33	Urea	S	Spheres – thin needles
	Purines and Related Substances		
114	Adenine	ML	many clusters – long thin needles
118	Guanine	L	long thin needles
121	Hypoxanthine	M	long thin needles
78	Xanthine	M	very long thin & thick needles
6,251	Caffeine	L	med. long med. thin needles
84	Isatin	L	spheres – long thin needles
	Enzymes		
37	Acid phosphatase	L	long thin needles
60	Aldolase	L	dense spheres – elongate thin needles
38	a-Amylase	M	long broad needles
39	ß-Amylase	L	long borad needles
40	Amyloglucosidase	L	long very broad needles
41	Catalase	M	spheres – short thin needles
61,140	Cellulase	L	spheres – large thick needles; spheres – small thin needles
62	Deoxyribonuclease	L	med. long very thin needles
42	Diastate/Clarase	L	small long thin needles
43	Enterokinase	L	dense spheres – thin short needles
44	Erepsin	L	very long thin needles
45	Glucose oxidase	L	med. long very thin needles
46	Invertase (bakers' yeast)	M	tiny spheres (0.012 mm dia) – short thin needles
47	Lipase (hog pancrease)	L	spheres – thin small needles
48	Macerase (Rhizopus sp.)	M	large spheres – long broad needles
49	Maltase (Aspergillus niger)	S	calcite with long induction time, no gel
50	Papain (Papaya)	L	med. long very thin needles
51	Pectinase (fungal)	L	med. long very thin needles
52	Pepsin	L	med. long very thin needles
53	Pronase	L	spheres – long thin & med. wide needles
54	Protease	ML	small very thin needles
55	Pyruvate kinase (rabbit)	M	med. long med thick needles

56	Rennet	L	large spheres – needles
58	Trypsin	L	spheres – med long needles
59	Urease	L	spheres – med long very thin needles
	Sugars and Sugar-based Compounds		
15,275	L-Arabinose	Tr	clusters – short med thick prisms
135	Cellobiose	L	spheres – long thin needles, insol
23,193	D-Fructose	S	large dense spheres – Et; dense spheres – short, thick calcite
132	D(+)-Glucose/Dextrose	L	clusters – long, med. thick needles
21	D-Lactose	S	large needles & tiny needles
22	D-Maltose	M	large needles
27	D-Manitol	M	long (>0.24 mm) thin needles
157, 282	D-Rhamnose	S	spheres – long med. thick needles
156,283,291	D-Ribose	S	short thick hex. prisms
113	D-Sorbitol	S	short med. thick needles
16	D-Sucrose	M	small thin needles
32	Xylan	M	bundles of med. needles
24	D-Xylose	S	clumps – short broad prisms
20	Inulin	L	large needle
110	Inositol	M	spheres – thin & thick needles
111	Myo-Inositol	L	very thin needles
185	Starch (potato)	L	very long med. thick needles with rounded tips
81	Arabinic acid	M	clustors – short med. thick crystals with rounded tips
168	Gum Arabic	S	small spheres – short rounded needles
108,279	Galacturonic acid	S	very short thick prisms
	Phosphates and Nucleotides		
90	Adenosine-2-monophosphric Acid	M	gel; calcite spheres, perhaps some AFM
133	ATP	L	long very thin needles
181	Ammonium phosphate dibasic	-	gel, no crystals after 8 months
170	Calcium phosphate tribasic	ML	spheres – med. long med thick needles
97	Cocarboxylase (thiamine phosphate) – Cl	M	gel; calcite spheres; long induction time
200	D-Glucose 6-phosphate	L	gel; calcite; long induction time
206	Phosphocreatine	M	large spheres – long thin crystals
205	Phosphoenol pyruvate	L	large spheres – med long med thick crystals
175	M-Phosphoric acid	L	spheres – needles
29	Potassium phosphate monobasic	-	gel – stable for 9 months
29	Glycerol phosphate, Na	L	large spheres – thin & thick needles
30	Hexametaphosphate, Na	-	gel, no crystals after 9 months
8	Phyroposphate, Na	L	long (0.2 mm) needles
	Vitamins		
122,126	B_1 Thiamine HCl	M	spheres – med long med thin needles
125,202	B_3 Niacin (nicotinic acid)	L	spheres – med. long med. thin needles
127	B_6 Pyridoxene HCl	S	spheres – med. long thin & thick needles
128	B_5 Pantothenic acid	L	long thin needles
71	B_2 Riboflavin	L	yellow dense clumps – radiating very thin needles
96	H Biotin	M	spheres – long thin needles

Stains and Related Substances			
52	Acid Fucsin	L	spheres – long extremely thin needles
153,227,228,240,241,242	Alizarin Red S	L	long thin needles; AFM plates; short prisms
154,220	Aniline blue	L	ultra thin fiber-like needles
230	Azocarmine B	L	thin med. long (0.1 mm) needles
231	Basic Fuchsin (no SO_3Na)	L	med. thick long (0.21 mm) blue needles
232	Calmagite	L	thin long (0.2 mm) needles
233	Congo Red	L	thin fiber-like needles (0.12 mm long)
234	Cotton Blue	L	thin fiber-like needles
235	Guinea Green	L	med thin, med. long needles
236	Evans Blue	L	med wide, long needles
237	Fast Green	L	thin long (0.36 mm) needles
238	Indigo Carmine	L	thin blue needles
239	Nuclear Fast Red	L	spheres – long thin needles
77	2(2-Thiazolazo)-p-Cresol	L	spheres – med. long very thin needles
130	1,4 Napthoquinone	ML	long very thin needles
131	1,2 Napthoquinone	L	clusters – med. long thin needles
Lignins and Surfactants			
179	Dowfax 8390 (sulfonate)	L	spheres – med. long thin needles
180	Sandopan JA36	L	spheres – long thick & med. thick needles with pointed tips
220,258	Polyfon O (lignosulfonate)	L	small (0.009 mm dia.) spheres – AFM & short (0.001 mm) needles
221	Reax 6BW (lignocarboxylate)	S	spheres – long (0.3 mm) needles
223	Reax 100 (lignosulfonate)	Tr	large long needles
176,284	Sodium Lauryl Sulfate	L	immed. prec., voluminous gel-like flocks, ultra thin long fibers
301	WRDA-82 (lignosulfonate + amine water reducer/retarder), 2.2 ppt	M	v. short thick crystals; rounded tips + gel
302	WRDA with Hycol (lignosulfonate + amine formate/acetate, 2.2 ppt	M	clusters – med. short med. thick
299	WRDA-82, 11 ppt	-	gel
300	WRDA with Hycol, 11 ppt	-	gel
Other Substances			
13	Allantoin	M	large & small long needles
99	AMO 1618	L	clusters – long thin needles
14	Amygdalin	ML	spheres – long thin needles
124	BHT	L	spheres – long thin needles
196	DL Buthionine Sulfoximine	L	spheres – long thin needles with pointed (?) tips
169,252	Casein	S	spheres – small (0.024 mm long) med. thin needles
10,116	Choline	L	long thin needles
172	Coumarin	M	spheres – long med. thick needles
117	Cytidine	M	clusters – short thick needles
100	DNA, Na	M	clusters – med. long thin needles
107	Dicumarol	L	spheres – med. long broad needles

173	Esculin	L	spheres – thin needles
174	Ethylenediammonium sulfate, Fe^{+2}	ML	spheres – med. long med. thick needles; gel
136	Ficin	L	spheres – short (0.07 mm) very thin needles; gel
102	D-Glucose amine HCl	M	clusters – med. long thick needles
109,271	D-Glucuranoalactone	M	spheres – long thick needles
224	Haematoxylin	L	long needles
138	Kanamycin	ML	spheres – med long (0.09 mm) med. thick & thin needles
25	Proteose peptone	M	spheres – exceptionally long thick needles
129	Sequestrine	L	med. long very thin needles
57	Streptomycin	L	dense spheres – large thick needles; tr gypsum
189	THAM	L	med. long, med. thin needles
73,190	Thioaceteamide	L	large spheres – med. long wide needles
208	Thiourea	L	spheres – med. long med. thick needles
123	Thymidine	L	spheres – long thin needles